

# The effects of the circadian clock on wound healing in skin

---

Katherine S.C. Heath, MSc

University College London

Thesis submitted for the degree of Doctor of Philosophy

2016

I, Katherine Heath, confirm that the work presented in this thesis is my own. Where information has been derived from other sources, I confirm that this has been indicated in the thesis.

# Abstract

Circadian rhythms are daily cycles of physiological functions which oscillate under the control of the circadian clock in order to coincide with the temporal demands of the light/dark cycle of the day. The importance of the integrity of the circadian clock in health and disease has emerged in recent years; perturbations of the circadian clock are associated with an increased risk of malignancy and metabolic syndrome. In this study, I aimed to examine whether RNAi modification of *Bmal1*, a core component of the circadian clock, could be used to improve wound healing.

Chronic wounds are a global problem, in part caused by diabetes and ageing. Currently there is no effective pharmaceutical treatment; wound care by specialist nurses and physical methods such as compression bandages are the main course of action. Originally, the aim was to use DNA antisense to transiently knock down *Bmal1*. It became clear that this was having a toxic effect so several other approaches to knocking down *Bmal1* expression were attempted. Ultimately, I used a lentiviral vector to transduce cells with an shRNA construct and also generated a *Bmal1*:luciferase reporter cell line to measure the oscillations of *Bmal1* *in vitro*. Experiments using the reporter cells demonstrated that commonly used methods to synchronise the circadian clock in mammalian cells confirmed that these measures are unnecessary. The generation of cells with *Bmal1* knockdown was only partially successful; however, an experiment using a heterogeneous population of *Bmal1* knockdown cells indicates that this intervention reduces the migration rate of these cells in a scratch wound assay but further experiments are required to definitively determine the effects once a stable knockdown cell line has been established. If these preliminary results are true then the knockdown of *Bmal1* is not likely to have a beneficial effect on wound healing.

## Contents

---

<b>List of Figures</b> .....	<b>7</b>
<b>List of Tables</b> .....	<b>10</b>
<b>Table of Abbreviations</b> .....	<b>11</b>
<b>Acknowledgements</b> .....	<b>14</b>
<b>1. General Introduction</b> .....	<b>15</b>
<b>1.1. The circadian clock</b> .....	<b>16</b>
<b>1.2. Core circadian clock genes</b> .....	<b>22</b>
<b>1.3. Circadian clocks and the skin</b> .....	<b>23</b>
<b>1.4. Wound Healing</b> .....	<b>25</b>
<b>1.5. Chronic wounds</b> .....	<b>28</b>
<b>1.6. Project background</b> .....	<b>30</b>
<b>1.7. Hypothesis</b> .....	<b>31</b>
<b>1.8. Thesis aims</b> .....	<b>31</b>
<b>2. Materials and Methods</b> .....	<b>32</b>
<b>2.1. Cell Culture</b> .....	<b>33</b>
2.1.1. Cell maintenance.....	33
<b>2.2. Molecular Biology</b> .....	<b>34</b>
2.2.1. Western Blotting .....	34
Table 2.1 Primary antibodies used in Western blotting .....	35
2.2.2. RT-PCR .....	37
2.2.3. cDNA synthesis .....	37
2.2.4. RT-PCR Analysis .....	40
2.2.5. Immunofluorescence.....	40
<b>2.3. Transfection protocols</b> .....	<b>41</b>
2.3.1. Fugene 6.....	41
2.3.2. Transduction .....	42
<b>2.4. Scratch Wound Assay</b> .....	<b>44</b>
<b>2.5. In vivo assays</b> .....	<b>45</b>
2.5.1. Analysis of in vivo wound healing .....	46
<b>2.6. In silico</b> .....	<b>46</b>
<b>3. Preliminary <i>in vivo</i> experiments</b> .....	<b>50</b>
<b>3.1. Introduction</b> .....	<b>51</b>
3.1.1. Background.....	51
3.1.2. Transiently disrupting the circadian clock.....	51
3.1.3. DNazymes.....	52
<b>3.2. Antisense Oligonucleotides</b> .....	<b>53</b>
3.1.1 Mechanisms of action .....	53

3.3.	Methods .....	55
3.4.	Results.....	56
3.5.	Discussion .....	70
4.	<b><i>In silico</i> antisense deoxyoligonucleotide expansion design and <i>in vitro</i> testing</b>	<b>72</b>
4.1.	Introduction .....	73
4.2.	Results.....	74
4.3.	<i>In vitro</i> testing of new asODNs .....	75
4.4.	Modified antisense DNA oligonucleotides .....	75
4.4.1.	Aptameric inhibition of off-target molecules.....	80
4.5.	Intracellular availability of ODNs.....	80
4.6.	<i>In vitro</i> testing of non-oligomerised mononucleotides .....	81
4.6.1.	Normalisation and analysis of Western Blots .....	82
4.7.	Discussion .....	93
5.	<b>Alternative methods of RNA interference .....</b>	<b>94</b>
5.1.	<b>Ribonucleic acid interference (RNAi).....</b>	<b>95</b>
5.1.1.	siRNA .....	96
5.1.2.	microRNA.....	97
5.1.3.	Short Hairpin RNA .....	98
5.1.4.	Overexpression of a dominant negative protein .....	99
5.2.	<b>Delivery methods .....</b>	<b>99</b>
5.2.1.	Transfection .....	99
5.2.2.	Transient versus Stable Transfection .....	101
5.2.3.	Physical methods of transfection .....	101
5.2.4.	RNAi delivery vectors .....	102
5.2.5.	Viral delivery .....	103
5.3.	<b>Methods and materials.....</b>	<b>103</b>
5.3.1.	siRNA .....	103
5.3.2.	miRNA.....	104
5.3.3.	Dominant negative Bmal1 .....	104
5.4.	<b>Transfection optimisation .....</b>	<b>105</b>
5.5.	<b>Results.....</b>	<b>107</b>
5.5.1.	Short Interfering RNA .....	107
5.6.	<b>Micro RNA .....</b>	<b>110</b>
5.6.1.	Transfection optimisation .....	111
5.7.	<b>Discussion .....</b>	<b>112</b>
6.	<b>Lentiviral vectors &amp; circadian clock synchronization <i>in vitro</i> .....</b>	<b>114</b>
6.1.	<b>Introduction to lentiviral vectors .....</b>	<b>115</b>
6.1.1.	Virally mediated RNAi – transduction .....	115

<b>6.2.</b>	<b>Introduction to circadian clock synchronisation <i>in vitro</i></b> .....	<b>118</b>
<b>6.3.</b>	<b>Methods</b> .....	<b>118</b>
6.3.1.	Lentiviral titre evaluation.....	118
6.3.2.	Transduction .....	119
6.3.3.	Circadian clock synchronisation assay .....	121
6.3.4.	RT-PCR .....	121
6.3.5.	Luciferase assay .....	122
6.3.6.	Incucyte scratch wound assay to assess functional effects of Bmal1 knockdown 122	
<b>6.4.</b>	<b>Results</b> .....	<b>123</b>
<b>6.5.</b>	<b>Discussion</b> .....	<b>128</b>
6.5.1.	Circadian clock synchronisation <i>in vitro</i> .....	128
6.5.2.	Scratch Wound Assay .....	132
<b>7.</b>	<b>Discussion</b> .....	<b>133</b>
7.1.	<b>General discussion</b> .....	<b>134</b>
7.2.	<b>Future directions</b> .....	<b>140</b>
	<b>References</b> .....	<b>141</b>
	<b>Appendix A</b> .....	<b>155</b>

---

# List of Figures

---

Figure 1.1 Circadian rhythms are seen in multiple aspects of human physiology.....	16
Figure 1.2 The regulatory pathways of central circadian clock.....	18
Figure 1.3 SCN signalling to the peripheral circadian clocks.....	21
Figure 1.4 Core circadian genes after (Froy, 2011) .....	23
Figure 1.5 Phases of wound healing .....	28
Figure 1.6 Chronic wound causes .....	29
Figure 2.1 Mouse wound model .....	45
Figure 3.1 DNAzyme schematic .....	52
Figure 3.2 Antisense down regulation of protein translation (Robinson, 2004).....	54
Figure 3.3 Antisense ODNs increase wound healing <i>in vivo</i> .....	56
Figure 3.4 ODN sequence Bmal 180 increases wound closure rate with comparison to no treatment.....	57
Figure 3.5 Macroscopic area measurements of the wounds cease to demonstrate the effects seen previously when the position of the control wound was moved. ....	58
Figure 3.6 No significance was seen between treated and control wounds in re-epithelialisation after the position of the control wound was moved.....	59
Figure 3.7 Antisense ODNs appear to decrease wound area significantly when the original experimental conditions were used.....	60
Figure 3.8 Re-epithelialisation measurements made from the same tissue as the macroscopic images in Figure 3.7 show no difference in healing rate between treated and untreated samples. ....	60
Figure 3.9 Macroscopic wound area is reduced with antisense ODN treatment. ....	61
Figure 3.10 Re-epithelialisation measurements made from the same tissue as the macroscopic images in Figure 3.9 show no difference in healing rate between treated and untreated samples. ....	62
Figure 3.11 Macroscopic images of the wounds used to produce the data in Figure 3.5	63
Figure 3.12 Representative macroscopic images used to produce the data in Figure 3.7 .....	64
Figure 3.13 The direction of tissue folding influences the macroscopic wound area. ....	65
Figure 3.14 Punch wound method .....	66
Figure 3.15 The position of the wound affects the degree of re-epithelialisation.....	66

Figure 3.16 The position of the control wound influences the size of the macroscopic wound area. ....	67
Figure 3.17 Combining anti-CLOCK and anti-Bmal1 asODNs lead to significantly reduced re-epithelialisation. ....	67
Figure 3.18 The asODNs do not significantly increase re-epithelialisation of the wounds. ....	68
Figure 3.19 Treatment with DNazymes does not significantly increase re-epithelialisation ....	69
Figure 4.1 Antisense DNA modifications .....	76
Figure 4.2 Scrambled asODN knocks down Bmal1 as effectively as the targeted sequence. asODNs also knockdown GAPDH.....	78
Figure 4.3 Bmal1 protein expression 6 hours after treatment is not due to a sequence specific effect of asODNs .....	83
Figure 4.4 Expression of the housekeeping proteins is not stable enough to use as a loading control .....	84
Figure 4.5 24 hours following treatment none of the sequences knocks down Bmal1 with comparison to the vehicle only control .....	85
Figure 4.6 At 24 hours both housekeeping proteins are significantly knocked down by the scrambled PO control .....	86
Figure 4.7 At 48 hours post-treatment all of the asODNs/NMPs except scrambled PO 2 knock down Bmal1 with comparison to the vehicle only control.....	87
Figure 4.8 48 hours post-treatment both of the housekeeping proteins are affected by the asODNS/NMPs .....	88
Figure 4.9 Bmal1 mRNA significantly increases in response to 24 hours' treatment with a phosphorothioate asODNs.....	89
Figure 4.10 Bmal1 mRNA significantly increases in response to 48 hours' treatment with a phosphorothioate asODNs .....	90
Figure 4.11 Bmal1 mRNA is not affected by antisense or dNMPs .....	91
Figure 4.12 asODNs do not increase migration rate of fibroblasts.....	92
Figure 5.1 The mechanism of action of siRNA .....	97
Figure 5.2 Mechanisms of miRNA regulation of gene expression.....	98
Figure 5.3 The mechanism of action of siRNA .....	100
Figure 5.4 A plasmid map displaying the qualities required for use in transfection ....	103
Figure 5.5 Neither miRNA nor siRNA knock down Bmal1 protein 48 hours post-treatment.....	107

Figure 5.6 neither siRNA nor overexpression of Bmal1 DN reduce the expression of Bmal1 48 hours post-treatment .....	108
Figure 5.7 Neither siRNA nor Bmal1 DN overexpression enhance the migration rate of NIH 3T3s.....	109
Figure 5.8 miRNA mimics do not reduce mRNA expression of Bmal1 .....	110
Figure 5.9 Representative images of immunofluorescent assessment of transfection efficiency. Interferin is the most successful transfection reagent for FAM-tagged siRNA .....	111
Figure 5.10 The optimised Interferin transfection protocol conditions did not produce a knock-down of Bmal1 or GAPDH after 72 hours .....	112
Figure 6.1 Viral particles are made within 293FT cells following transfection with transfer, packaging and envelope plasmids.....	116
Figure 6.2 Virally mediated transduction of shRNA constructs .....	117
Figure 6.3 Plasmid map of the Genecopoeia shRNA clones targeted to Bmal1.....	120
Figure 6.4 Plasmid map of the Bmal1:LUC construct.....	121
Figure 6.5 The control has as much effect as the treatment in cell synchronisation of Bmal1 with serum shock.....	123
Figure 6.6 Dexamethasone has no more effect than the control in the synchronisation of Bmal1 in NIH 3T3s.....	123
Figure 6.7 Changing the culture medium for fresh culture medium induces circadian oscillations in Bmal1 as effectively as the cell synchronisation protocols widely used in the literature. ....	124
Figure 6.8 The amplitude of the wave in circadian rhythm of Bmal1 with serum shock is larger than with dexamethasone or medium change.....	125
Figure 6.9 Synchronisation by serum shock resulted in a longer period length than by the dexamethasone or medium change. ....	125
Figure 6.10 ShRNA knockdown construct 4 significantly reduces the mean wound density of transduced NIH 3T3 fibroblasts .....	126
Figure 6.11 Representative image of fluorescent cells expressing mCherry overlaid over a brightfield image of the same field of view (20 x).....	127
Figure 6.12 Per2 oscillations in NIH 3T3 cells expressing mPer2:LUC can be re-initiated by treatment with forskolin or by fresh medium.....	128
Figure 6.13 Mechanism by which Bmal1 stimulates protein translation.....	130
Figure 6.14 The interaction between glucocorticoids and mTOR (Shimizu et al., 2011) .....	131

## List of Tables

---

Table 2.1 Primary antibodies used in Western blotting .....	35
Table 2.3 Secondary antibodies used in Western blotting .....	36
Table 2.4 Buffers and reagents used for SDS-PAGE .....	36
Table 2.5 Primers for RTPCR.....	39
Table 2.6 Antibodies used for immunofluorescence.....	41
Table 3.1 Antisense sequences used in preliminary experiments .....	55
Table 4.1 16mer asODNs were elongated to produce 25-30mer sequences.....	74
Table 4.2 asODNs used for further <i>in vitro</i> testing .....	77
Table 5.1 Electroporation settings .....	105
Table 5.2 Transfection reagents tested.....	106
Table 6.1 Statistical differences in mean wound density between NIH 3T3s transduced with shRNA construct 4 compared to NIH 3T3s transduced with the scrambled control .....	126

## Table of Abbreviations

---

ACTH	Adrenal cortex to adrenocorticotrophic hormone
ANOVA	Analysis of variance
BCA	Bicinchoninic acid
cAMP	Cyclic AMP
CLOCK	Circadian locomotor output cycles Kaput
CREB	cAMP response element binding protein
CT	Cycle threshold
DBS	Donor Bovine Serum
DMEM	Dulbecco's Modified Eagle Medium
DN	Dominant negative
DRN	Dorsal raphe nucleus
dsRNA	double stranded RNA
ELISA	Enzyme-linked immunosorbent assay
ERK	Extracellular signal-regulated kinase
FACS	Fluorescence-activated cell sorting
FAM	5(6)-carboxyfluorescein
FBS	Foetal bovine serum
FITC	Fluorescein isothiocyanate
GAPDH	Glyceraldehyde 3-phosphate dehydrogenase
GM	Genetic modification
HBOT	Hyperbaric oxygen therapy
HEPES	(4-(2-hydroxyethyl)-1-piperazineethanesulfonic acid)
HPLC	High performance liquid chromatography
HRP	Horse radish peroxidase
HUVEC	Human umbilical vein endothelial cells
ICU	Intensive care unit
IGL	Intergeniculate leaflet
IRES	Internal ribosome entry site
LB	Luria-Bertani
LNA	Locked nucleic acids
LP	Lentiviral particles

miRNA	microRNA
NMP	Nucleoside mono phosphate
ODN	Oligodeoxynucleotide
PACAP	Pituitary adenylate cyclase-activating peptide
PBS	Phosphate buffered saline
PCR	Polymerase chain reaction
PEI	Polyethylenimine
PES	polyththersulfone
PFA	Parafolmaldehyde
PMO	Phosphorodiamidate morpholino oligomers
PO	Phosphodiester
PS	Phosphothioate
RAR	Retinoic acid receptor
RHT	Retinohypothalamic tract
RIPA	Radio immunoprecipitation assay
RISC	RNA-induced silencing complex
RLT	Proprietary lysis buffer from Qiagen
RNA	Ribonucleic acid
RNAi	Ribonucleic acid interference
ROR	RAR-related orphan receptors
ROS	Reactive oxygen species
RPE	Proprietary ethanol based washing buffer from Qiagen
RTPCR	Reverse transcription polymerase chain reaction
RW	Qiagen wash buffer
SCN	Superchiasmatic nuclei
SDHA	Succinate dehydrogenase complex, subunit A,
SEM	Standard error of the mean
shRNA	Short hairpin RNA
siRNA	Short interfering RNA
SS	Serum shock
SYBR	SYBR green is a nucleic acid stain used for RTPCR from Life Tech
TBS	Tris buffered saline
TIFF	Tagged Image File Format <sup>l</sup>
TMP	Thymidine monophosphate
UVB	Ultra-violet light B

WT	Wild type
XPA	Xeroderma Pigmentosum, Complementation Group A

# Acknowledgements

---

I would like to thank my supervisors Dr Christopher Thrasivoulou, Professor David Whitmore and Professor John Parnavelas for their help, support and guidance.

I thank Professor Whitmore for making it possible for me to do this project, Dr Thrasivoulou for his unrelenting support and for believing in me throughout and Prof Parnavelas for adopting me for the last couple of years and being so kind and generous with his laboratory space, time and expertise.

I would also like to thank Tim Robson, Danial Ciantar and Jane Pendjiky for all of their help over the years. I thank Jane for making me the image of the mouse wounding technique and for being a font of knowledge about all things related to Photoshop and for our great chats over the years.

I am grateful to the BBSRC for funding my project.

I would also like to thank all of my colleagues and friends, from labs past and present, and the 5<sup>th</sup> and 6<sup>th</sup> floor Rockefeller building for their intellectual conversations and for making the place much nicer place to be. In particular I would like to thank Dr Noemie Hamilton for giving me so much help when I needed it most and Dr Bill Andrews for teaching me so much of his expertise in the lab.

I thank my family for their understanding and encouragement.

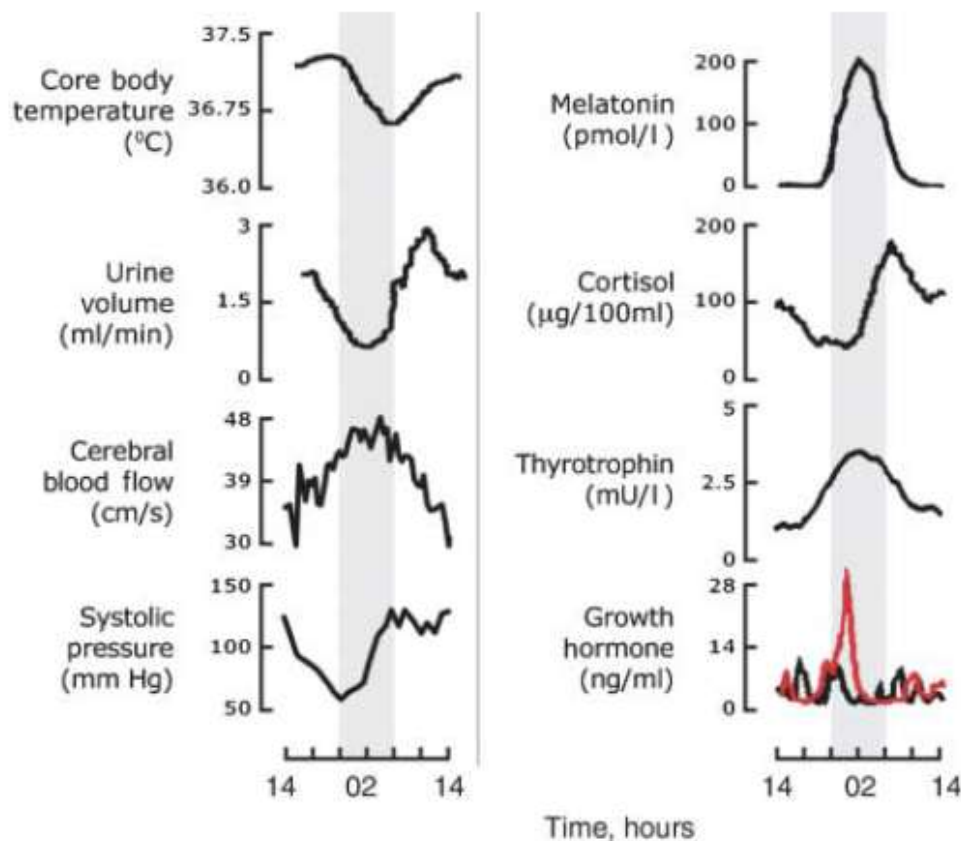
And lastly, but by no means least, I thank my wonderful husband Jamie, who has supported me in every way. I would never have been able to do this PhD without him.

# 1. General Introduction

---

## 1.1. The circadian clock

Circadian rhythms control aspects of one's daily life such as the sleep/wake cycle, diurnal fluctuation in hormones relating to metabolic control and body temperature amongst other numerous examples.



(Hastings, O'Neill, & Maywood, 2007)

### **Figure 1.1 Circadian rhythms are seen in multiple aspects of human physiology.**

As shown above, the circadian clock controls daily fluctuations in body temperature, micturition volume, blood flow and blood pressure (left hand graphs) and daily fluctuations in multiple hormones (right hand graphs).

There are numerous reviews on the subject (R. Y. Moore, 1997; Ripperger & Schibler, 2001; Reppert & Weaver, 2002; Takahashi, Hong, Ko, & McDearmon, 2008; Pevet & Challet, 2011). A circadian clock that regulates biological processes is found in all organisms, including plants, bacteria, insects and mammals. See **Figure 1.1** The work

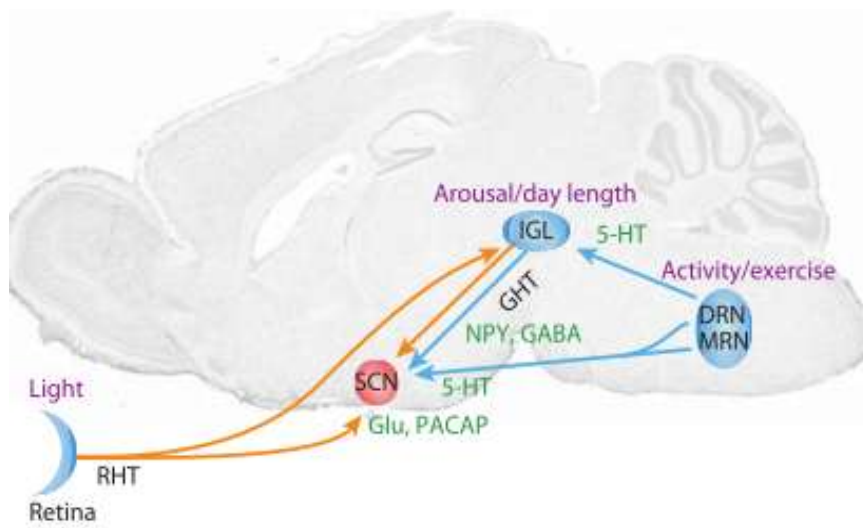
'circadian' derives from 'circa' meaning around and 'dies' meaning day. For a biological rhythm to be deemed circadian it must repeat approximately every 24 hours, must persist in the absence of external cues (for example, daylight), must be entrainable, i.e. adaptable according to environmental conditions, for example they can be synchronised with the local time. An example of this phenomenon is the sleep-wake cycle. When one travels across time zones, the sleep-wake cycle adjusts to the local time over the course of several days.

In mammals the circadian clock is regulated primarily by the *Zeitgeber* (meaning 'time-giver' in German) daylight. There are many other factors that can influence circadian rhythms, such as time of feeding and exercise, but daylight has the greatest influence. Typically the effect on circadian rhythms in constant dark is that the period (the unit of repeating circadian patterns) lengthens. This is called 'free-running'.

Light is detected by melanopsin (Hattar et al., 2002) in photo-sensitive retinal ganglion cells which send photic information via the retino-hypothalamic tract (R. Y. Moore & Lenn, 1972) to the suprachiasmatic nuclei (SCN) which act as the central circadian clock. See **Figure 1.2**. Light dependent synchronisation is the same in diurnal and nocturnal animals (Mrosovsky, Edelman, Hastings, & Maywood, 2001; Caldelas, Poirel, Sicard, Pvet, & Challet, 2003). The inputs to the SCN are both photic and non-photoc; daylight is detected by the photosensitive cells of the retina which send a signal to the ventrolateral part of the SCN via the retinohypothalamic tract (RHT) (R. Y. Moore & Lenn, 1972). This causes the release of glutamate and pituitary adenylate cyclase-activating protein which in turn induce the expression of clock genes (Hannibal et al., 1997). The main intracellular pathway for this is via the extracellular signal-regulated kinase pathway (ERK). Activation of ERK causes the phosphorylation of

cyclic adenosine monophosphate (cAMP) response element binding protein (CREB) which then binds to cAMP response elements in the promoters of genes such as Per1 and Per2 (Period transcripts) and activates their transcription (Kornhauser, Mayo, & Takahashi, 1996; Obrietan, Impey, & Storm, 1998; Grewal, York, & Stork, 1999; Coogan & Piggins, 2003). These genes are only inducible when light hits the retina during the dark phase, resulting in the periodic phase either advancing or being delayed in mammals; this is called 'resetting'. This effect is not seen in mice with Per1/Per2 mutations (Akiyama et al., 1999).

Light derived signals also reach the SCN via the intergeniculate leaflets (IGL) and along the geniculo-hypothalamic tract (GHT) (R. Y. Moore & Card, 1994). This occurs slightly after the RHT signal, so it may modulate the response to light. The IGL is also stimulated by non-phototic signals via dorsal raphe nucleus (DRN) and integrates these signals to the SCN. Non-phototic cues such as activity/exercise are sent to the SCN from the DRN via serotonin signalling (Kiss, Leranath, & Halasz, 1984; van den Pol & Tsujimoto, 1985).



(Dibner, Schibler, & Albrecht, 2010)

## Figure 1.2 The regulatory pathways of central circadian clock

Photo-sensitive retinal ganglion cells detect light and stimulates the suprachiasmatic nuclei via the retino-hypothalamic tract to regulate the central circadian clock

The SCN sends messages to the body by several means; in the brain there are various efferents which terminate in different areas but there must also exist a paracrine element to the signalling as projections of SCN neurons are not required for establishment of locomotor activity rhythms and additionally transplanted SCN tissue can restore rhythms in many areas of the brain (Silver, LeSauter, Tresco, & Lehman, 1996).

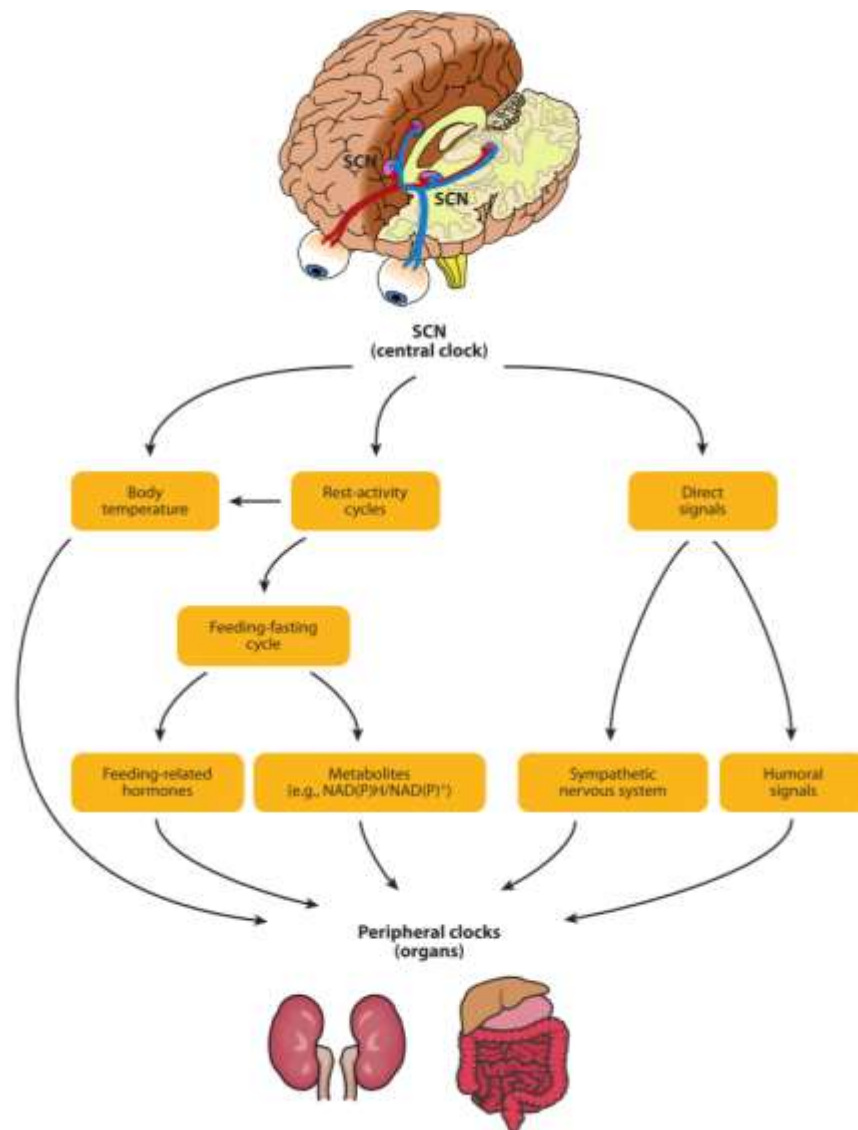
The SCN is also thought to control hormone rhythms such as melatonin and corticosterone, i.e. hormone release from the pineal gland and the adrenal cortex. The sensitivity of the adrenal cortex to adrenocorticotrophic hormone (ACTH) changes throughout the day which affects the amount of corticosterone secreted (Buijs et al., 1999; Kaneko, Hiroshige, Shinsako, & Dallman, 2012). See Figure 1.3. Exposure to light affects gene expression in both the adrenal gland and liver (Ishida et al., 2005).

In the SCN the phase of clock expression is the same in diurnal and nocturnal animals due to its dependence of light cues for synchronisation but the phase of circadian gene expression varies greatly in the peripheral tissues of diurnal and nocturnal animals (i.e. the downstream effects of SCN signalling differ in diurnal vs. nocturnal animals.) (Vosko, Hagenauer, Hummer, & Lee, 2009)

Another way in which the circadian clock can be entrained is via timing of feeding. If food availability is limited to a small window within the day the circadian rhythms adjust to correlate with food availability (Stephan, 2002). On a molecular level, the peripheral circadian clocks share the same regulatory proteins as found in the SCN (K Yagita, Tamanini, van Der Horst, & Okamura, 2001) . Up to 10% of all genes are expressed in a rhythmical fashion that indicates that they are under circadian control. Feeding related synchronisation is independent of the SCN - it occurs even in animals with ablated SCN and conversely it does not shift the timing phases within the SCN.

Even double CLOCK knockout animals can be entrained with food (Oishi, Miyazaki, & Ishida, 2002). Restricted feeding results in an altered glucocorticoid rhythm (this is usually under SCN control).

Restricted feeding results in a reduction in nocturnal core temperature (Damiola, 2000). If the incubation temperature of cultured fibroblasts is lowered correspondingly, it enables the pattern of circadian oscillations to persist for longer following synchronisation (Welsh, Yoo, Liu, Takahashi, & Kay, 2004; S. A. Brown et al., 2008). In mice, elevating the night-time housing temperature causes a change in circadian gene expression in the liver but not the SCN, indicating that this is another modulator of peripheral circadian clocks (Cailotto et al., 2009). Peripheral circadian clocks can be altered locally via sympathetic nerve ablation in the pineal gland or liver which causes the cessation of Per gene expression. The reverse effect can be achieved using adrenergic agonists, indicating that some of the control of peripheral circadian rhythmicity is under the influence of the sympathetic nervous system (Cailotto et al., 2009).



(Dibner et al., 2010)

**Figure 1.3 SCN signalling to the peripheral circadian clocks**

The central clock controls the peripheral circadian clocks via neural, endocrine and paracrine signalling.

## 1.2. Core circadian clock genes

The molecular clocks within the SCN neurons consist of a transcription-translation feedback loop. The 2 core genes are *Clock* and *Bmal1* which encode the transcription factors CLOCK (circadian locomotor output cycles Kaput) (Vitaterna et al., 1994) and Bmal1 (Brain and muscle Aryl hydrocarbon receptor nuclear translocator-like protein (ARNTL)). These transcription factors heterodimerise and bind to E-box sequences, where they activate the transcription of *Period* and *Cryptochrome* genes. See **Figure 1.4**. Alternatively CLOCK homologues, such as NPAS2 bind to Bmal1 to perform the same function (Debruyne et al., 2006; Asher & Schibler, 2006). In turn, the Period (Per) and Cryptochrome (Cry) proteins form oligomers which translocate to the nucleus where they inhibit CLOCK:Bmal1 induced transcription (Froy, Chang, & Reppert, 2002; Reppert & Weaver, 2002). All of the clock genes undergo 24 hour oscillations in mammals with the exception of CLOCK (Dunlap, 1999).

Bmal1 is also negatively regulated by reverse erythroblastosis virus  $\alpha$  (REV-ERB $\alpha$ ) (Preitner et al., 2002) and positively regulated by retinoic acid receptor-related orphan receptors (ROR $\alpha$  and ROR $\gamma$ ) via ROR response elements (Sato et al., 2004). See **Figure 1.4**. The function of the circadian clock depends on Bmal1 to maintain normal oscillations. Unlike other core components that exist in paralog pairs (e.g. Per1 & Per2), Bmal1 knockdown also affects its paralog, Bmal2, so the ablation of Bmal1 alone serves to disrupt the circadian clock (Shi et al., 2010). CLOCK can be functionally replaced by Npas2 but not in the periphery (DeBruyne, Weaver, & Reppert, 2007). In 2000, Bunger et al. demonstrated that Bmal1<sup>-/-</sup> mice lack circadian rhythms.

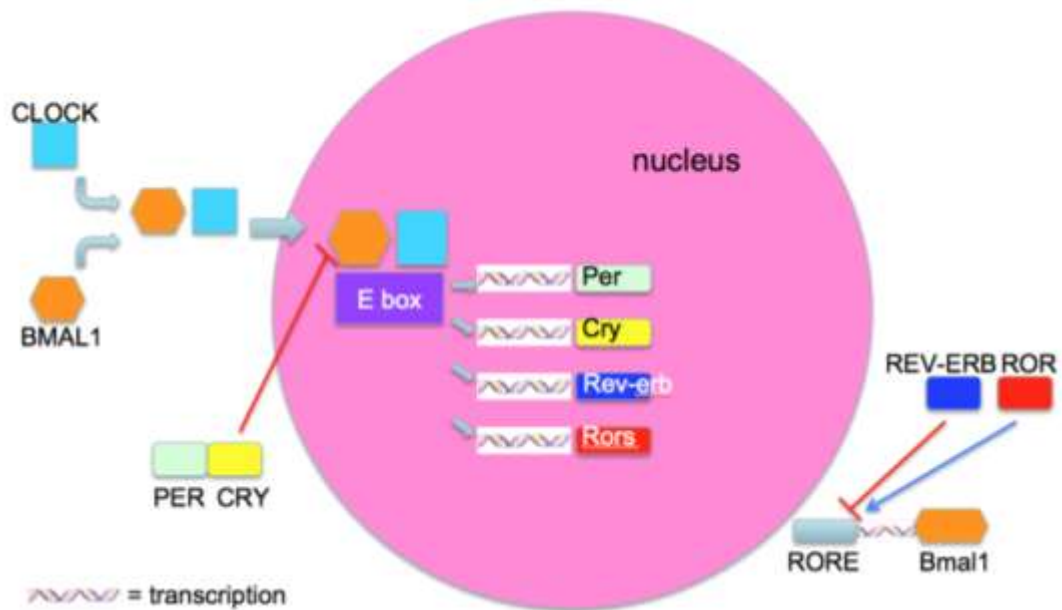


**Figure 1.4 Core circadian genes** after (Froy, 2011)

The oscillations of core circadian genes are regulated via a double negative feedback loop; the CLOCK:BMAL1 heterodimer activates the transcription of Period and Cryptochrome proteins which in turn inhibit their own transcription. Rev-erb and Rors negatively feedback onto their transcription via a similar mechanism.

### 1.3. Circadian clocks and the skin

The core circadian genes have been shown to be expressed in several types of mouse skin (dorsal, flank, vibrissa) oscillating in a circadian manner under both light/dark and dark/dark conditions in both keratinocytes and fibroblasts. This rhythmicity is under the control of the central clock in the SCN; external light has no impact on the expression levels of the core circadian proteins (Bjarnason et al., 2001; Tanioka et al., 2009).

The clock proteins have also been shown to be expressed in primary skin cells and fibroblast cell lines (W. Brown, 1991; Balsalobre, ADamiola & Schibler, 1998; Kazuhiro Yagita & Okamura, 2000; Zanello, Jackson, & Holick, 2000; K Yagita et al., 2001; Nagoshi, Saini, Bauer, Laroche, Naef, Schibler, et al., 2004; Nagoshi, Brown, Dibner, Kornmann, & Schibler, 2005; S. A. Brown et al., 2005; Menger et al., 2007). In immortalised fibroblast cell lines the clock has been shown to be out of phase in

neighbouring cells but synchronization can be achieved by the addition of the glucocorticoid agonist dexamethasone (Ripperger & Schibler 2001, Balsalobre et al. 2000) . Synchronization can also be induced by stimulation of the cells with glucose (Hirota et al., 2002); high serum treatment (Balsalobre, ADamiola & Schibler, 1998; Nagoshi et al., 2005; Osland et al., 2011); forskolin (K Yagita & Okamura, 2000); prostaglandin E (Tsuchiya, Minami, Kadotani, & Nishida, 2005) even merely changing the culture medium has been said to induce some synchronicity of clock protein expression (Yamazaki, 2000). The same peripheral clock also exists in human skin (Bjarnason et al., 2001; Sandu et al., 2012) however, the outputs are at the opposite phases as mice are nocturnal (W. Brown, 1991).

Bmal1 has been shown to be of key importance in the circadian regulation of cell proliferation in skin; In a Bmal1 homozygous knockout mouse, there was shown to be constantly elevated epidermal cell proliferation. This was demonstrated to be specific to Bmal1 intrinsic to keratinocytes via the creation of a keratinocyte-only Bmal1 selective deletion model which proved that Bmal1 is fundamental for the “time-of-day dependant” proliferation of keratinocytes during cell division in the epidermis (Geyfman et al., 2012). The same authors also demonstrated that the sensitivity to UVB induced DNA damage is highest late at night in mice during the maximal S phase (i.e. when it would be dark). This is the opposite in humans – S phase in the epidermis being in the afternoon and possibly explains the susceptibility of humans to skin cancers (Gaddameedhi, Selby, Kaufmann, Smart, & Sancar, 2011a; Geyfman et al., 2012).

Janich et al (2011) used a Bmal1<sup>-/-</sup> mouse model to investigate the effects of the circadian clock on the skin. They found that these mice had reduced levels of epidermal differentiation genes resulting in the reduced activation of basal inter-follicular

epidermal cells and consequently inefficient epidermal self-renewal and concomitant accumulation of terminally differentiated corneal cells at 5 months old.

## **1.4. Wound Healing**

Normal wound healing is a process involving four distinct but overlapping phases (See Figure 1.4); initially there is haemostasis; damage to cells in the wound results in the up regulation of stress signal pathways which is induced by the phosphorylation cascade of signalling molecules. (Kobayashi, Aiba, Yoshino, & Tagami, 2003) This results in changes to cell survival, metabolism and gene expression. Damaged cells leak endogenous molecules, such as damage-associated molecular pattern molecules. (Bianchi, 2007)

The first response to injury is clotting; platelets are activated and aggregate to form an insoluble fibrin clot. This arrests the bleeding and also provides a temporary matrix for the regrowth of the wound bed. Growth factors attach to the clot and cells migrate through it to initiate the healing process. (Nurden, Nurden, Sanchez, Andia, & Anitua, 2008) The platelets and serum in the clotted blood also release growth factors to enhance the healing process. (Bahou & Gnatenko, 2004)

There is subsequently an inflammatory phase where there is an influx of neutrophils to remove bacteria and damaged tissue via phagocytosis. Mechanical signals caused by the wound and electrical signals resulting from disrupted membranes may also be cues to induce healing (Nuccitelli, Nuccitelli, Ramlatchan, Sanger, & Smith; Kippenberger et al., 2000). Toll-like receptors on the surface of macrophages recognize any invading pathogens and evoke an inflammatory response (Shaykhiev, Behr, & Bals, 2008). Damaged blood vessels leak leucocytes (predominantly neutrophils) into the wound and immune cells within the wound are activated (Noli & Miolo, 2001).

Growth factor signals then attract more neutrophils and macrophages to the wound site. The inflammatory cells kill micro-organisms and clear up cellular debris (Dovi, Szpaderska, & DiPietro, 2004; M.-H. Kim et al., 2008). The nitric oxide and reactive oxygen species that they generate help to exert an effect on wound repair, but must be cleared by catalytic enzymes to prevent tissue damage (Schäfer & Werner, 2008). The inflammatory cytokines also help to regulate angiogenesis. Angiogenesis is the sprouting of wound edge capillaries into the wound bed where they form a microvasculature within the granulation tissue to permit the delivery of nutrients and oxygen (Tonnesen, Feng, & Clark, 2000).

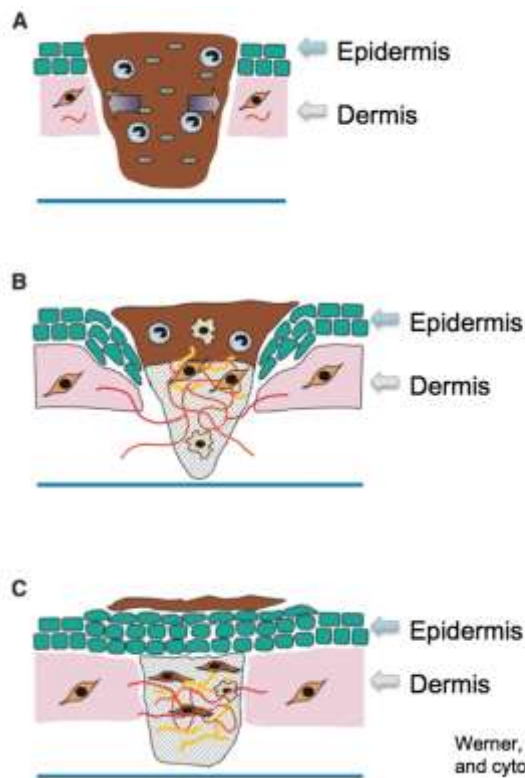
The dermis is repaired via formation of granulation tissue secondary to invasion of fibroblasts which secrete a collagen matrix (Hinz, 2007). These fibroblasts are derived from the wound edge, fibrocytes in circulation and bone marrow progenitor cells (Abe et al., 1998). Some of the fibroblasts become contractile myofibroblasts expressing  $\alpha$ -smooth muscle actin. Their contractile action helps to draw the edges of the wound together and help to align the collagen fibre in the scar tissue (Hinz, 2007).

The epidermis is repaired via re-epithelialisation; keratinocytes migrate to close the wound which requires them to alter their adhesion state so that they can move from the basement membrane through the clot (Nguyen, Gil, & Carter, 2000; Iliina & Friedl, 2009). They migrate using lamellipodia made largely from actin (Mitchison & Cramer, 1996). Additionally, epidermal and follicular stem cells are recruited to form a new epidermal layer (Fuchs, 2008). This requires partial digestion of the clot by matrix metalloproteinases to permit the cells to migrate between the scab and the healthy underlying tissue (Pilcher et al., 1999). The final stage of wound healing is called resolution; the barrier function of the skin is repaired and the skin regains its typical

appearance to a greater or lesser extent depending on the amount of scarring. Once the keratinocytes close the wound they must cease to migrate and proliferate and instead re-stratify. Additionally the microvasculature in the scar matures and the extra-cellular matrix is remodelled and the myofibroblasts undergo apoptosis (Ulrich et al., 2007; Hinz, 2007).

Neutrophils leave the site of the wound via apoptosis or by migrating back to the circulation (Haslett, 1992; Mathias et al., 2006) and macrophages are de-activated, the inflammatory markers are taken up by non-functional receptors on inflammatory cells (D'Amico et al., 2000). Anti-inflammatory molecule production is the final step to dampen down the inflammatory response (Schwab, Chiang, Arita, & Serhan, 2007; Perretti & Gavins, 2012).

Problems that can occur in the resolution phase are that the inflammation can persist or that the keratinocytes over-proliferate, leading to keloid scar formation (Wynn, 2008).



## Phases of wound healing

### A (minutes)

- Haemostasis occurs immediately after the injury

### B (in the first 24 hours)

- Inflammation follows
- granulation tissue forms
- fibroblasts and keratinocytes migrate to the wound site

### C (days – years)

- Remodelling

Werner, S., & Grose, R. (2003). Regulation of wound healing by growth factors and cytokines. *Physiological reviews*, 83(3), 835-70.

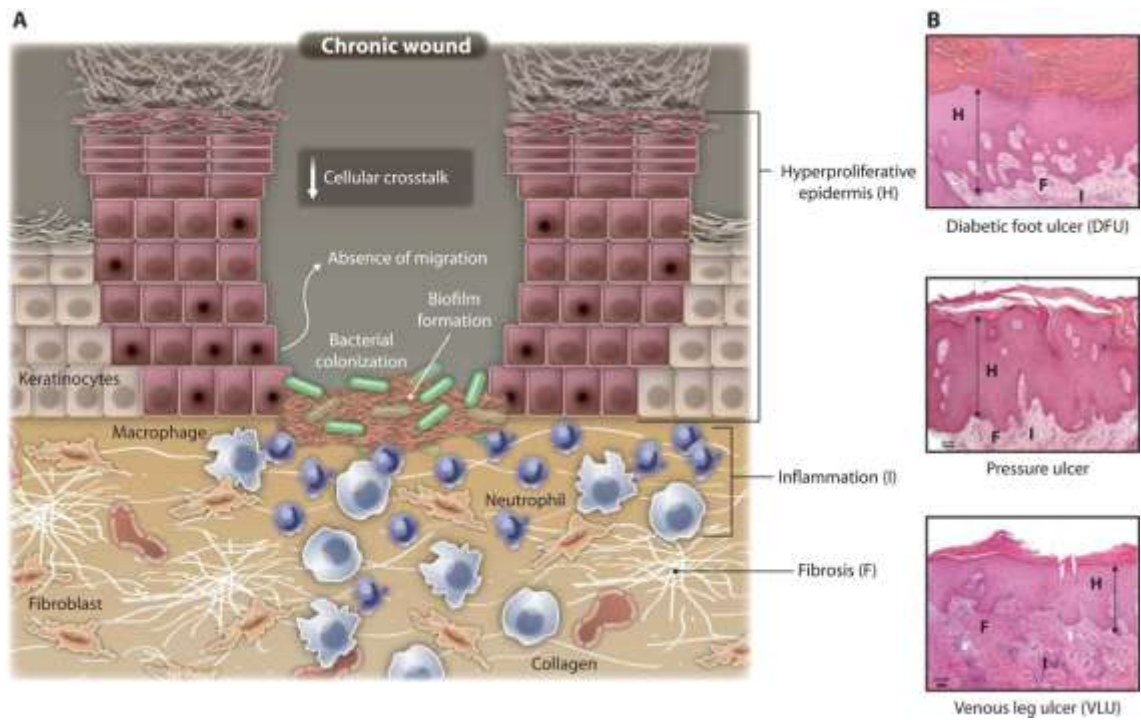
(Werner & Grose, 2003)

### Figure 1.5 Phases of wound healing

In normal wound healing there are distinct but overlapping phases. Haemostasis is the first phase, mediated via the activation and aggregation of platelets to form a clot. This is followed by an inflammatory phase; immune cells clear any infection and damaged tissue. Concurrently the wound is resolved via the migration of skin cells to the wound site and the production of granulation tissue. Remodelling of the scar tissue occurs over subsequent days – years.

## 1.5. Chronic wounds

Chronic wounds are those that are characterised by a prolonged healing time, failure to heal or recurrence of the wound. One factor in the aetiology of chronic wounds is an excessive inflammatory response, resulting in excessive secretion of matrix metalloproteinase by neutrophils, causing degradation of the connective tissue underlying the wound. Additionally these hard-to-heal wounds often have a large quantity of reactive oxygen species present that also leads to tissue damage and hinders the healing process See Figure 1.6.(Diegelmann & Evans, 2004).



(Eming, Krieg, & Davidson, 2007)

### Figure 1.6 Chronic wound causes

A major cause of chronic wounds is an excessive inflammatory response which degrades the underlying connective tissue. Coupled with an absence of cell migration the healing process is hindered and the failure to resolve the wound increases the risk of recurrent infection.

Chronic wounds are a common problem, causing poor quality of life and morbidity. The five year mortality rate for patients with diabetic or ischaemic ulcers is higher than that of prostate or breast cancer patients (Armstrong, Wrobel, & Robbins, 2007) although arguably this could be a reflection of the severity of their diabetes, not a direct effect of the ulcers per se. The financial costs of treating chronic wounds are estimated at being in excess of 1 billion pounds a year in the UK (P Kranke, Mh, M, Schnabel, & Se, 2012). The most common types of chronic wound in the West are diabetic or vascular ulcers, pressure sores and those secondary to oncological radiation therapy (P Kranke et al., 2012). Given the increasingly ageing population and the rising prevalence of diabetes it is likely that the extent of this problem will continue to worsen. Currently an effective therapeutic solution for chronic wounds is lacking. In recent years several studies have attempted to harness the effects of recombinant growth factors, delivered locally (Barrientos, Brem, Stojadinovic, & Tomic-Canic, 2014). For example, a study

using recombinant human granulocyte macrophage colony stimulating factor had some encouraging results, albeit in a small sample size (50% of the treated ulcers healed over 6 months) (Da Costa, Jesus, Aniceto, & Mendes, 1999). Another study used platelet derived growth factor applied topically as a gel; they saw a 39% increase in complete healing of ulcers with a median size of 1.5 cm<sup>2</sup> (Smiell et al., 1999). Vascular endothelial growth factor 1 has used in a phase I clinical trial to ameliorate wound healing in chronic neuropathic diabetic wounds (Hanft et al., 2008). Although these studies are encouraging, the consensus on these treatments so far is that more extensive testing is required (Rennert et al., 2013; Barrientos et al., 2014).

## **1.6. Project background**

Studies have shown an interesting effect of ‘switching off’ the circadian clock on the migration of zebrafish fibroblasts. In zebrafish the fibroblasts are not normally seen to migrate, but when their circadian clock was knocked down they spontaneously started to migrate. In mammalian fibroblasts that were stably knocked down with shRNA against CLOCK, a core circadian gene, an increased rate of migration was observed in comparison to controls (Becker/Whitmore labs, unpublished data). These findings indicated that ‘stopping’ the circadian clock within the wound area might have a beneficial effect in wound healing. It was proposed that the use of RNAi to transiently stop the clock might reduce the risks of off-target effects. The Becker lab had already had success in developing an antisense oligodeoxynucleotides (asODNs) targeted to knock down connexin 43; therefore this work follows on from a pilot study in the use of asODNs to knock down Bmal1 and in silico expansion of the asODN sequences to optimise their efficacy.

## **1.7.Hypothesis**

Transient knockdown of key circadian clock regulating genes can accelerate wound healing in mammalian cells and is a potential target for therapeutic use.

## **1.8.Thesis aims**

This study aims to discover whether manipulation of the circadian clock, by various means, has beneficial effects on wound healing.

The main aims were:

- 1) Optimisation of asODNs by continuing *in vivo* experiments and by *in silico* expansion of the sequences to ensure a more biologically stable asODN
- 2) Development of a tool to knockdown Bmal1 in order to disrupt the circadian clock.
- 3) Measuring the functional effects of knocking down Bmal1 wound healing *in vitro*.

## 2. Materials and Methods

---

## **2.1. Cell Culture**

### **2.1.1. Cell maintenance**

All experiments (unless stated otherwise) were done using NIH 3T3 cells which are a murine fibroblast cell line generated in 1962 from Swiss mouse embryos and have become a standard fibroblast cell line. 3T3 refers to the manner in which they were immortalised; “3-day transfer, inoculum  $3 \times 10^5$  cells”(Todaro & Green, 1963). The cells were maintained in Dulbecco’s Modified Eagle Medium (DMEM) with added GlutaMAX™, supplemented with 10% Donor Bovine Serum (DBS) and penicillin-streptomycin at 100 U/ml (all Life Technologies Ltd.) at 37 °C with 5% CO<sub>2</sub> in a humidified incubator. Cells were grown in T175 flasks (Nunclon Easyfilter), unless otherwise stated, until near confluence and then split as required. They were split by aspirating the culture medium, rinsing with sterile PBS and incubation with 6 ml Trypsin-EDTA (Life Technologies Ltd.) until all had detached. The trypsin was then inactivated by the addition of 6 ml of growth medium and transferred to fresh flask(s) containing pre-warmed growth medium.

### **Cell storage**

Stocks were frozen down in growth medium supplemented with 10% DMSO (Sigma-Aldrich Company Ltd.) in cryovials and stored at -80°C until needed.

### **Cell counting**

Where required cells were counted in the following way: They were removed from the flasks by trypsinisation and inactivation as described above. 10 µl of the concentrated cells solution was mixed with 10µl Trypan Blue (Life Technologies Ltd.) and added to a haemocytometer (Bright Line, Sigma-Aldrich Ltd.). Any dead cells stain blue. Cells were counted in each large quadrant and an average was taken. This number was

multiplied by 2 to account for the dilution with Trypan Blue and 10,000 to give the number of cells per millilitre.

## **2.2. Molecular Biology**

### **2.2.1. Western Blotting**

#### **Protein extraction**

Cells were grown and treated in 6-well plates. They were harvested by aspiration of culture medium and rinsing and aspiration with sterile PBS. RIPA buffer containing freshly dissolved PhosStop and cOmplete Protease Inhibitor Cocktail Tablets (1 of each per 10ml of buffer) was added directly to the wells (typically 100  $\mu$ l) over ice and incubated for 2 minutes. The cells were scraped from the dishes and the lysate was transferred to 1.5 ml Eppendorf tubes. The lysate was centrifuged for 15 minutes at full speed in a bench-top Eppendorf micro-centrifuge to aggregate the DNA so that it could be removed from the lysate. Protein concentration was determined using the Pierce™ BCA Protein Assay Kit (Life Technologies Ltd). This is a colorimetric assay that enables accurate quantification of the protein concentration by using protein standards to generate a standard curve. Typically the protein samples were diluted 1:5 in RIPA buffer so this was factored into the calculations.

#### **SDS-PAGE**

Prior to SDS-PAGE the protein samples were all diluted with RIPA buffer to the same concentration, typically 1 $\mu$ g/ $\mu$ l in a volume of 30  $\mu$ l. Thereafter 10 $\mu$ l of 4x NuPAGE LDS sample buffer (Life Technologies Ltd.) containing 20%  $\beta$ -mercaptoethanol was added to the protein samples and they were heated at 95°C for 5 minutes to denature the proteins. Then they were transferred to ice and briefly centrifuged to reincorporate any condensation.

30 µl of each sample was loaded into each lane in a 12% acrylamide gel (12% Mini-PROTEAN® TGX™ Precast Gel, Bio-Rad Ltd.). Precision Plus Protein™ standard (Bio-Rad Ltd.) was loaded into at least one lane. The gels were inserted into a mini-Protean Tetra system (Bio-Rad Ltd.) and electrophoresed at 70 V for 10 minutes and thereafter at 100 V for 70 minutes under 1X Tris-Bis running buffer (Bio-Rad Ltd.)

The gels were blotted onto nitrocellulose membranes (Bio-Rad Ltd.) using the mini-Protean Tetra blotting unit with 1X transfer buffer containing 20% methanol. The lanes were removed from the gels which were then sandwiched between the nitrocellulose membrane, blotting paper and transfer sponges which had been pre-soaked in transfer buffer (all Bio-Rad Ltd.). The gels were blotted for 60 minutes at 100 V.

The membranes were incubated with Ponceau (Sigma-Aldrich Ltd.) to ensure even blotting prior to being incubated on a shaker with blocking solution (5% non-fat milk in TBS) for an hour at room temperature. Then the primary antibodies were added at the following concentrations (Table 1) overnight at 4°C on a shaker, followed by 3 x 5 minute washing prior to incubation in the appropriate secondary antibody (Table 2) for 60 mins at room temperature.

**Table 2.1 Primary antibodies used in Western blotting**

Primary antibody	Catalogue code	Manufacturer	Raised in	Concentration of use
Bmal1	H170	Santa Cruz	Rabbit	1:400
GAPDH	G9545	Sigma	Rabbit	1:4000
β-actin	Ab8227	Abcam	Rabbit	1:4000
α-tubulin	13090310	AbD Serotec	Rat	1:2500
Cyclophilin A	Ab41684	Abcam	Rabbit	1:4000

**Table 2.2 Secondary antibodies used in Western blotting**

Secondary antibody	Catalogue code	Manufacturer	Raised in	Concentration
Anti-rabbit HRP conjugated	A0545	Sigma	Goat	1:4000
Anti-rat HRP conjugated	AP136P	Calbiochem (now Chemicon)	Goat	1:4000

**Table 2.3 Buffers and reagents used for SDS-PAGE**

Running buffer for separation of proteins via electrophoresis	Tris/Glycine/Sodium Dodecyl Sulphate (SDS)	25 mM Tris 192 mM Glycine 0.1 % w/v SDS pH 8.3
Transfer buffer for blotting the proteins onto the membranes	Tris/Glycine	2 5mM Tris 192 mM Glycine 20 % methanol pH 8.3
Buffer for washing the blots	Tris Buffered Saline-Tween 20 (TBS-T)	20 mM Tris 500 mM NaCl pH 7.5 Tween 20 0.1%
Blocking solution	10 % non-fat powdered milk (Bio-Rad) in TBS-T	

All components were purchased from Bio-Rad or Sigma-Aldrich

The membranes were washed at least 3 times over 30 minutes on a shaker to remove background signal then they were incubated with Pierce Enhanced Chemiluminescence

Western Blotting Substrate for 2 minutes prior to being imaged on a Chemi-Doc MP imaging system (Bio-Rad).

### **2.2.2. RT-PCR**

#### **RNA isolation**

Cells for RT-PCR were grown in 6 well plates. RNA was isolated using the Qiagen RNeasy Plus kit. 350µl of RLT buffer was used to lyse the cells. The lysate was transferred to QiaShredder tubes and centrifuged for 2 minutes at full speed to homogenise the lysate and shear the DNA. The lysate was transferred to gDNA spin columns and centrifuged at full speed for 1 minute to remove genomic DNA. This lysate was mixed with an equal volume of 70% ethanol and added to an RNeasy column and centrifuged for 30 seconds. Columns were washed with RW buffer (350 µl), then RPE buffer (500µl) and centrifuged for 30 seconds each. Then 500µl RPE buffer was added and the spin columns were centrifuged for 2 minutes. At each step the flow-through was discarded and the columns were transferred to clean 2ml collection tubes. The spin columns were then centrifuged for 2 minutes with open lids to enable the membranes to dry and any residual ethanol to evaporate. Thereafter 30µl of RNase and DNase free water was used to elute the RNA. The concentration and purity of the RNA was evaluated via a spectrophotometer (Nanodrop ND-1000). The minimum value for the 260/280 nm and 260/230 nm absorbance ratios accepted was 2. If the samples were not up to this standard they were concentrated and cleaned up using the MinElute kit (Qiagen).

#### **2.2.3. cDNA synthesis**

1µg of RNA was used for cDNA synthesis, diluted to a volume of 10 µl in RNase-free water in RNase and DNase-free 0.5 ml microcentrifuge tubes (Axygen). To this 3µl of Master mix 1 was added and the first part of the PCR programme was run. Meanwhile

Mastermix 2 was prepared on ice. 7uL of Mastermix 2 was added to each tube and the remainder of the programme was run.

Mastermix 1 (volumes per sample)

1uL each of Random Primers, Oligo dT and dNTP (all Life Technologies Ltd.)

Mastermix 2 (volumes per sample)

4 µl 5x first strand buffer

2 µl DTT

0.5 µl RNase out

0.5 µl Superscript II Reverse Transcriptase

(all components were from Life Technologies Ltd.)

Additionally one tube of cDNA was made without the Reverse Transcriptase as a control.

#### **PCR programme for cDNA synthesis**

Initial denaturing step            65°C for 5 minutes

Holding step                        10°C until recommenced (during addition of the 2<sup>nd</sup> mastermix)

25°C for 10 minutes

42°C for 1 hour

70°C for 15 minutes

#### **geNorm Assay**

The primers for normalisation were selected following a geNorm™ analysis of a panel of 12 housekeeping gene primer sets from Primer Design Ltd. This assay established the more stable housekeeping genes in this system. The best combination of genes was determined to be GAPDH and SDHA.

The assay required testing 5 untreated samples and 5 treated samples in triplicate for each gene and the QBase+™ software used a bespoke algorithm to establish which gene or combination of genes were the most stable under the conditions measured.

**Table 2.4 Primers for RTPCR**

	Official	gene	Accession	Anchor	Context length	sequence
species	symbol		number	Nucleotide	(bp)	
MOUSE	Arntl (Bmal 1)		NM_007489	926	98	
MOUSE	GAPDH		NM_008084.2	793	180	
MOUSE	SDHA		NM_023281.1	2018	181	

The cDNA was diluted 10 times for RTPCR. The mastermix for each gene was as follows:

Per well:

10 µl SYBR green (Sigma-Aldrich Ltd.)

1 µl primer (Primer Design Ltd.)

4 µl water

15 µl of this mastermix was added per well of a white 96-Well Skirted PCR Plate (Bio-Rad)

per sample in triplicate. 5 µl of diluted cDNA was added to each well in triplicate for each sample and mixed thoroughly. The plates were sealed with Microseal® 'B' Adhesive Seals, Optical, (Bio-Rad) and kept at 4°C as required. Just prior to running the RTPCR programme the plates were briefly centrifuged to ensure all of the mixture was incorporated.

Plates were run on a Bio-Rad CFX96 PCR detection system.

### **RT-PCR Programme**

The signal was amplified as follows:

1. 94°C for 2 mins
2. 94°C for 15 seconds
3. 60°C for 30 seconds
4. 72°C for 30 seconds
5. Plate read

Steps 2 to 5 were repeated 39 times then the melting curve was measured at 60°C to 90°C.

#### **2.2.4. RT-PCR Analysis**

The arithmetic mean and standard deviation of the CT values were determined to enable the possibility of erasing any outliers from the technical triplicates. Thereafter the standard  $\Delta\Delta\text{CT}$  method was used to calculate the relative fold expression of the gene of interest. The arithmetic mean of the housekeeping genes was subtracted from the arithmetic mean of the gene of interest to give the  $\Delta\text{CT}$  value. The highest  $\Delta\text{CT}$  value was then subtracted from each  $\Delta\text{CT}$  value to produce the  $\Delta\Delta\text{CT}$  values.

$$\text{Relative fold expression} = 2^{(-\Delta\Delta\text{CT})}$$

The Reverse Transcriptase control CT values were checked to ensure that there was no amplification of genomic DNA affecting the RNA expression analysis.

#### **2.2.5. Immunofluorescence**

Immunofluorescence was used to assess the transfection or transduction efficiency of several types of RNAi.

Cells were seeded at the same density as the requirement for each different protocol in Millicell© EZ slides with a surface area per well of 1.2 cm<sup>2</sup> (Merck Millipore) and transfected accordingly. 48 or 72 hours after transfection the cells were washed twice with PBS then fixed for 5 minutes with PFA at room temperature. Then the cells were permeabilised with PBS-Triton 0.1% (Sigma-Aldrich Ltd.) for 10 minutes at room temperature if antibody staining was required. Then the proteins were blocked with Universal Protein Blocking Reagent (Genetex, Inc.) diluted 1:100 in PBS-Triton 0.1% for 30 minutes at room temperature. Primary antibodies were incubated overnight on a shaker at 4°C diluted in blocking solution. After three five minute washes in PBS-Triton 0.1% on a shaker the cells were incubated with the secondary antibody for a hour at room temperature then washed three times with PBS-Triton 0.1% and Hoechst (Life Technologies Ltd.) was added as a nuclear stain for 5 minutes followed with a further

wash. The slides were mounted with Citifluor™ and the coverslips (22 x 50 mm, VWR) were sealed with clear nail varnish and allowed to dry prior to imaging.

Slides were imaged using a Leica fluorescence microscope. The same settings were used for each well. For transfection efficiency the number of cells as measured by nuclear staining were divided by the number of cells expressing the protein or fluorophore of interest and multiplied by 100 to give percentage efficiency.

Where the constructs I was introducing contained a fluorophore the protocol was as above but excluding the blocking and antibody steps.

**Table 2.5 Antibodies used for immunofluorescence**

		Catalogue code	Manufacturer	Raised in	Concentration
Primary antibody	Monoclonal anti-flag M2	F3165	Sigma	Mouse	1:200
Secondary antibody	Alexa Fluor™ 488 anti-mouse	A-11029	Life Technologies Ltd.	Goat	1:500

## 2.3. Transfection protocols

### 2.3.1. Fugene 6

For the majority of experiments Fugene 6 (Roche) was used according to the manufacturer's recommendations. The ratio of Fugene to DNA was optimised by transfecting fluorescent probes in a plasmid vector at ratios of 6:1, 4:1, 3:1 and 1.5:1. Cell density was also varied for each of these conditions and the optimal protocol was deemed to be at a cell density of 60-70% confluence with a ratio of Fugene to DNA of 4:1.

Cells were seeded to be 60% confluent the following day. Two hours prior to transfection the culture medium was replaced with warmed culture medium that did not contain antibiotics which can affect transfection. Transfection mixes were made by

adding Fugene 6 to OptiMEM™ (Life Technologies) at room temperature and swirling gently to mix. After five minutes incubation the DNA was added and flicked to mix. The transfection mix was left to incubate and form complexes for half an hour at room temperature. The transfection complexes were added to the cells drop wise and the plates were swirled gently to mix. Cells were assayed typically after 48 hours to assess the transfection efficiency.

### **2.3.2. Transduction**

Approval for performing genetic modification (GM) using lentiviral vectors was obtained from UCL GM Safety Officer following a risk assessment (see Appendix). 293 FT cells (Life Technologies Ltd.) were maintained in DMEM containing 10% FBS, penicillin-streptomycin at 100 U/ml and Geneticin at 500µg/ml (all Life Technologies Ltd.) at 37 °C with 5% CO<sup>2</sup> in a humidified incubator. Prior to transduction cells were seeded in DMEM containing 10% FBS, penicillin-streptomycin (P-S) at 100 U/ml and 25 mM 4-(2-hydroxyethyl)-1-piperazineethanesulfonic acid (HEPES) buffer. The buffer protects the viability of the viral particles; 293FT cells are fast-growing and can cause the culture medium to become too acidic otherwise. Second generation viral particles were generated by transfecting 293FT cells with the following plasmids:

pCMV-dR8.2, pCMV-VSV-G and transfer plasmids psi-LVRU6MP containing four different shRNA clones targeted against murine Bmal1 and one scrambled shRNA control.

6 - 24 hours later the culture medium was changed. 48 and 72 hours thereafter the virus-containing supernatant was harvested and filtered through a .45 µM syringe-driven filter to remove any cell debris.

3<sup>rd</sup> generation viral particles were generated using the Lenti-Pac™ system from Genecopoeia. 2 days prior to transfection 293FT cells were seeded at  $1.4 \times 10^6$  cells per 10cm dish. On the day of transfection complexes were made as following:

2.5 µg transfer plasmid containing the shRNA knockdown constructs +5 µL of Lenti-Pac™ were diluted in 200 µL OptiMEM (Life Technologies).

15 µL Endofectin (Genecopoeia) was diluted in 200 µL OptiMEM (Life Technologies). The diluted Endofectin was added to the DNA mix drop-wise whilst gently vortexing. Complexes were incubated at room temperature for 15 minutes before transfection. 14 hours later the culture medium was replaced with 10 mL fresh culture medium containing 20 µL TitreBoost™ (Genecopoeia). 48 hours post-transfection the supernatant was harvested, centrifuged at 500 x g for 5 minutes and then filtered through a 0.45 µm polyethersulfone (PES) membrane to remove any cell debris.

Viral supernatant was concentrated by adding 4 volumes of PEG-it™ polyethylene glycol solution to the viral supernatant, mixing thoroughly by inversion and refrigeration for at least 24 hours. The 'pegged' viral solution was then centrifuged at 4°C for 30 minutes at 1500 x g. The pellet was resuspended in HEPES buffered DMEM (as above) at a 10 -100 times concentration with comparison to the neat viral supernatant. Viral titre was established using a Alliance HIV-1 P24 antigen ELISA Kit. NIH 3T3 cells were transduced with the concentrated virus solution at concentrations of 0.1 viral particles to 1000 viral particles per fibroblast in the presence of 8mg/ml polybrene or DEAE-Dextran (both Sigma). 48 hours following transduction the cells were either assayed for signs of the expression of a fluorescent marker (mCherry) or resistance to puromycin via the addition of DMEM containing 10% FBS, 10,000IU P-S and 2 µg/ml puromycin.

pCMV-dR8.2 dvpr was a gift from Bob Weinberg (Addgene plasmid # 8455)

pCMV-VSV-G was a gift from Bob Weinberg (Addgene plasmid # 8454)

## **2.4. Scratch Wound Assay**

A scratch wound assay is a standard in vitro experiment to assess cell migration into an artificially created 'wound' as a proxy for wound healing (Liang, Park, & Guan, 2007). Cells were seeded in 96 well Image Lock Essenbio plates (EssenBio, U.K.) and uniform horizontal scratches were made with the 'Wound-maker'(EssenBio). The wells were gently washed twice to with sterile PBS to remove any loose cells and warm culture medium was replaced. The plates were imaged in an INCUCYTE™ imager within a humidified cell culture incubator at 37°C and 5% CO<sup>2</sup> and imaged approximately every hour for 3 days. The cell migration rate was analysed using a plugin for ImageJ written by Mr Daniel Ciantar of the UCL Confocal Unit. In brief, the images from the same well were stacked and the average pixel distance of the 'wound edge' was measured across the whole image to provide a pixels/hour migration rate.

## 2.5. In vivo assays

6 week old ICR mice were maintained according to UK Home Office regulations. The mice were induced with 4% isoflurane and buprenorphine was administered subcutaneously for analgesia. The dorsal area was shaved and the skin cleaned with 70% ethanol. Four 6mm full thickness wounds were made using a biopsy punch. See **Figure 2.1**. Antisense or DNzyme sequences were applied in 30% pluronic gel at 100mM. Each mouse was treated with one vehicle-only control and three different sequences in the other wounds. Three days later the mice were humanely sacrificed and the tissue was harvested and fixed in 4% paraformaldehyde at 4°C for a minimum of 24 hours. Then the tissue was bisected and half was sent to be paraffin embedded, sectioned and stained with haematoxylin and eosin (H & E) at UCL IQpath (Institute of Neurology, UCL) to facilitate histological analysis of the extent of re-epithelialisation.

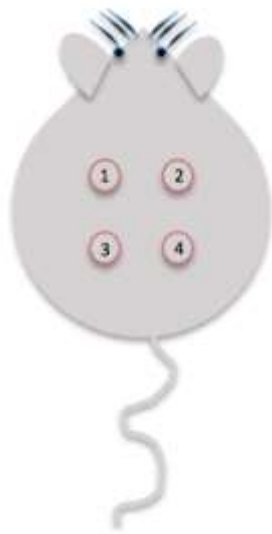


**Figure 2.1 Mouse wound model**

Four 6 mm full thickness wounds were made in the dorsal skin of the mice, using a punch biopsy. The numbering relates to the positions of the treatments.

### **2.5.1. Analysis of in vivo wound healing**

Macroscopic images were taken of all wounds using a dissection microscope (Leica MZFLIII) at a fixed magnification of 1.25x fitted with a Leica DFC310FX camera. The change in macroscopic wound area after 3 days was measured using ImageJ (NIH). H & E stained slides were imaged using a DM2500 Leica bright-field microscope at a magnification of 20X. The images were exported as TIFFS. The distance of re-epithelialisation was measured by tracing the distance from the wound edge to the end of the outgrowth of the keratinocyte layer on each side of the wound and analysed using ImageJ.

The first experiment analysed by the author was undertaken by other lab members prior to the start of the PhD project. Some of the treatments used in the first experiment were DNAzymes. One observation from the macroscopic analysis of the data was that the DNAzyme equivalent of an antisense treatment also tested at that time appeared to be more effective at reducing the macroscopic area of the wound. (For example Bmal 750 antisense is the same as Bmal 23 but without the catalytic loop). Therefore for the second experiment this was tested by making some antisense sequences from DNAzymes and vice versa.

## **2.6. In silico**

The original 16 mer antisense sequences were designed using the principles set out by Law et al (Law, Zhang, & Stott, 2006) by Dr Peter Cormie (unpublished data, Becker/Whitmore labs). Further to extensive *in vivo* testing not yielding any positive effects from these sequences it was hypothesised that one reason for this might be due to the relative shortness of the sequences rendering them sensitive to rapid clearing by endogenous nucleases. Previous studies in the lab have shown that 30 mer

oligonucleotides are more resilient to catalysis. The original anti-Bma1 sense sequences were used as a template.

Up to 29 bases of the Bma1 sense code were added to the beginning or the end of the template sequences in this way:

ttagaatatgcagaacacca**ggaaggatcaagaatg**caagggaggcccacagtcagatt

ggaaggatcaagaatgcaagggaggcccac  
aggaaggatcaagaatgcaagggaggccca  
aaggaaggatcaagaatgcaagggaggccc  
caaggaaggatcaagaatgcaagggaggcc  
ccaaggaaggatcaagaatgcaagggaggc  
accaaggaaggatcaagaatgcaagggagg  
caccaaggaaggatcaagaatgcaagggag  
acaccaaggaaggatcaagaatgcaagggga  
aacaccaaggaaggatcaagaatgcaaggg  
gaaccaaggaaggatcaagaatgcaagg  
agaaccaaggaaggatcaagaatgcaag  
cagaaccaaggaaggatcaagaatgcaa  
gcagaaccaaggaaggatcaagaatgca  
tgagaaccaaggaaggatcaagaatgc  
atgcagaaccaaggaaggatcaagaatg

722

catggaaggttagaatatgcagaacacca**ggaaggatcaagaatg**caagggaggcccacagtcagattgaaaaga  
**aggaaggatcaagaatg**caagggaggccca**cagtcagattgaaaag**aggcgtcgggacaaaatgaacagtttcatt

atggaaggttagaatatgcagaacaccaag  
tggaaggttagaatatgcagaacaccaagg  
ggaaggttagaatatgcagaacaccaagga  
gaaggttagaatatgcagaacaccaaggaa  
aaggttagaatatgcagaacaccaaggaa  
aggttagaatatgcagaacaccaaggaa  
ggttagaatatgcagaacaccaaggaa  
gttagaatatgcagaacaccaaggaa  
ttagaatatgcagaacaccaaggaa  
tagaatatgcagaacaccaaggaa  
agaatatgcagaacaccaaggaa  
gaatatgcagaacaccaaggaa  
aatatgcagaacaccaaggaa  
atatgcagaacaccaaggaa  
tatgcagaacaccaaggaa  
atgcagaacaccaaggaa  
tgagaaccaaggaa  
gcagaaccaaggaa  
cagaaccaaggaa  
agaaccaaggaa  
gaaccaaggaa  
aacaccaaggaa

**a**ac**ca**agg**a**aggatcaagaatg**ca**agg**ga**  
**c**ac**ca**agg**a**aggatcaagaatg**ca**agg**gag**  
**a**cc**aa**gg**a**aggatcaagaatg**ca**agg**gagg**  
**cc**aagg**a**aggatcaagaatg**ca**agg**gaggc**  
**ca**agg**a**aggatcaagaatg**ca**agg**gaggcc**  
**aa**gg**a**aggatcaagaatg**ca**agg**gaggccc**  
**ag**g**a**aggatcaagaatg**ca**agg**gaggccca**  
**g**g**a**aggatcaagaatg**ca**agg**gaggcccac**  
**ga**aggatcaagaatg**ca**agg**gaggcccaca**  
**aa**ggatcaagaatg**ca**agg**gaggcccacag**  
**ag**gatcaagaatg**ca**agg**gaggcccacagt**  
**gg**atcaagaatg**ca**agg**gaggcccacagtc**  
**ga**tcaagaatg**ca**agg**gaggcccacagtc**  
**at**caagaatg**ca**agg**gaggcccacagtcag**  
**tc**aagaatg**ca**agg**gaggcccacagtcaga**  
**ca**agaatg**ca**agg**gaggcccacagtcagat**  
**aa**gaatg**ca**agg**gaggcccacagtcagatt**  
**ag**aatg**ca**agg**gaggcccacagtcagattg**  
**ga**atg**ca**agg**gaggcccacagtcagattga**  
**aa**tg**ca**agg**gaggcccacagtcagattgaa**  
**at**g**ca**agg**gaggcccacagtcagattgaaa**  
**tg**caagg**gaggcccacagtcagattgaaaa**  
**g**caagg**gaggcccacagtcagattgaaaag**

The emboldened letters above represent the reverse complement of the antisense sequence (i.e. the sense sequence). Initially this was kept intact and a total of 14 bases were added, shifting the template one base at a time. Then this was expanded further so that as little as one base from the original sequence was included in the potential 30 mer. Thereafter several exclusion rules whittled down the number of candidates. These rules are as follows:

1. The sense sequence must not begin with ‘a’ (as the antisense should not end in ‘t’)
2. CpG (i.e. c adjacent to g 5’ – 3’) could not be included as these are not found in an unmethylated form in mammalian cells and can trigger an immune response(Becker, Lin, & Green, 1999).

3. No sequence should contain more than one G triplet or any G quartet as these can fold into secondary structures or form G quadruplexes via hydrogen bonding.
4. For a similar reason the sense sequence must not have more than three Cs or Gs in the first 5 bases.

Once these rules were applied the resulting possible candidates (see example below) were copied into Microsoft Excel and the reverse complement was generated using ApE (A plasmid Editor) v. 2.0.45 (Davis, n.d.).

Subsequently these reverse complement antisense sequences were run through the Sigma Genosys DNA calculator (Sigma, n.d.) to generate the melting temperature, GC content, prediction of likelihood of forming a secondary structure or primer dimer.

Sequences were eliminated if the melting temperature was lower than 37°C or if the GC content was lower than 40% or higher than 65% or if there was a prediction of primer dimer formation or a secondary structure classified as being stronger than 'weak'.

The remaining candidate sequences were screened for sequence homology with other genes. Any sequences with at least 3 mismatches for other genes were included at this point. This was checked using FASTA (Pearson, n.d.; Pearson & Lipman, 1988). Thereafter the remaining candidates were also checked for homology with human Bmal1 and other genes as the ultimate goal would be to produce an antisense that would be effective in aiding human wound healing.

### 3. Preliminary *in vivo* experiments

---

## **3.1.Introduction**

### **3.1.1. Background**

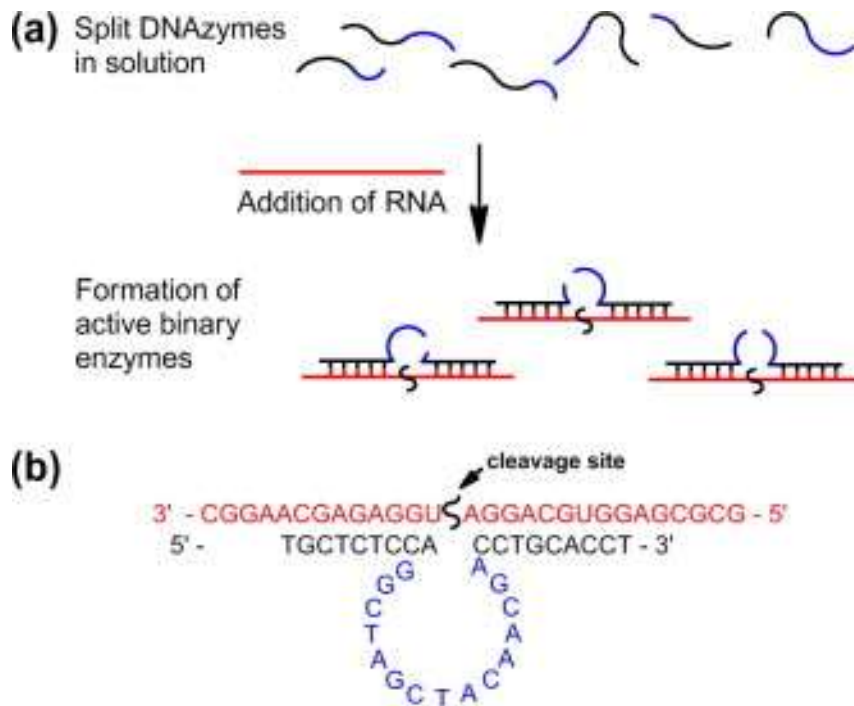
The original basis for this project was an observation made by a previous post-doctoral fellow that zebrafish fibroblasts lacking a functional circadian clock migrate in culture whereas, normally, these cells do not migrate (personal communication, Dr Peter Cormie, unpublished observations). Work in the Becker laboratory has for some time focused on wound healing and the manipulation of connexin expression in the skin via antisense oligodeoxynucleotides (asODNs)(Qiu et al., 2003; Mendoza-Naranjo et al., 2012). These observations lead to the idea that transiently disrupting the circadian clock might lead to increased cell migration in skin wounds and could be used therapeutically to ameliorate the healing of chronic wounds. This chapter describes the preliminary findings of *in vivo* studies undertaken to provide a proof-of-concept data. With exception to the first *in vivo* experiment (figure 3.3) all of the following work was done by the author including the analysis of the first experiment.

### **3.1.2. Transiently disrupting the circadian clock**

As described in Chapter 1, the core genes controlling the circadian clock are *Bmal1* and *CLOCK*. Dr Cormie designed 16 mer asODNs targeted to *Bmal1* and *CLOCK* using the starting point of DNzyme design as described by Law et al. (2006) See table 3.1 .

### 3.1.3. DNAzymes

DNAzymes are RNA cleaving molecules that consist of a catalytic region of 15 deoxynucleotides with a substrate-recognition domain of approximately 8 deoxynucleotides on each end (Santoro & Joyce, 1997, 1998).



(Ruble, Richards, Cheung-Lau, & Dmochowski, 2012)

#### Figure 3.1 DNAzyme schematic

DNAzymes bind to the complementary RNA and cleave the RNA so that it is not translated.

They are designed by selecting AU or GU sites in the target mRNA, generating the reverse complement of this sequence and replacing the A or G with the catalytic sequence **ggctagctacaacga** (Santoro & Joyce, 1997, 1998; Law et al., 2006). See Figure 3.1. They are useful as a tool for selecting sites on the mRNA which are susceptible to catalysis; i.e. sites that are accessible. Additionally, they can be rapidly tested *in vitro* by incubation of the target mRNA with the DNAzyme and running the products on an agarose gel to determine if the mRNA has been cleaved (Law et al., 2006; Baum & Silverman, 2008). One limitation of DNAzymes is that they are rapidly degraded *in vivo*

and, therefore, their potential use as a therapeutic drug is greatly reduced (Baum & Silverman, 2008). For this reason, the majority of the DNAzyme sequences were then converted to asODNs by removal of the catalytic sequence prior to testing *in vivo*.

## **3.2. Antisense Oligonucleotides**

Antisense oligonucleotides (ODNs) were first developed as a method to analyse the relationship between deoxyribonucleic (DNA), messenger ribonucleic acid (mRNA) and the proteins they encode (Paterson, Robertst, & Kuff, 1977) Shortly after this, in 1978, antisense was used to inhibit the production of Rous sarcoma virus in infected chick embryo fibroblast cultures (Zamecnik & Stephenson, 1978; Stephenson & Zamecnik, 1978).

The laboratory in which this project originated believes that antisense DNA is a safe and effective way of knocking down a target protein *in vivo*. The Becker lab uses antisense as a topical application for enhancing wound healing. The antisense is delivered in the medium of 30% pluronic gel (Becker et al., 1999) which has the advantage of being a non-toxic gel that is liquid at 4°C, but sets when it warms up, e.g. on contact with the skin. This enables accurate topical application and ensures that the ODN stays in contact with the wound area for prolonged period.

### **3.1.1 Mechanisms of action**

During transcription, RNA polymerase synthesises mRNA from the template (or non-coding) strand of DNA. This is the reverse complement of the template DNA, and is an exact match for the coding DNA 5' to 3' sequence with the exception that thymines are substituted for uracils in mRNA. Thereafter the mRNA is translated into protein in the cytoplasm of the cell via ribosomal RNA. Antisense ODNs utilise the cells' own protein

translation mechanism to disrupt *de novo* synthesis of proteins via one of the three following mechanisms: the first is that the short sequence of DNA (typically 15 - 30 nucleotides long, or 15mer - 30mer) binds to the complementary sequence on the mRNA and activates RNase H, which cleaves the mRNA and leads to its degradation; secondly, translation can be blocked via steric hindrance; thirdly, translation can be disrupted by the inhibition of splicing; and fourthly, the ODN can destabilise translation by binding to pre-mRNA. Any of these modes of action can ultimately result in down regulation of the target protein. See Figure 3.2.

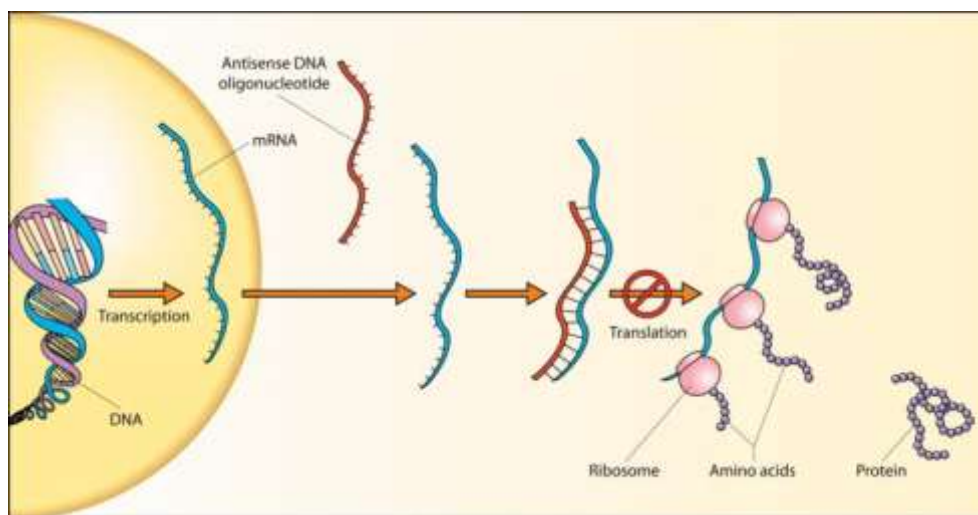


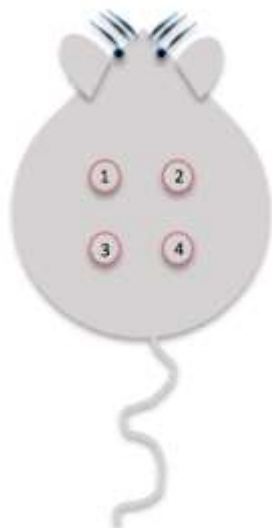
**Figure 3.2 Antisense down regulation of protein translation**

(Robinson, 2004)

Binding of the Antisense DNA oligonucleotide to the mRNA interferes with the translation of the mRNA into their protein.

### 3.3.Methods

Animal experiments were undertaken as per Chapter 2, section 2.5. In the first *in vivo* experiment the treatments were oriented as follows:



Position 1	Pluronic (or untreated) control
Positions 2-4	Antisense ODNs

**Table 3.1 Antisense sequences used in preliminary experiments**

		antisense
bmal	180	catcgttatgggacta
bmal	722	cattcttgatcctcc
bmal	750	ctttcaatctgactg
bmal	1639	atgaaaatactcataa
bmal	1749	gtgataaaagaacct
bmal	1782	gggttcatgaaagtga
bmal	2044	gatgaccctttatcc
bmal	2056	tggaaggaatgtctgg
bmal	2337	gcatctgctccaaca
clock	15	tccaccaacctcaaa
clock	8	gtcaacaatgagctca

The sequences were named for their starting base position on the target mRNA.

### 3.4. Results

Figure 3.3 and Figure 3.4 depict data from the first *in vivo* experiment analysed by the author. The experiment had previously been conducted by other lab members. Due to an insufficiency of (vehicle only) pluronic gel during the experiment, one set of mice had a ‘no treatment’ control wound.

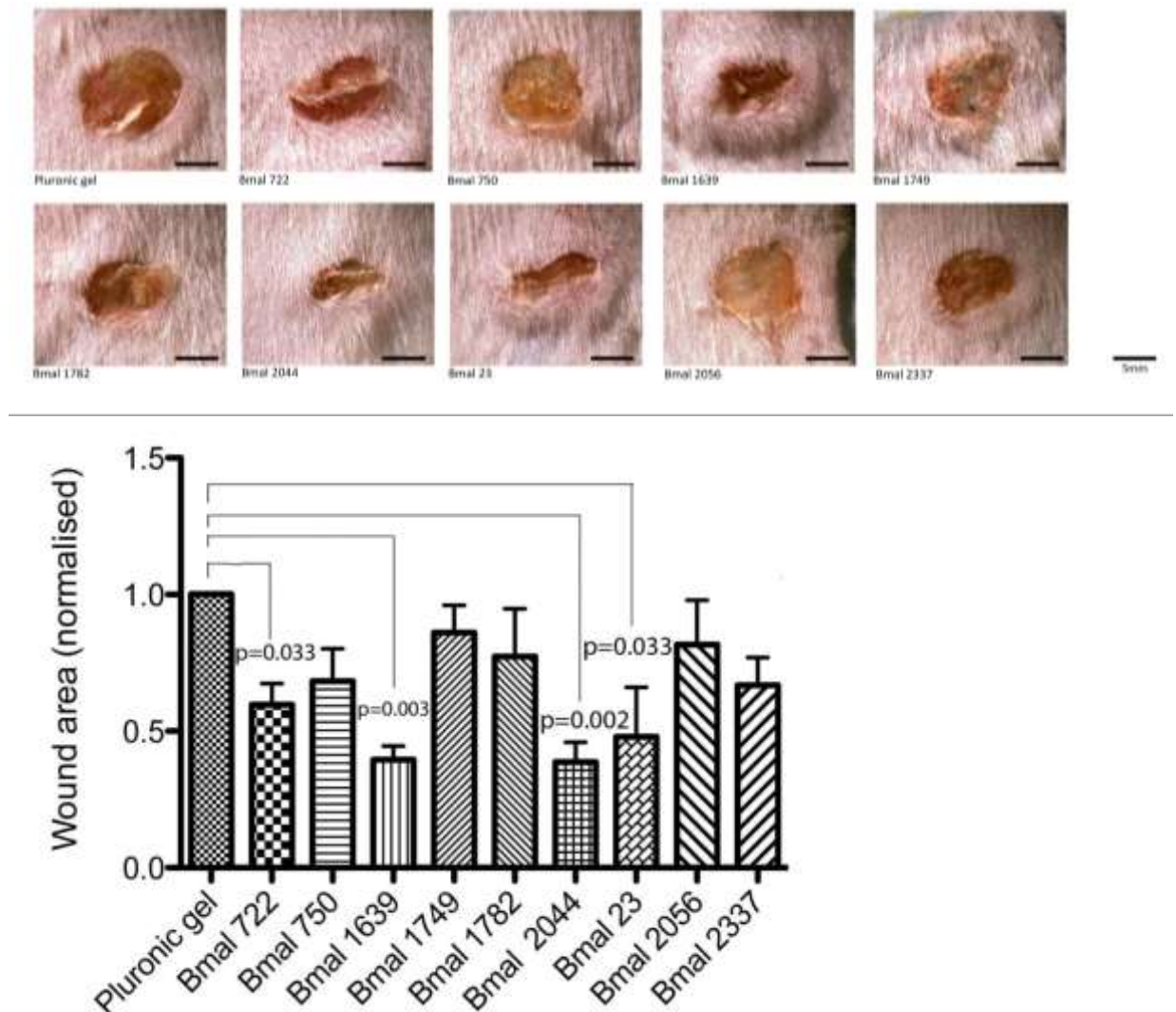
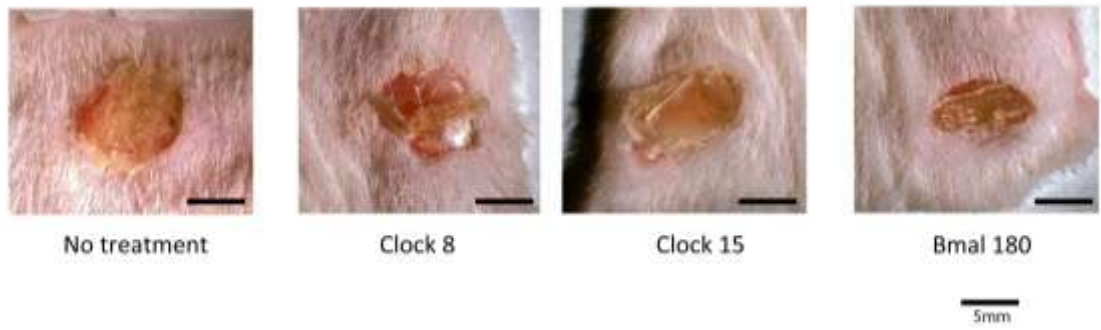


**Figure 3.3 Antisense ODNs increase wound healing *in vivo***

4 full thickness dorsal skin wounds were treated with antisense sequences as indicated in 0. 3 days later the tissue was harvested and macroscopic images were taken with a Leica dissection microscope at a fixed magnification. (a) representative images of the wounds from each treatment in the ‘pluronic control’ group. (b) the macroscopic area of the wounds normalised to the pluronic control wound in each mouse. Statistical analysis was done by Kruskal-Wallis with Dunnett’s post-hoc test. n=6

a



b

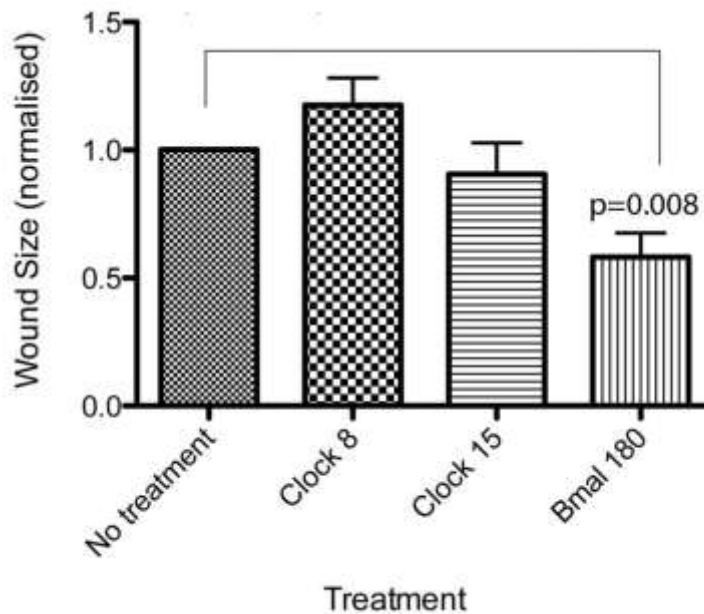


**Figure 3.4 ODN sequence Bmal 180 increases wound closure rate with comparison to no treatment**

4 full thickness dorsal skin wounds were treated with antisense sequences as indicated in Methods 2.5. 3 days later the tissue was harvested and macroscopic images were taken with a Leica dissection microscope at a fixed magnification. (a) representative images of the wounds from each treatment in the group where ‘no treatment’ was the control wound. (b) shows the macroscopic area of the wounds normalised to the untreated control wound in each mouse. Statistical analysis was done by Kruskal-Wallis with Dunnett’s post-hoc test. n=6

Following the promising results on the basis of the macroscopic analysis of the first *in vivo* experiment the macroscopic results arising from the following experiment were quite disappointing. See Figure 3.5. In hindsight, it is likely that this was mainly due to moving the position of the pluronic control from the top left position to the bottom right position on the mouse. This phenomenon is discussed in more detail below. Another fault with this experiment was that some of the DNzyme converted to antisense or antisense converted to DNzyme sequences did not follow the rules of their design properly so these were omitted from the subsequent analysis of the re-epithelialisation See Figure 3.3.

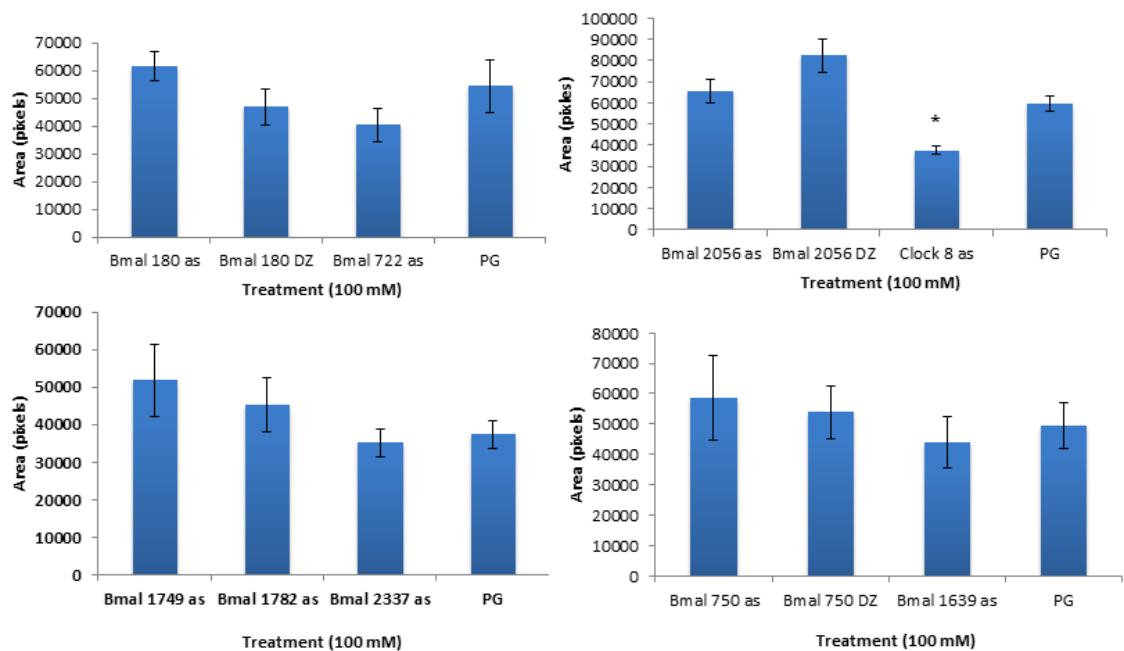


**Figure 3.5 Macroscopic area measurements of the wounds cease to demonstrate the effects seen previously when the position of the control wound was moved.**

4 full thickness dorsal skin wounds were treated with antisense sequences as indicated in Methods 2.5. 3 days later, the tissue was harvested and macroscopic images were taken with a Leica dissection microscope at a fixed magnification. Wound area was measured using ImageJ. Columns depict mean area in pixels  $\pm$  SEM. ANOVA with Bonferroni post hoc tests were used for the statistical analysis .n = 6\* p<0.05 Independent samples t test (SPSS)

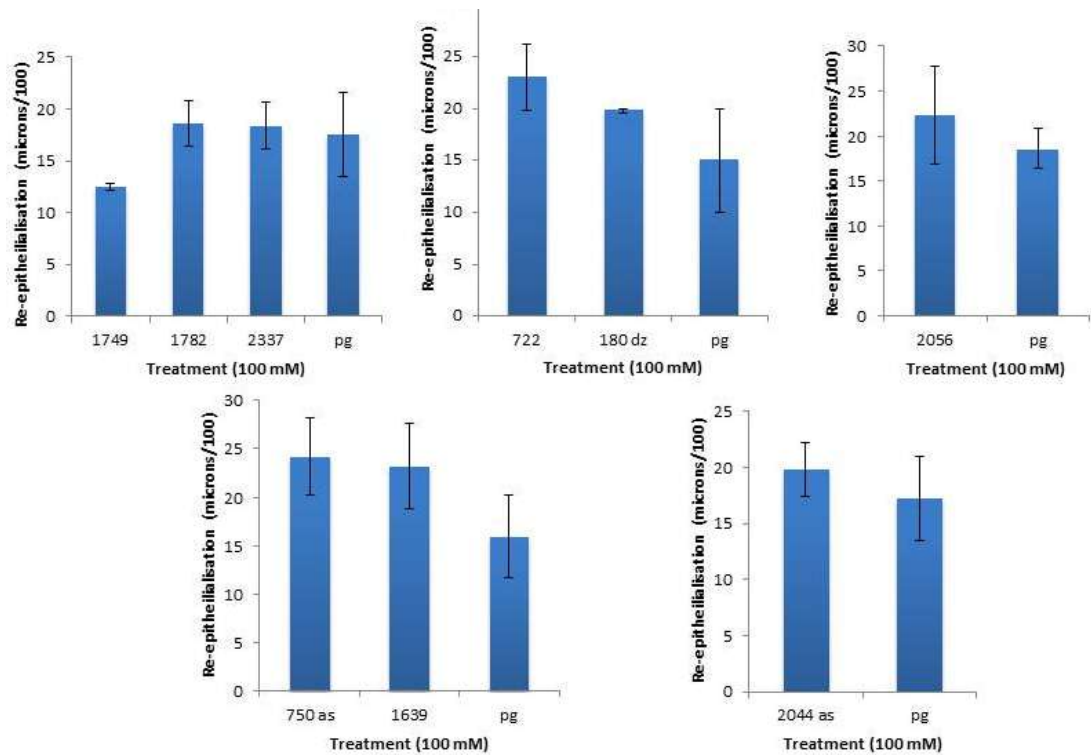


**Figure 3.6 No significance was seen between treated and control wounds in re-epithelialisation after the position of the control wound was moved.**

4 full thickness dorsal skin wounds were treated with antisense sequences as indicated in Methods 2.5. 3 days later, the tissue was harvested and sent for embedding and H & E staining. These are the same wounds measured in Figure 3.5. The distance of re-epithelialisation was measured using ImageJ. Columns depict mean distance in microns/100  $\pm$  SEM. ANOVA with Bonferroni post hoc tests were used for the statistical analysis.  $n = 6$

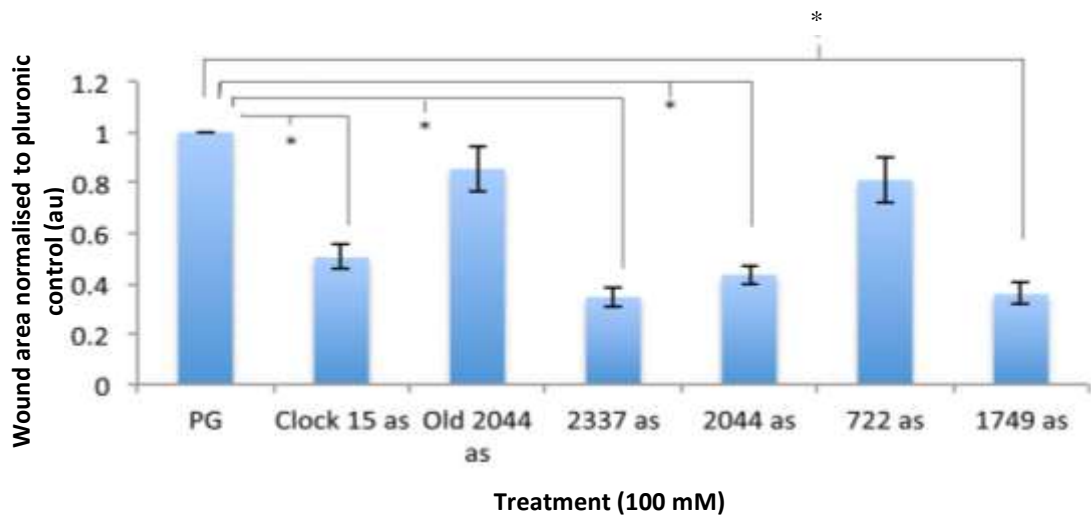


**Figure 3.7 Antisense ODNs appear to decrease wound area significantly when the original experimental conditions were used.**

4 full thickness dorsal skin wounds were treated with antisense sequences as indicated in Methods 2.5. 3 days later, the tissue was harvested and macroscopic images were taken with a Leica dissection microscope at a fixed magnification. Wound area was measured using ImageJ. Columns depict mean area in pixels  $\pm$  SEM. ANOVA with Bonferroni post hoc tests were used for the statistical analysis. n = 6

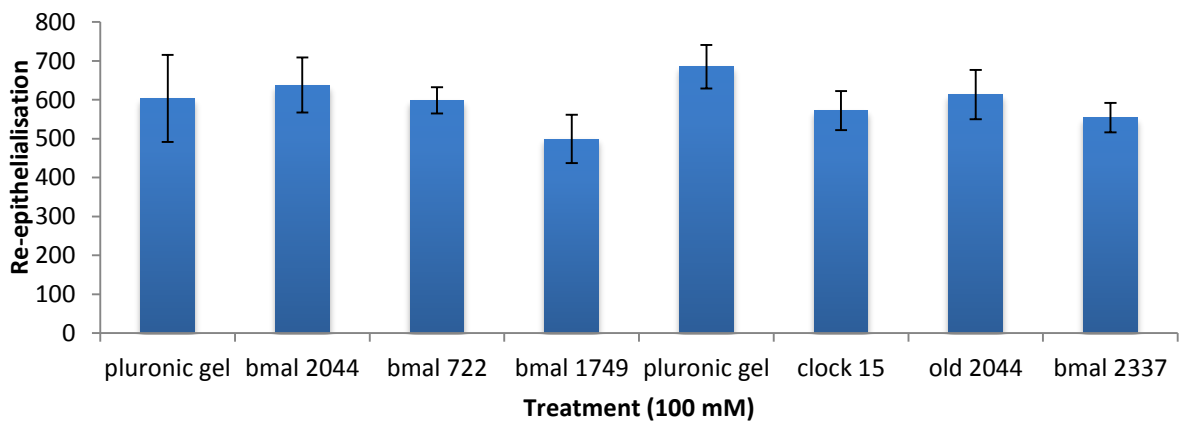


**Figure 3.8 Re-epithelialisation measurements made from the same tissue as the macroscopic images in Figure 3.7 show no difference in healing rate between treated and untreated samples.**

4 full thickness dorsal skin wounds were treated with antisense sequences as indicated in Methods 2.5. 3 days later, the tissue was harvested and used for embedding and H & E staining. The distance of re-epithelialisation was measured using ImageJ. Columns depict mean distance in microns/100  $\pm$  SEM. ANOVA with Bonferroni post hoc tests were used for the statistical analysis. n = 6

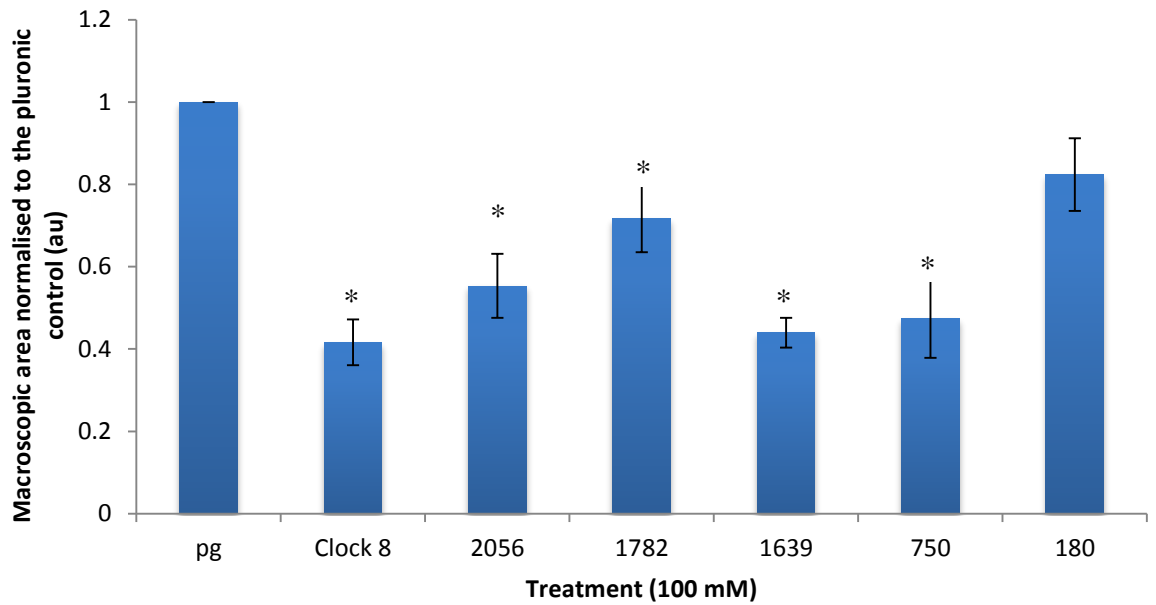


**Figure 3.9 Macroscopic wound area is reduced with antisense ODN treatment.**

4 full thickness dorsal skin wounds were treated with antisense sequences as indicated in Methods 2.5. 3 days later, the tissue was harvested and macroscopic images were taken with a Leica dissection microscope at a fixed magnification. Wound area was measured using ImageJ. Columns depict mean area in pixels and normalised to the pluronic control in each mouse  $\pm$  SEM. ANOVA with Bonferroni post hoc tests were used for the statistical analysis. n = 6

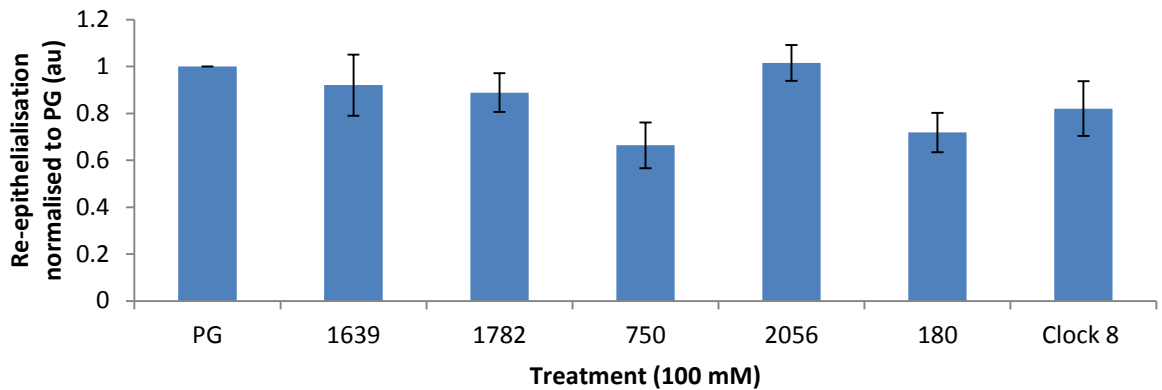


**Figure 3.10 Re-epithelialisation measurements made from the same tissue as the macroscopic images in Figure 3.9 show no difference in healing rate between treated and untreated samples.**

4 full thickness dorsal skin wounds were treated with antisense sequences as indicated in Methods 2.5. 3 days later, the tissue was harvested send for embedding and H & E staining. The distance of re-epithelialisation was measured using ImageJ. Columns depict mean distance normalised to pluronic control  $\pm$  SEM. ANOVA with Bonferroni post hoc tests were used for the statistical analysis. n = 6

It was observed that the macroscopic data from the *in vivo* experiments to this point had a tendency to show that the bottom right hand wound was the smallest. It was hypothesized that this is probably an artefact due to the stretching of the skin and the direction of the tissue folding when the punches were made. In addition, the sequences that were used in the bottom right hand wound do not perform as well when moved to another position. See overleaf for examples of images.

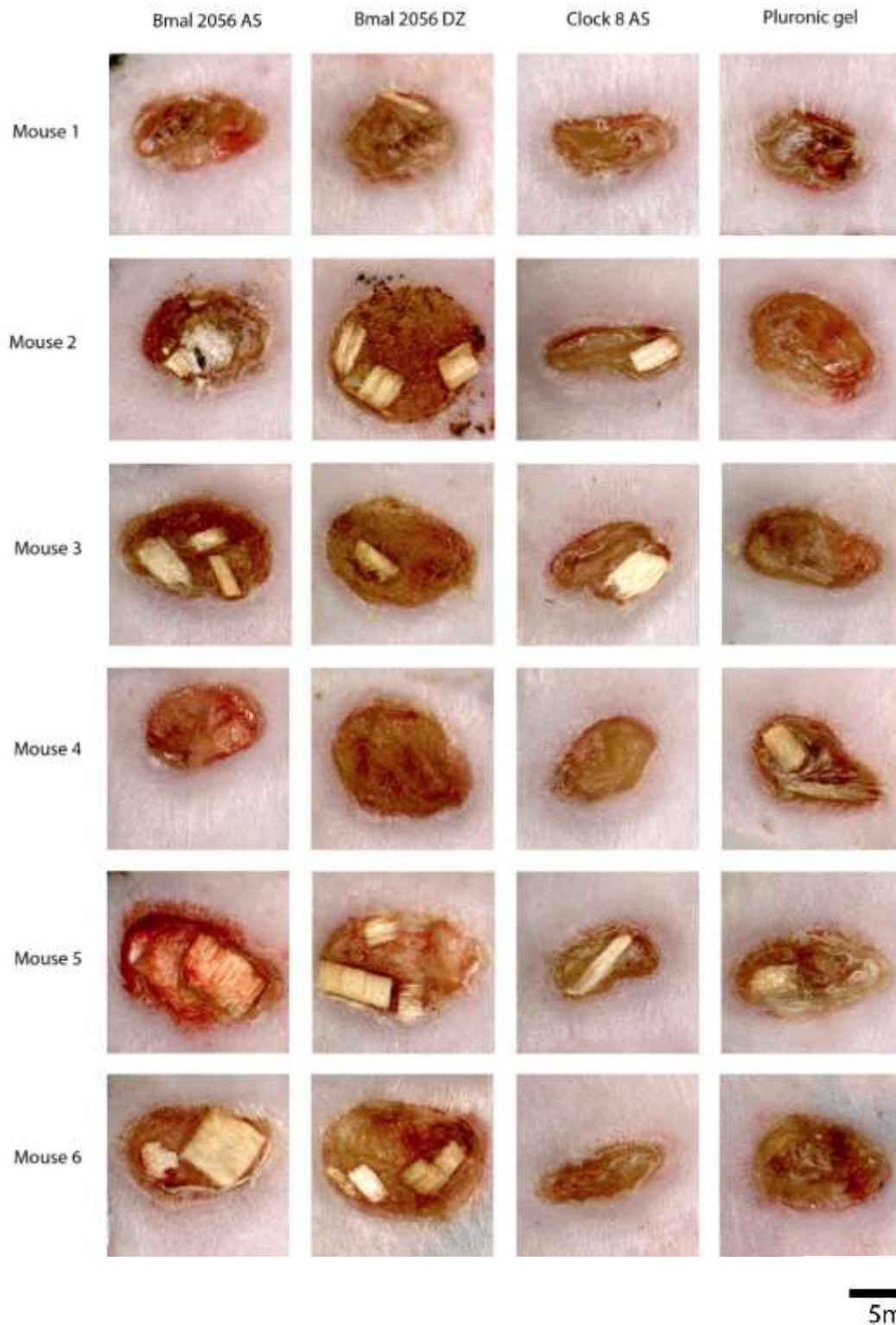
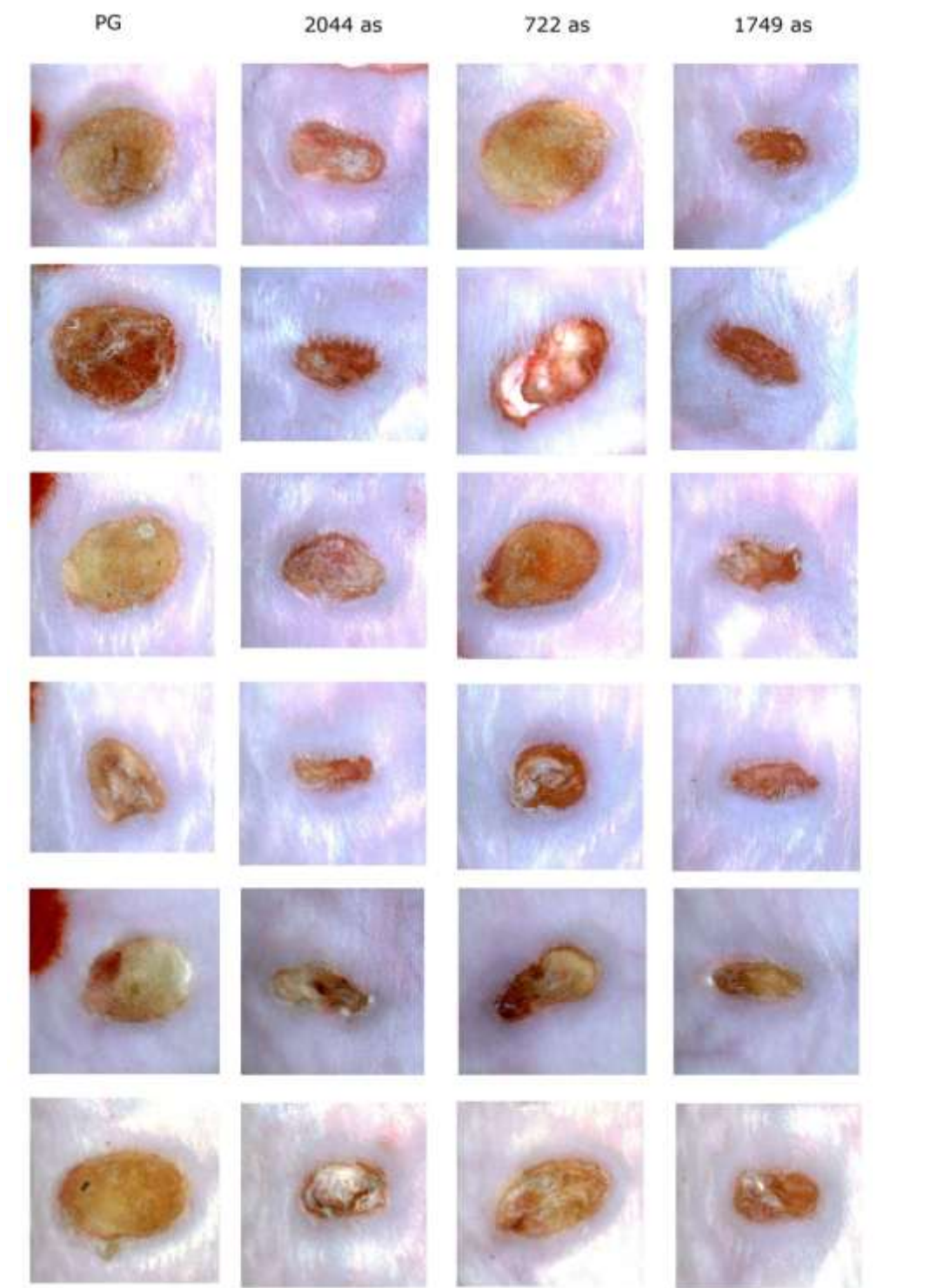


**Figure 3.11 Macroscopic images of the wounds used to produce the data in Figure 3.5**

In the above images, the order of the wounds on the mouse from left to right as you see them on the page are top right, top left, bottom right, bottom left. The pieces of woodchip are from the animals' bedding; this was subsequently changed to an absorbent matting to prevent inclusion of foreign material in the wounds. In the above experiment the tissue was folded from the mouse's left to right to make the punch wounds.



5mm

**Figure 3.12 Representative macroscopic images used to produce the data in Figure 3.7**

In the above images, the order of the wounds on the mouse from left to right as you see them on the page are top right, top left, bottom right, bottom left. In this experiment the tissue was folded from the mouse's right to left to make the punch wounds.

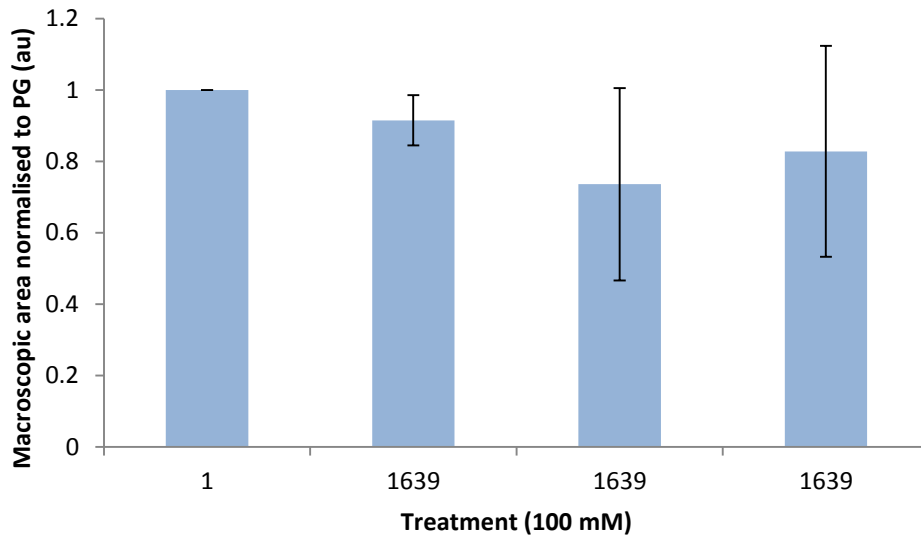


**Figure 3.13 The direction of tissue folding influences the macroscopic wound area.**

4 full thickness dorsal skin wounds were treated with the same antisense sequences in wounds 2, 3 and 4 and the direction of the tissue fold was alternated when making wounds.

3 days later, the tissue was harvested and macroscopic images were taken with a Leica dissection microscope at a fixed magnification. Wound area was measured using ImageJ. Columns depict mean area normalised to pluronic control  $\pm$  SEM. ANOVA with Bonferroni post hoc tests were used for the statistical analysis. n = 2

This experiment demonstrated that there are two main factors that affect the size of the wounds; the position on the mouse and the direction of the fold. The wounds nearer to the head and over the most humped part of the spine are larger and more stretched, whereas those nearer to the tail are smaller and more elliptical, probably because the skin in this area is looser. Additionally, the wounds that are on the underside of the fold when the punch-holes are made are smaller, possibly due to the way the skin retracts as the mouse is turned onto its side. See Figure 3.14. In light of this, it was recognised that the macroscopic data are not a very reliable indicator of the efficacy of the treatments, and that the primary outcome measurement should be re-epithelialisation.

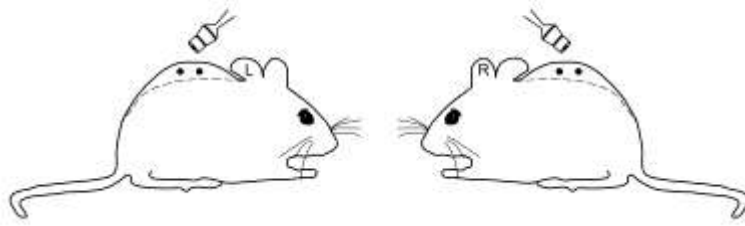


### Figure 3.14 Punch wound method

Wounds were made by lying the anaesthetized mice on their sides, stretching the loose dorsal skin and making 2 full thickness punch biopsies through both layers of the fold, resulting in 4 wounds

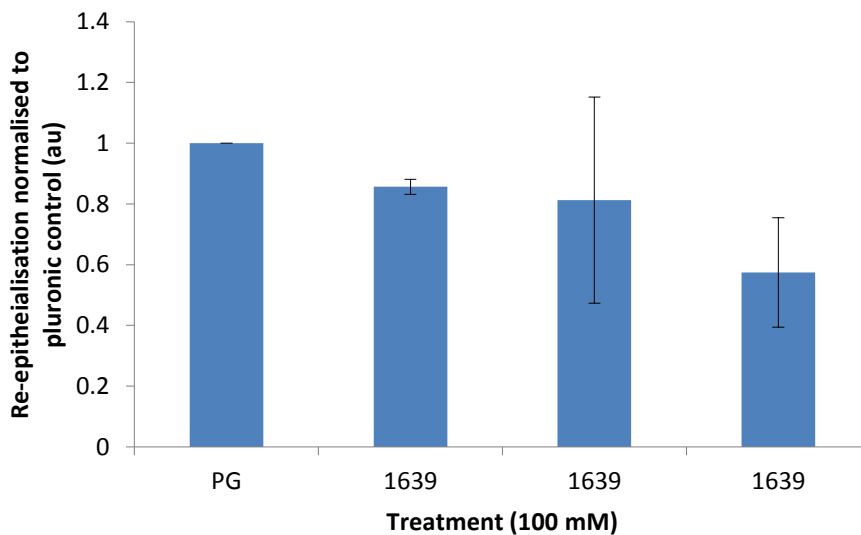


### Figure 3.15 The position of the wound affects the degree of re-epithelialisation

4 full thickness dorsal skin wounds were treated with the same antisense sequences in wounds 2, 3 and 4 and the direction of the tissue fold was alternated when making wounds. 3 days later, the tissue was harvested send for embedding and H & E staining. The distance of re-epithelialisation was measured using ImageJ. Columns depict mean distance of re-epithelialisation normalised to pluronic control  $\pm$  SEM

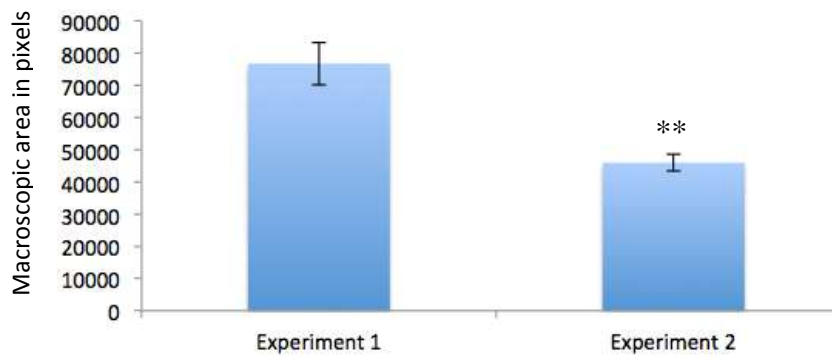


**Figure 3.16 The position of the control wound influences the size of the macroscopic wound area.**

An analysis of the mean macroscopic size of the pluronic control wounds when they were in the top left versus bottom right. In experiment 1 the pluronic control was in the top left, in experiment 2 it was in the bottom right. This also demonstrates the effect of the wound position on macroscopic wound area measurement.

Statistical analysis was done using Independent samples Student’s t-test on SPSS.  $p < 0.05$ . (Experiment 1  $n = 15$ , experiment 2  $n=30$ )

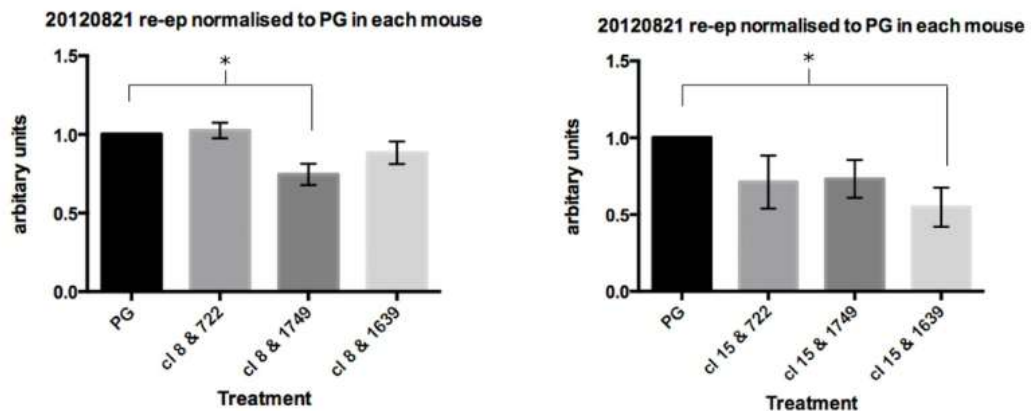


**Figure 3.17 Combining anti-CLOCK and anti-Bmal1 asODNs lead to significantly reduced re-epithelialisation.**

4 full thickness dorsal skin wounds were treated with antisense sequences as indicated in Methods 2.5. 3 days later, the tissue was harvested and sent for embedding and H & E staining. The distance of re-epithelialisation was measured using ImageJ. Columns depict mean distance normalised to pluronic control ± SEM. ANOVA with Dunnett’s post hoc tests were used for the statistical analysis.  $n = 6$

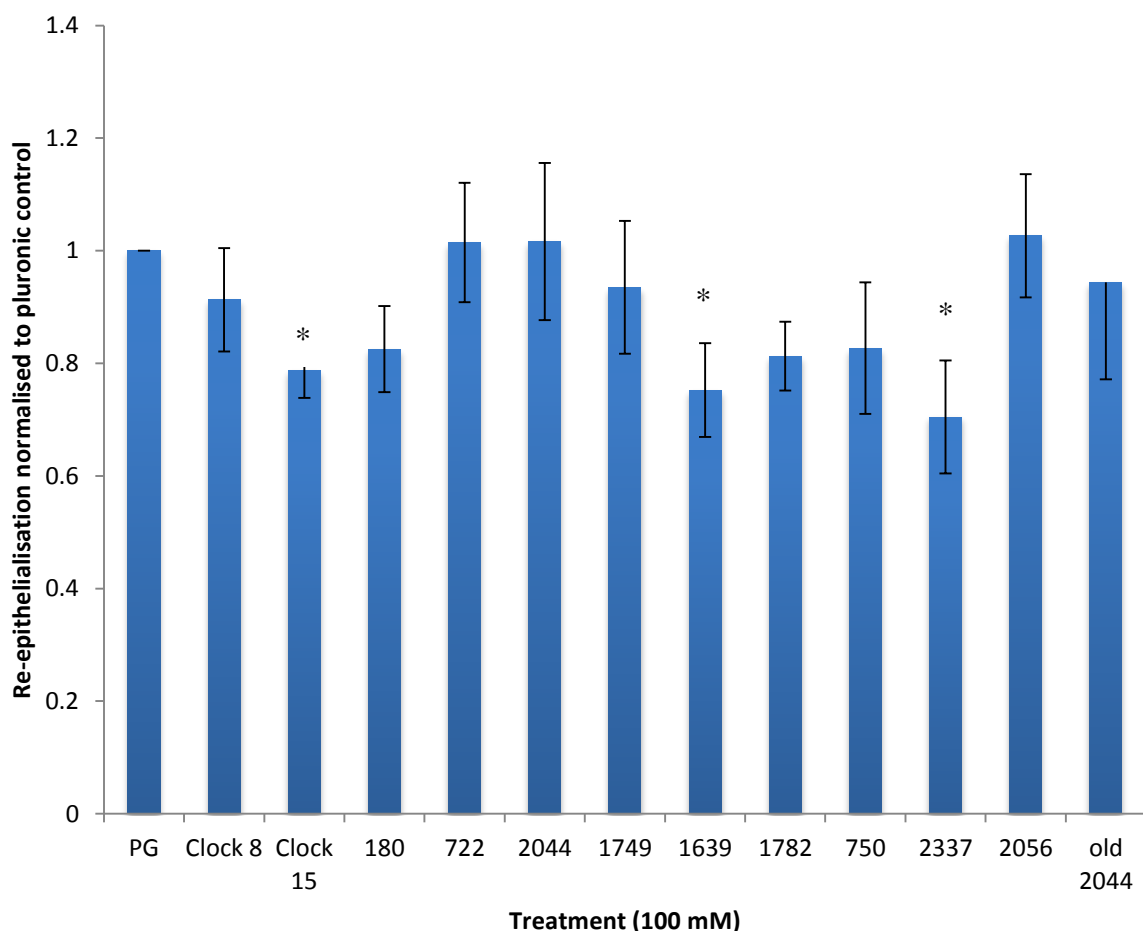


**Figure 3.18 The asODNs do not significantly increase re-epithelialisation of the wounds.**

Re-epithelialisation data from all of the comparable experiments using single asODN treatments were pooled and re-analysed. The only significant findings arising from the re-analysis were negative; a significant reduction in re-epithelialisation. Statistical analysis of significance was done using Kruskal-Wallis with Dunnett’s post-hoc on SPSS. n=10-16. \*= p<0.05

After having reviewed the original data, it was decided that it might be worth trying some of the DNAzymes that had been tested for their functional ability to cleave the RNA in a biochemical assay and shown some promise *in vitro* in previous studies in fibroblast cell cultures (scratch wound assays and Western Blot) by past lab members (although the n numbers were too small for statistical significance).

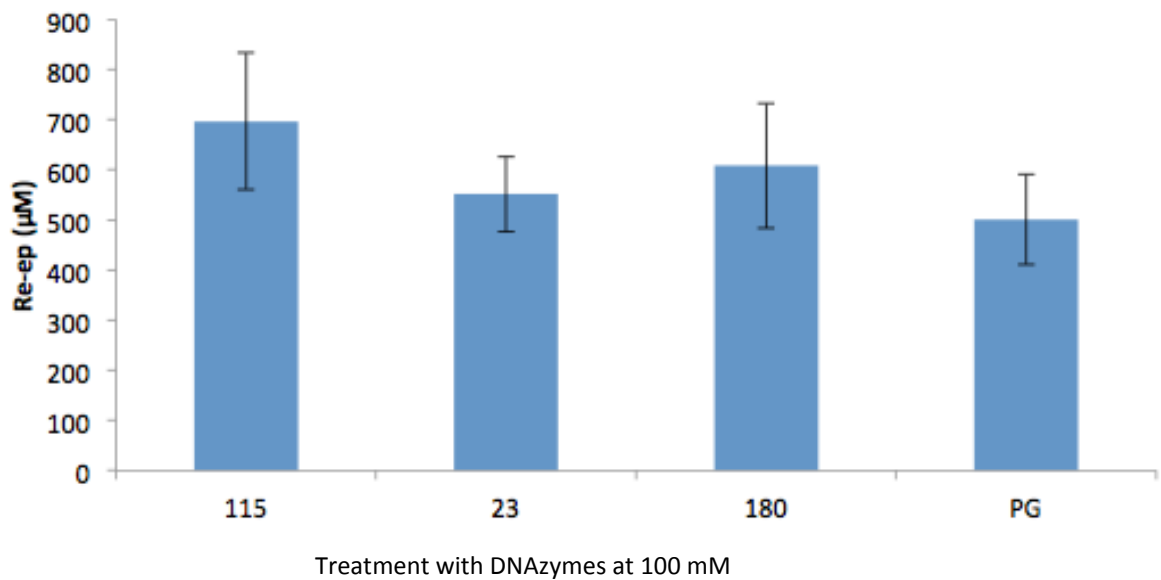


**Figure 3.19 Treatment with DNazymes does not significantly increase re-epithelialisation**

4 full thickness dorsal skin wounds were treated with the same antisense sequences in wounds 2, 3 and 4 and the direction of the tissue fold was alternated when making wounds.

3 days later, the tissue was harvested and sent for embedding and H & E staining. The distance of re-epithelialisation was measured using ImageJ. Columns depict mean distance of re-epithelialisation in micrometres  $\pm$  SEM. Statistical analysis was done with ANOVA on SPSS.

No significant difference was found between treated and untreated samples. n=6.

### 3.5. Discussion

Initially the macroscopic appearance of the asODN treated wounds was very promising. It appeared as though there had been a strong effect of the asODNs on some of the wounds. It was possible that the use of wood chip as bedding material was confounding the data as the wounds with wood chip inclusions seemed to heal less well (see figure 3.11). Following further investigation, a pattern developed and it became apparent that there was a distinct order to the size of the wounds, regardless of the treatments. This is illustrated by figures 3.11 and 3.12; the wounds are in order of their position on the back. It is clearly evident that the wounds in the 4<sup>th</sup> column of these two figures are different sizes. Two main factors affect the size of the wounds; the position on the mouse and the direction of the fold. The wounds nearer to the head and over the most humped part of the spine are larger and more stretched, whereas those nearer to the tail are smaller and more elliptical, probably because the skin in this area is looser and hence contracted the wound more effectively than the rostral region of the back. Additionally, the wounds that are on the underside of the fold when the punch-holes are made are smaller, possibly due to the way the skin retracts as the mouse is turned onto its side. In light of this, it was recognised that the macroscopic data are not a very reliable indicator of the efficacy of the treatments and that the primary outcome measurement should be re-epithelialisation. It is unfortunate that the macroscopic appearance of the wounds indicated a positive effect that turned out to be an artefact, but this delay was partly due to problems experienced in sectioning the very fragile tissue by cryostat which was later resolved by having the tissue paraffin embedded. The data from the *in vivo* work shows that there was no significant effect on wound healing of the original 16 mer asODNs.

There are several possible reasons why the original sequences did not have a functional effect. Firstly, there were some actual errors in the sequences; 3 of the sequences had transposition errors; a **c** where there should have been a **g** or vice versa. Secondly, the sequences were only 16 nucleotides long which makes them much less stable *in vivo*. They are more vulnerable to endogenous nucleases at this size (Aartsma-Rus et al., 2009). It is regrettable that these sequences had not been screened *in vitro* prior to starting the *in vivo* work.

The DNAzymes did not produce a beneficial effect *in vivo* either; however, this is not surprising as there is considerable data to suggest that DNAzyme are not very long-lived *in vivo* (Law et al., 2006; Baum & Silverman, 2008). The next logical step to develop these sequences was to expand them to being 30 bases (30 mer) long; previous work in the laboratory had shown a 30 mer asODN sequence targeted against connexin 43 to be effective. The next chapter addresses the *in silico* development and *in vitro* testing of the new elongated sequences.

Subsequent to the discovery of the artefacts introduced by the mouse model wounding methods the standard operating procedure for the laboratory was modified. Additionally the practice of alternating the wound position and blinding of the treatments was introduced.

4. *In silico* antisense  
deoxyoligonucleotide  
expansion design and *in*  
*vitro* testing

---

## 4.1. Introduction

Following the hypothesis that the lack of beneficial effect seen with the 16mer asODNs was due to the rapid catalysis, the asODNs were elongated as described in Methods 2.6. Antisense design is a systematic process based on a set of rules which help to reduce the number of possible candidates. The key rules are that the binding site must be accessible structurally; the melting temperature must be above 37°C, preferably above 48°C (Aartsma-Rus et al., 2009), and the sequence must not fold itself into any stable secondary structures or form primer-dimers that would be stable enough to prevent their binding to their target mRNA. There are several motifs which must be avoided; G quartets or repeats of G triplets can cause the asODNs to form stacks via hydrogen bonding in the *P* orbital; CpG motifs must be avoided as they are not found in mammalian DNA in an unmethylated state so the cell recognizes DNA containing CpGs to be of bacterial origin which can illicit an inflammatory response (Becker et al., 1999).

Due to endogenous nucleases asODNs are cleared relatively quickly which reduces the risks of toxicity or off-target effects. Additionally the use of asODNs as a topical gel directly applied to the wounds reduces any undesired potential systemic effects. The disadvantages of this rapid degradation are that it reduces the time available for effective silencing of protein translation and that the products of the degradation could potentially cause off-target silencing or other side effects as was seen in unmodified siRNA (Miller, Braiterman, & Ts'o, 1977; de Fougères, Vornlocher, Maraganore, & Lieberman, 2007).

## 4.2. Results

The asODN candidate sequences were systematically selected using the criteria previously mentioned. Following this, they were discounted if they did not share sufficient homology to human Bmal1.

**Table 4.1 16mer asODNs were elongated to produce 25-30mer sequences**

mer number	asODN candidate	homology to human Bmal1?
30	ccttggtgttctgcatattctaacctcca	y, partial, 1 mismatch
30	tccttccttggtgttctgcatattctaacc	y, partial, 1 mismatch
30	atccttccttggtgttctgcatattctaac	y, partial, 1 mismatch
30	gaccttccttggtgttctgcatattctaa	y, partial, 1 mismatch
30	ttccttggtgttctgcatattctaacctc	y, partial, 1 mismatch
30	tccttggtgttctgcatattctaacctcc	y, partial, 1 mismatch
30	atctgctccaagaggctcatgatgacagc	complete
29	cttggtgttctgcatattctaacctcca	y, partial, 1 mismatch
29	ccttccttggtgttctgcatattctaacc	y, partial, 1 mismatch
28	cttccttggtgttctgcatattctaacc	y, partial, 1 mismatch
28	gagtcctccatttagaatcttcttgcc	y, partial, 1 mismatch
28	gcttccaagaggctcatgatgacagcca	complete
27	ttccttggtgttctgcatattctaacc	y, partial, 1 mismatch
26	tctgtaaaactgcctgtgacattc	y, partial, 1 mismatch
26	gtctgtaaaactgcctgtgacattc	y, partial, 1 mismatch
26	tccttggtgttctgcatattctaacc	y, partial, 1 mismatch
25	gttactgggactactgatccttg	complete
25	gagtcctccatttagaatcttcttg	y, partial, 1 mismatch

### **4.3. *In vitro* testing of new asODNs**

The efficacy of the asODNs to knock down Bmal1 protein was assessed via Western blot; mRNA knockdown was assessed by RT-PCR and functional changes were assessed by Scratch Wound Assay as described in Methods section 2.2. Initially the results were promising. In the absence of a satisfactory control for the asODNs, a mock transfected ‘vehicle only’ control was used. A scrambled asODN control was designed in collaboration with the custom oligo department of Sigma Aldrich Ltd. It soon became apparent that the scrambled control (which has no homology to any murine mRNA) was as effective at knocking down Bmal1 protein as the targeted sequence (see Fig. 4.1). Additionally it was observed that GAPDH was also being affected by the asODNs (scrambled or otherwise). This effect has also been observed by the Becker lab when testing their asODN targeted to Connexin 43 *in vitro* and also *in vivo* by a colleague at the Cancer Institute (personal communication). For this reason, the asODNs were modified to have a phosphorothioate backbone in place of the usual phosphodiester backbone.

### **4.4. Modified antisense DNA oligonucleotides**

As early as 1978, it was established that modifications to the ends of ODNs improved their efficacy (Zamecnik & Stephenson, 1978). These authors demonstrated that the ‘blocked’ ODNs which had chemical modifications to the 5’ and 3’ ends of the sequences had a more pronounced effect on silencing the production of the Rous sarcoma virus due to the protective effects that these modifications conferred on degradation via cellular nucleases to the phosphodiester bonds in native DNA.

In 1987, Matsukura et al (1987) introduced phosphorothioate (PS) internucleoside linkages to further reduce the susceptibility of the ODNs to cleavage by endonucleases,

Subsequently, 2'-O-methyl-modified nucleotides at the 5' and 3' ends were introduced as an alternative way to stabilise the molecular integrity of ODNs (Agrawal, Mayrand, Zamecnik, & Pederson, 1990).

There have been several different types of chemical modification used to enhance the effect of ODNs. The main ones are depicted below:

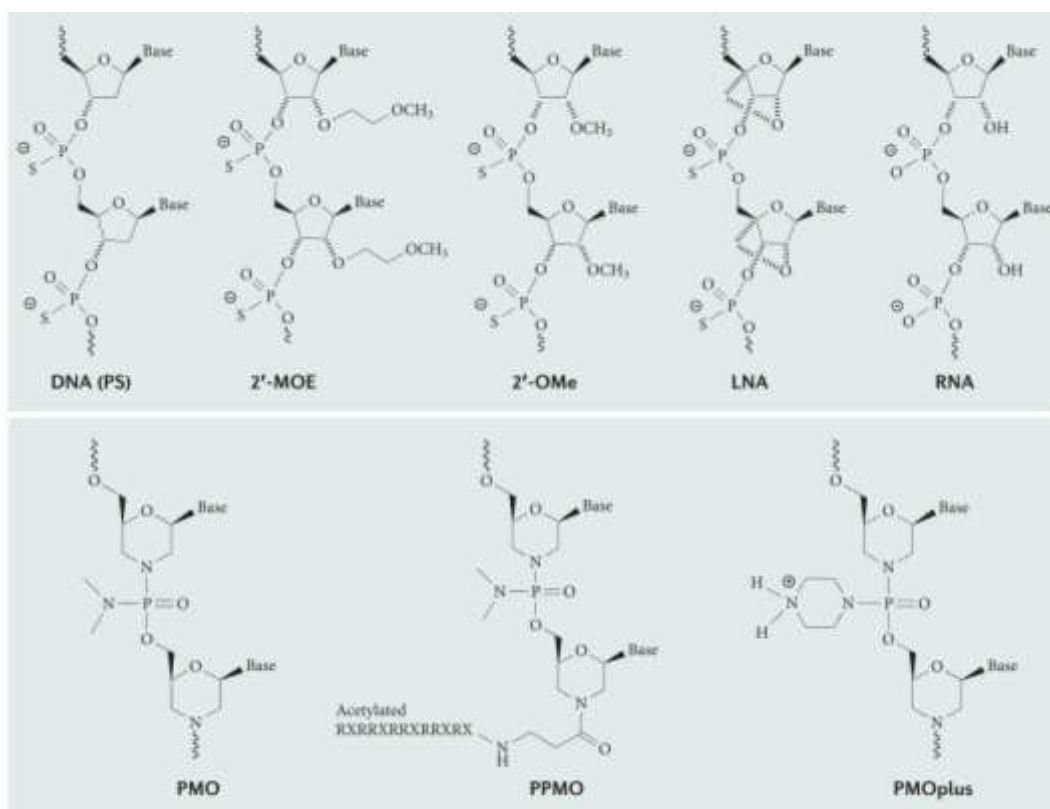


### Figure 4.1 Antisense DNA modifications

From RNA therapeutics: beyond RNA interference and antisense Oligonucleotides (Kole, Krainer, & Altman, 2012)

Figure 4.1 depicts several of the commonly used antisense DNA modifications which are predominantly designed to slow down the degradation rate of the sequences *in vitro* / *in vivo*

Of these modifications, the phosphorothioate (DNA (PS)), 2' -O-methoxyethyl (2' -MOE) and 2' -O-methyl (2' -OMe) moieties are designed to reduce degradation by endonucleases. Locked nucleic acids (LNA) increase the binding to the target mRNA.

Phosphorodiamidate morpholino oligomers (PMOs) are a more substantial modification where the nucleic acids are substituted for morpholine rings, and the internucleoside groups are replaced with uncharged phosphorodiamidate groups, resulting in degradation resistance and neutral charge. PMOplus contain positively charged piperazine groups; peptide-conjugated PMOs contain positively charged arginine-rich peptides. Both of these modifications improve the intracellular uptake of the oligomers (Kole et al., 2012).

For the purposes of this project, the only modification used was PS – phosphorothioate as the aim was to create a patentable asODN and the other modifications mentioned above are either prohibitively expensive or proprietary modification designs (Summerton & Weller, 1997) and, therefore, not appropriate for the original aims cited in the grant application for the project.

**Table 4.2 asODNs used for further *in vitro* testing**

asODN name	Sequence
Antisense 1 (PO)	TCCTTCCTTGGTGTTCTGCATATTCTAACC
Scrambled 1 (PO)	GCAGTCTCAATTCCTCGCTTACCTTTATGT
Scrambled 2 (PO)	GGAACTCTCCTGGTATCGTCTAATAT
Antisense 1 (PS)	T*C*C*T*T*C*C*T*T*G*G*T*G*T*T*C*T *G*C*A*T*A*T*T*C*T*A*A*C*C
Scrambled Antisense 1 (PS)	G*C*A*G*T*C*T*C*A*A*T*T*C*C*T *C*G*C*T*T*A*C*C*T*T*T*A*T*G*T

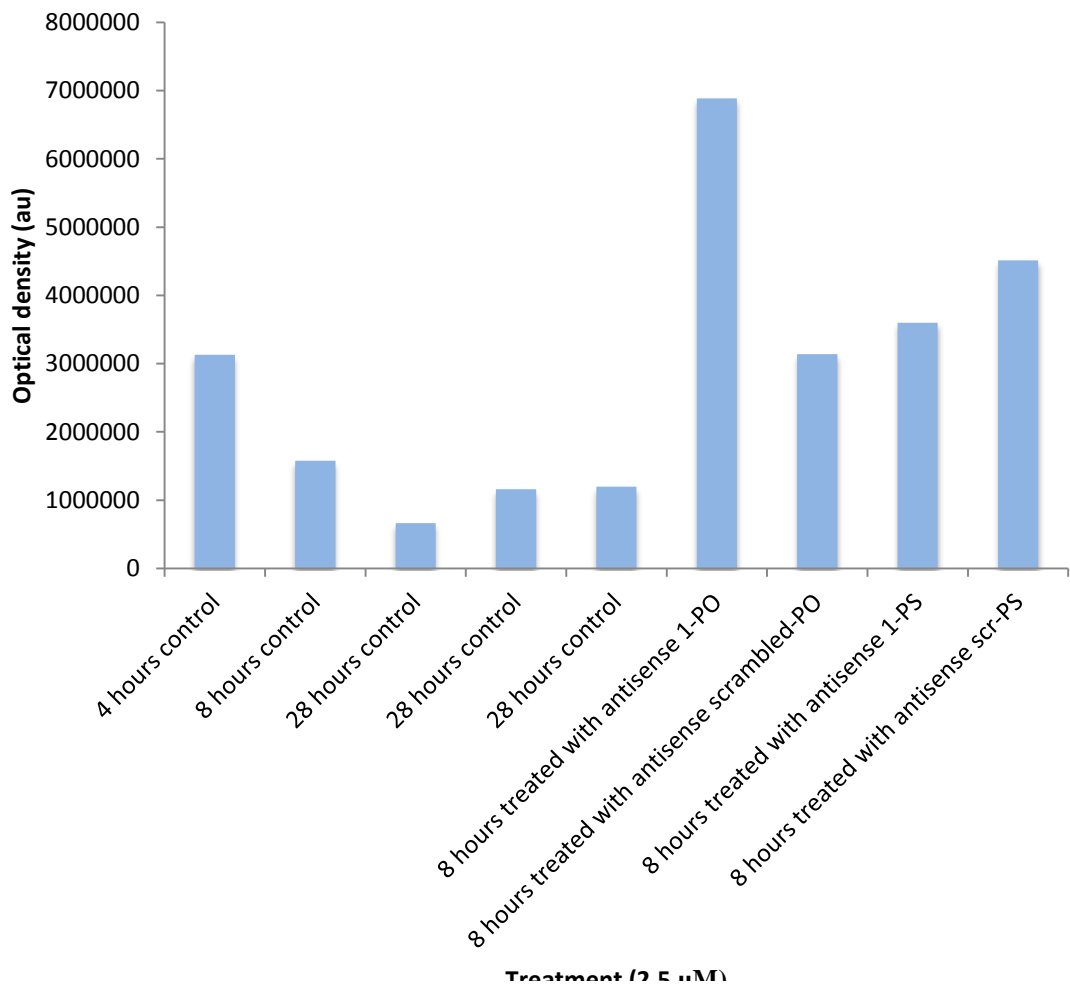


**Figure 4.2 Scrambled asODN knocks down Bmal1 as effectively as the targeted sequence. asODNs also knockdown GAPDH.**

NIH 3T3 cells were transfected with antisense and harvested at the intervals as above. Protein was extracted and Western blotting done as per section 2.2.1. This is one representative experiment of many. The columns represent Bmal1 protein normalised to GAPDH, but as is evident above in the circled image of the GAPDH bands, GAPDH is being affected by the treatments in a similar manner to incubating cells in old medium. Although the Bmal1 bands to the right hand side of the blot appear to have a similar optical density, when normalised it appears that antisense 1PO is less effective at reducing the expression of Bmal1 as the optical density of GAPDH is noticeably lower in that lane. This phenomenon raised some serious queries as to the sequence specificity of the antisense; scrambled asODN is as effective as reducing Bmal1 protein. Also the knockdown of housekeeping proteins might suggest that there is some level of toxicity.

In the mid-nineteen nineties there was research into the use of ODNs as treatment for chronic myeloid leukaemia by targeting anti BCR/ABL (Giles, Spiller, Green, Clark, & Tidd, 1995; Wu et al., 1995). This was called into question when Vaerman et al investigated the mechanisms involved (Vaerman et al., 1997). They believed that many of the biological effects observed were not due to 'sequence-specific inhibition of genetic expression'. Following their study of the degradation of ODNs in culture medium, they concluded that the cytotoxicity of the ODNs was due to the 'stepwise hydrolysis of the ODN phosphate linkages' as previously shown (Wickstrom, 1986). Further to this, these authors examined the relative anti-proliferative effects of the deoxynucleotide mono-phosphates (dNMPs) and found that this phenomenon only occurred post-hydrolysis (and not in the more stable phosphothioate oligos) and that the intensity of the cytotoxicity was strongest with deoxyguanosine monophosphate (dGMP) followed by thymidine monophosphate (TMP), then deoxyadenine monophosphate (dAMP), with deoxycytosine monophosphate (dCMP) showing no anti-proliferative effects whatsoever.

This work was expanded further by Koziolkiewicz et al (2001). This group studied the effects of dNMPs and their phosphorothioate analogues, dNMPSs. They measured the breakdown of dNMPs over 48 hours by high performance liquid chromatography (HPLC) and found that dGMP was completely hydrolysed to deoxyguanosine and subsequently to guanine (15%) and xanthine (85%) within that time-frame. This rate of degradation was similar for the other dNMPs, but the hydrolysis of dNMPSs was much lower. Similarly to Vaerman et al, they found that dGMP and TMP were more toxic to both human umbilical vein endothelial cells (HUVECs) and cervical cancer cells (HeLas). A 72 hour incubation with 100  $\mu$ M deoxyguanosine reduced cell numbers by 40-50% and incubation with guanine reduced cell growth by 60%.

Conversely, they found that dNMPSs did not inhibit cell proliferation at all, even over 96 hours of incubation; in fact, with the exception of dCMPS, they stimulated the proliferation of promyelocytic HL-60 cells and HUVECs by 20-60%. They hypothesized that this effect was due to the rapid dephosphorylation of the dNMPSs by ecto 5'nucleotidase (ecto 5'NT) - when they inhibited ecto 5'NT in these cells the proliferative effects of the dNMPSs was obliterated. The authors concluded that this might be due to an as yet unknown interaction with P2 receptors.

#### **4.4.1. Aptameric inhibition of off-target molecules**

Another potential side effect that has been found for ODNs is the non-sequence specific binding to off target molecules. ODNs have been shown to inhibit thrombin (Bock, Griffin, Latham, Vermaas, & Toole, 1992; Bergan, Kyle, Connell, & Neckers, 1995) and protein-tyrosine kinase in a non-antisense based mechanism. This is due to the secondary or tertiary structure binding to the (non)target.

### **4.5. Intracellular availability of ODNs**

Earlier studies ( a R. Thierry & Dritschilo, 1992) compared the uptake of native ODNs (POs), phosphorothioate analogues (PSs) and end-capped phosphorothiate ODNs (cap-PSs). Incubation in culture medium resulted in total degradation of POs, but when encapsulated in liposomes they were intact after 5 days. PS and cap-PS oligos were much more resistant, with 21% and 40% of oligos undegraded after a 48 hour incubation. The cellular uptake of the three variants, when delivered naked was non-detectable in POs, slow in PS and faster in cap-PS. Once liposomally encapsulated, the uptake of PS was 18-fold and the cap-PS was 7-fold when compared to naked delivery. This was assessed via fluorescein isothiocyanate (FITC) labelling. The authors concluded that the liposomal encapsulation conferred protection to the oligos, reduced their efflux from

the cells and additionally permitted a gradual release from endocytic vesicles. Their best results were with cap-PS and encapsulated ODNs – they exhibited the highest intracellular uptake, the best distribution and longevity within the cell ( a R. Thierry & Dritschilo, 1992).

#### **4.6. *In vitro* testing of non-oligomerised mononucleotides**

Further to the discovery that the housekeeping proteins used as a loading control were being affected and in light of the work done by Koziolkiewicz et al (2001) more Western blots were performed to:

- a) Compare the effects of non-oligomerised mononucleotides (NMPs) versus the phosphodiester asODNs. See Figure 4.6 and Figure 4.7
- b) Test the stability of the housekeeping proteins to all treatments by using a total protein stain as a loading control. See Figure 4.3.
- c) Retest the effects of the antisense sequences on Bmal1 using total protein staining as a loading control. See Figure 4.3

Amido Black (Sigma Aldrich Ltd) was used prior to blocking the membranes. Membranes were briefly exposed to the stain (0.1% w/v) then destained with 25% methanol, 10% acetic acid destaining solution until visible bands against the destained background. Colorimetric images were obtained using the Bio-Rad ImageLab MP used for the chemiluminescent imaging. Thereafter the Western blot process was the same as described in Methods 2.2.1.

The non-oligomerised equivalents of the asODNs were formulated by making 1 mM solutions of each dNMP and then mixing them in the same ratio as found in the

asODNs. Thereafter, they were diluted as appropriate to obtain 2.5  $\mu$ M final concentration.

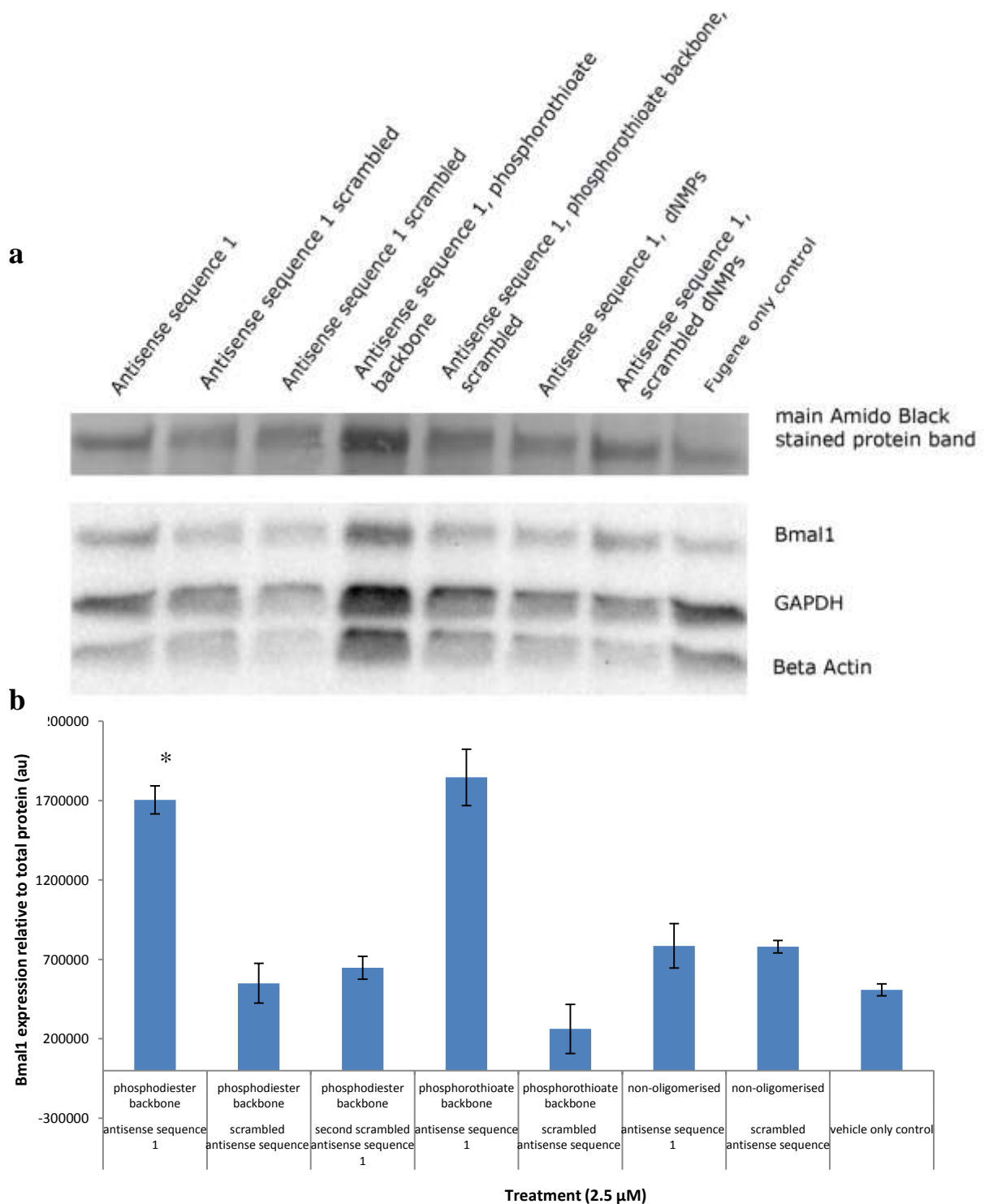
#### **4.6.1. Normalisation and analysis of Western Blots**

For normalisation between blots an untreated protein lysate was made, aliquotted and stored at -20°C so that the same volume of the identical batch of protein could be loaded into the last lane of each Western blot. Thereafter, all proteins on the blot were normalised to the optical density (od) of predominant protein band divided by the control lane on the colorimetric amido black images.

$$\text{Normalised od between blots } (k) = \frac{\text{optical density of predominant amido black band}}{\text{optical density of control amido black band}}$$

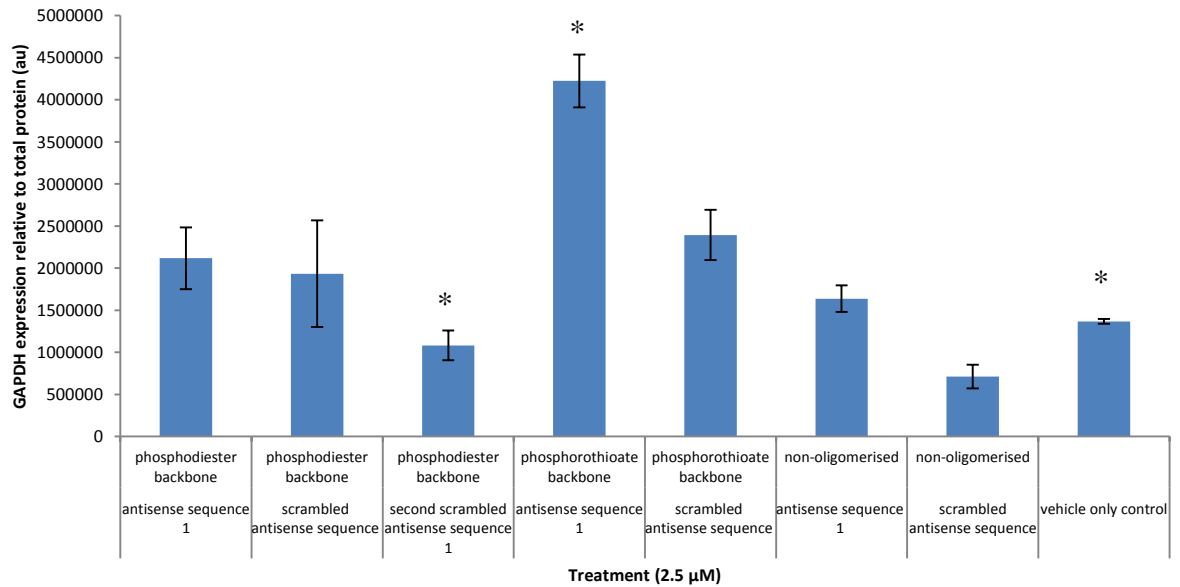
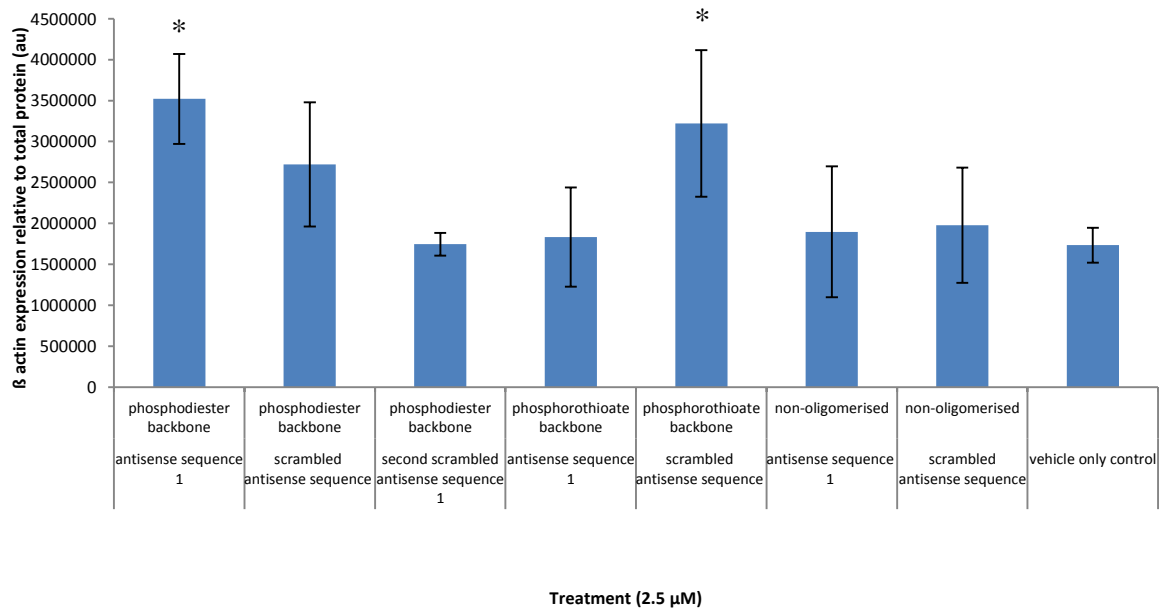
$$\text{Normalised od of the sample bands} = \text{od of chemiluminescent band} \times k$$

Cells were harvested 6, 24 and 48 hours after treatment in order to assess whether the affects seen were due to cytotoxicity. The median half-life of proteins in NIH 3T3s has been measured as being 46 hours whereas the median half-life of mRNA was found to be 9 hours (Schwanhäusser et al., 2011).



**Figure 4.3 Bmal1 protein expression 6 hours after treatment is not due to a sequence specific effect of asODNs**

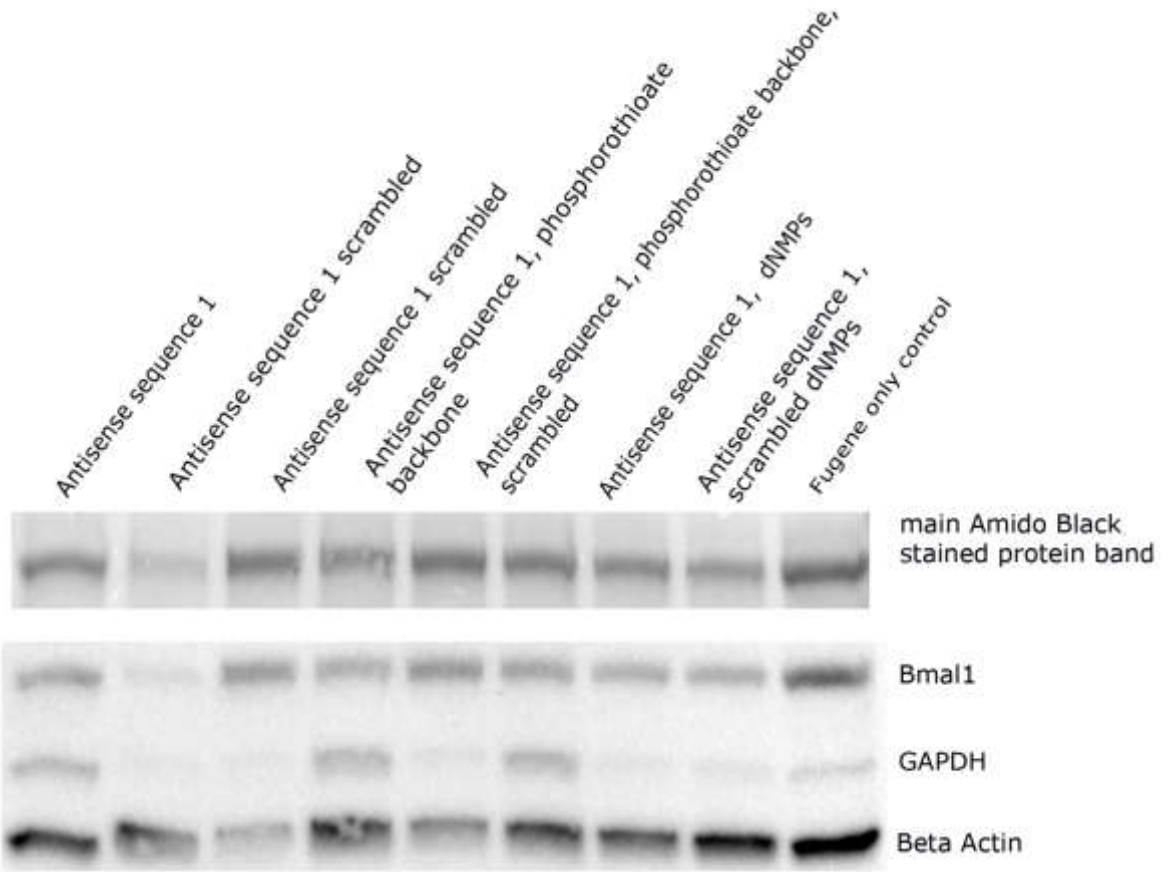
NIH 3T3 cells were seeded to be 60-70% confluent the following day. 2 hours prior to treatment the culture medium was refreshed. Thereafter they were treated as indicated above with asODNs, transfected with Fugene 6™. The cells were harvested 6 hours later and protein was extracted for Western blot analysis. a) Representative image of the membrane post blotting. b) The columns represent mean ± SEM Bmal1 protein relative to total protein loaded n=3. One-way ANOVA with Bonferroni post-hoc test was used to test statistical differences. \* p<0.05

**a****b**

#### Figure 4.4 Expression of the housekeeping proteins is not stable enough to use as a loading control

NIH 3T3 cells were seeded to be 60-70% confluent the following day. 2 hours prior to treatment the culture medium was refreshed. Thereafter they were treated as indicated above with asO<sub>d</sub>Ns, transfected with Fugene 6<sup>TM</sup>. The cells were harvested 6 hours later and protein was extracted for Western blot analysis. The columns represent mean  $\pm$  SEM: (a) GAPDH protein relative to total protein loaded n=3. (b)  $\beta$ -Actin protein relative to total protein loaded n=3. One-way ANOVA with Bonferroni post-hoc test was used to test statistical differences. \* p<0.05

a



b

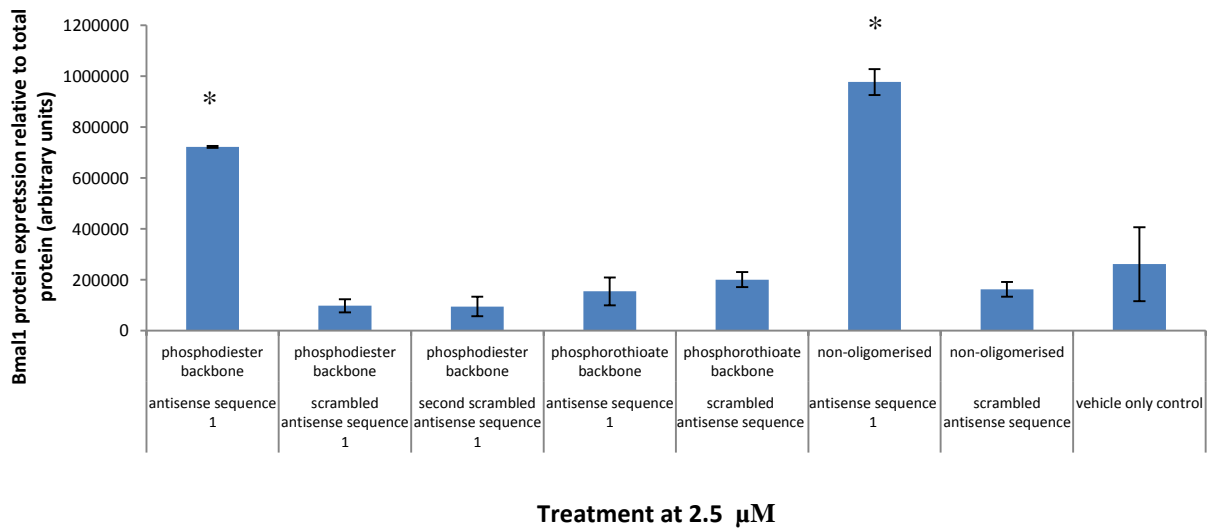


**Figure 4.5 24 hours following treatment none of the sequences knocks down Bmal1 with comparison to the vehicle only control**

NIH 3T3 cells were seeded to be 60-70% confluent the following day. 2 hours prior to treatment the culture medium was refreshed. Thereafter they were treated as indicated above with asODNs, transfected with Fugene 6™. The cells were harvested 24 hours later and protein was extracted for Western Blot analysis. a) Representative image of the membrane post blotting. b) The columns represent mean  $\pm$  SEM Bmal1 protein relative to total protein loaded n=3. One-way ANOVA with Bonferroni post-hoc test was used to test statistical differences. \* p<0.05

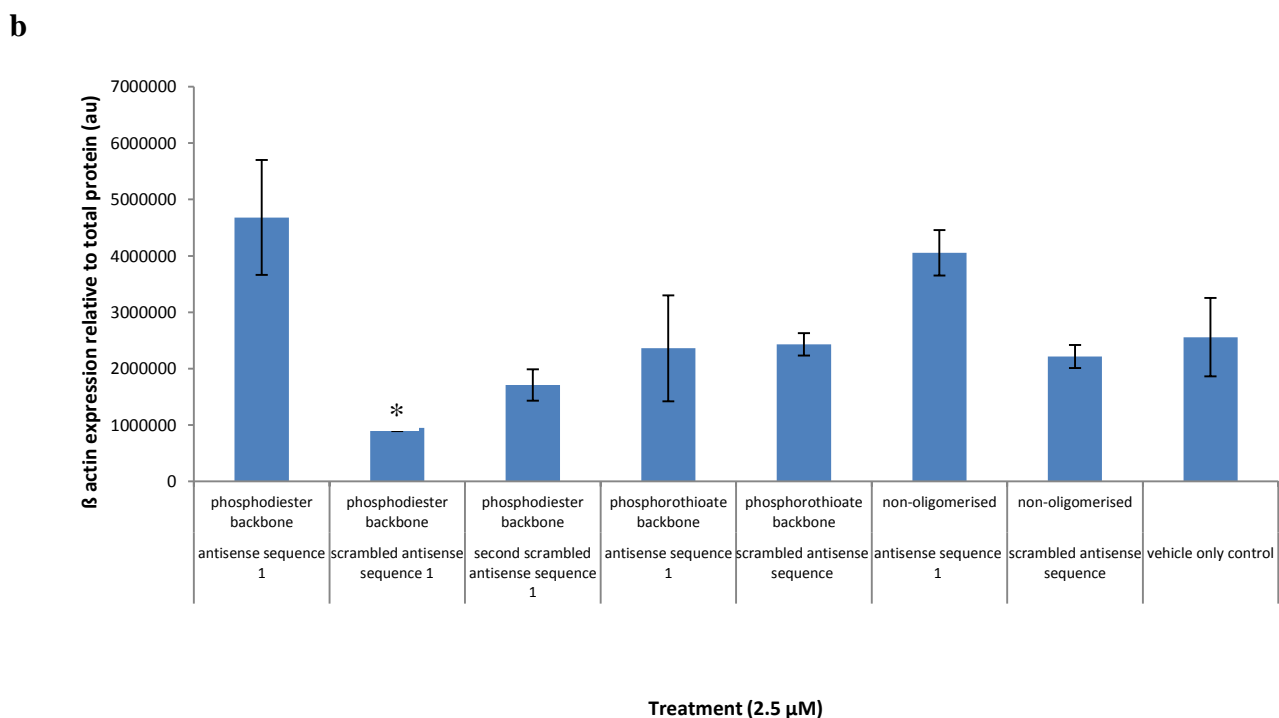
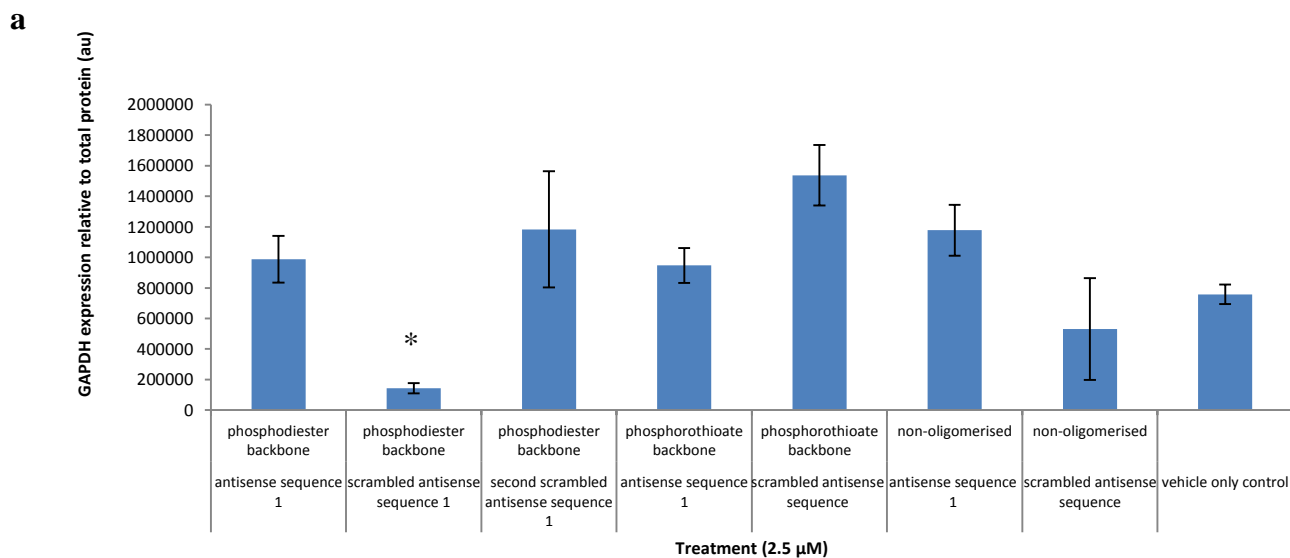
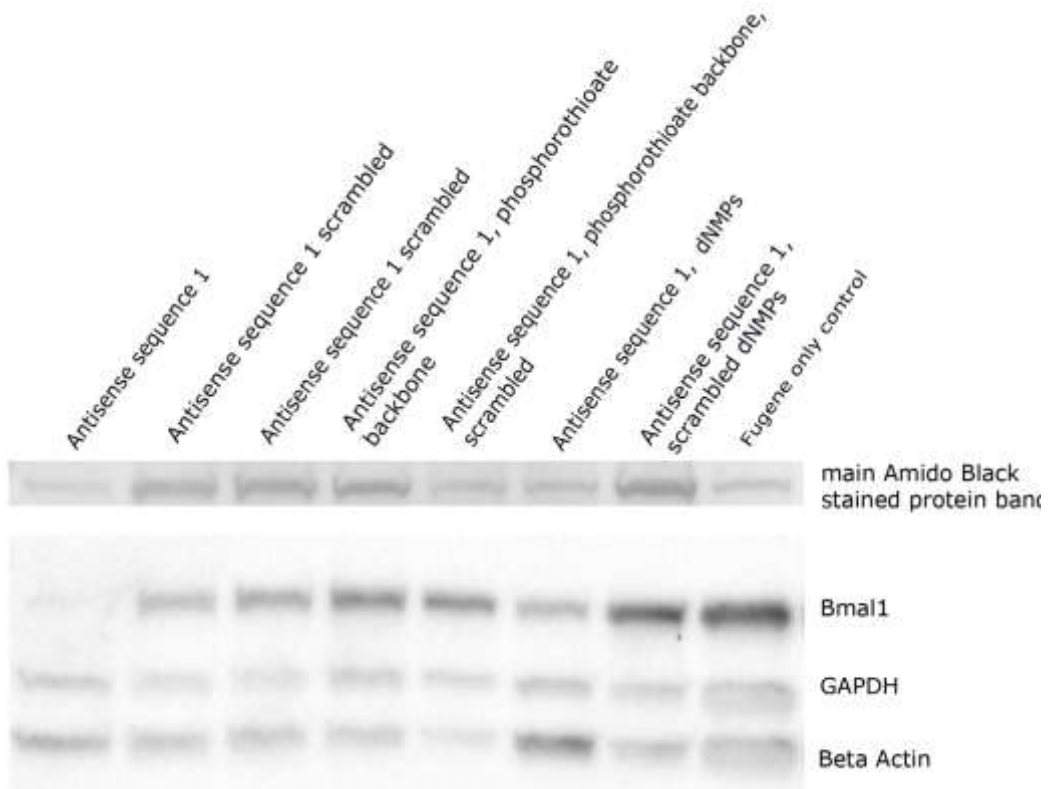


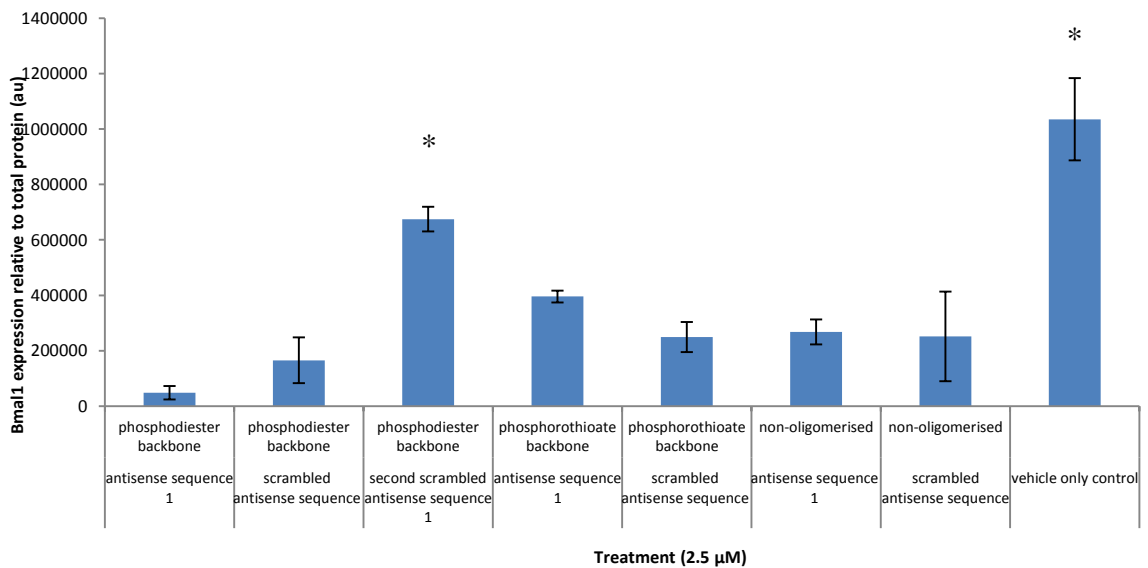
**Figure 4.6 At 24 hours both housekeeping proteins are significantly knocked down by the scrambled PO control**

NIH 3T3 cells were seeded to be 60-70% confluent the following day. 2 hours prior to treatment the culture medium was refreshed. Thereafter they were treated as indicated above with asODNs, transfected with Fugene 6™. The cells were harvested 24 hours later and protein was extracted for Western Blot analysis. The columns represent mean  $\pm$  SEM: (a) GAPDH protein relative to total protein loaded n=3. (b)  $\beta$ -Actin protein relative to total protein loaded n=3. One-way ANOVA with Bonferroni post-hoc test was used to test statistical differences. \* p<0.05

a

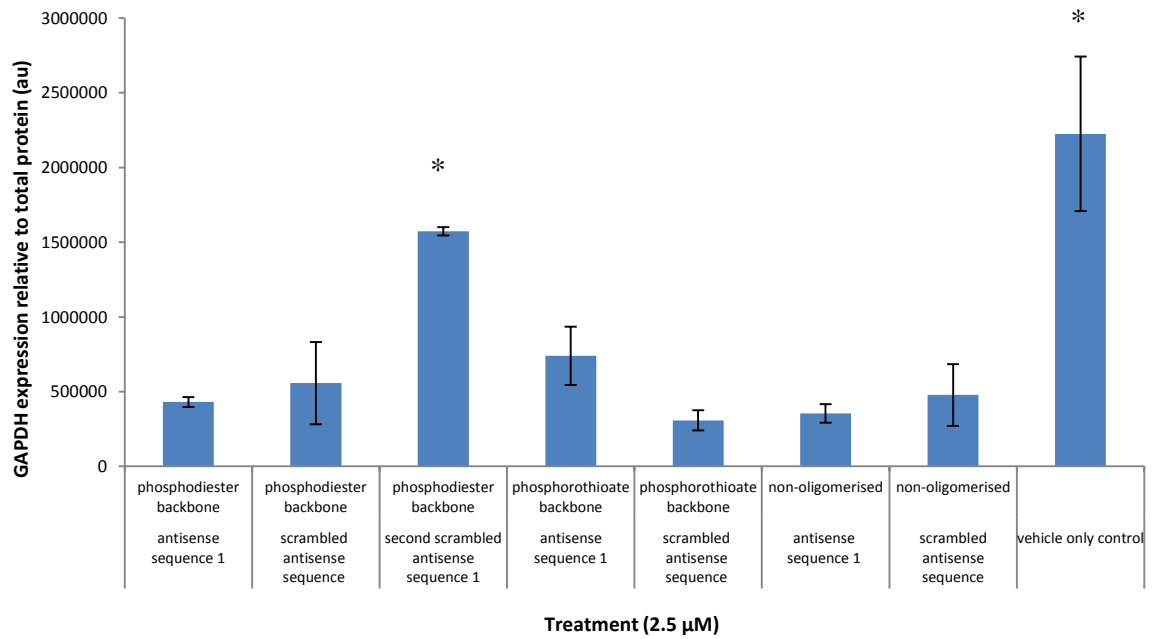
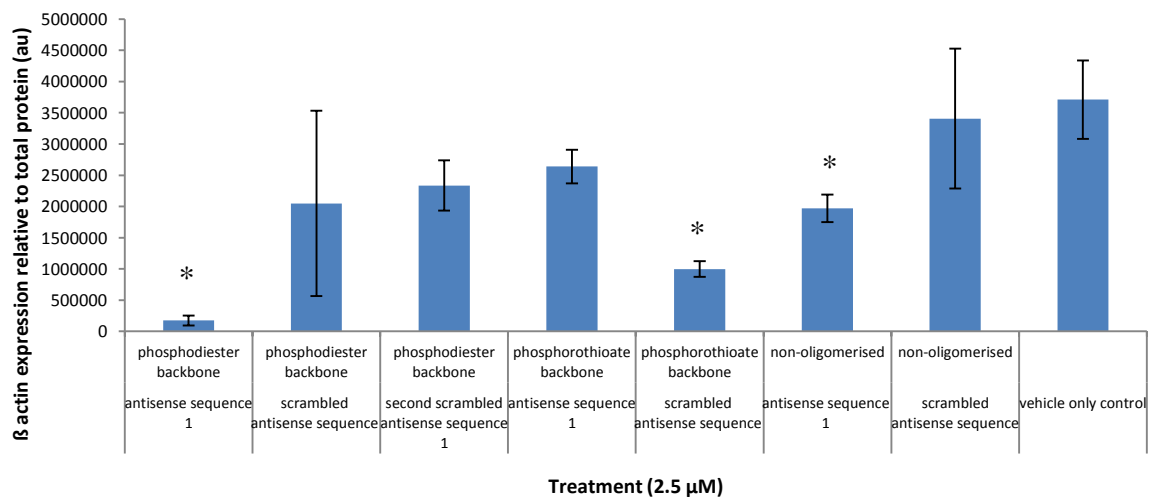


b



**Figure 4.7 At 48 hours post-treatment all of the asODNs/NMPs except scrambled PO 2 knock down Bmal1 with comparison to the vehicle only control**

NIH 3T3 cells were seeded to be 60-70% confluent the following day. 2 hours prior to treatment the culture medium was refreshed. Thereafter they were treated as indicated above with DNA in an aqueous solution, transfected with Fugene 6™. The cells were harvested 48 hours later and protein was extracted for Western blot analysis. a) Representative image of the membrane post blotting. b) The columns represent mean ± SEM Bmal1 protein relative to total protein loaded n=3. One-way ANOVA with Bonferroni post-hoc test was used to test statistical differences. \* p<0.05

**a****b**

### Figure 4.8 48 hours post-treatment both of the housekeeping proteins are affected by the asODNS/NMPs

NIH 3T3 cells were seeded to be 60-70% confluent the following day. 2 hours prior to treatment the culture medium was refreshed. Thereafter they were treated as indicated above with asODNs, transfected with Fugene 6<sup>TM</sup>. The cells were harvested 48 hours later and protein was extracted for Western Blot analysis. The columns represent mean  $\pm$  SEM: (a) GAPDH protein relative to total protein loaded n=3. (b)  $\beta$ -Actin protein relative to total protein loaded n=3. One-way ANOVA with Bonferroni post-hoc test was used to test statistical differences.  $p < 0.05$

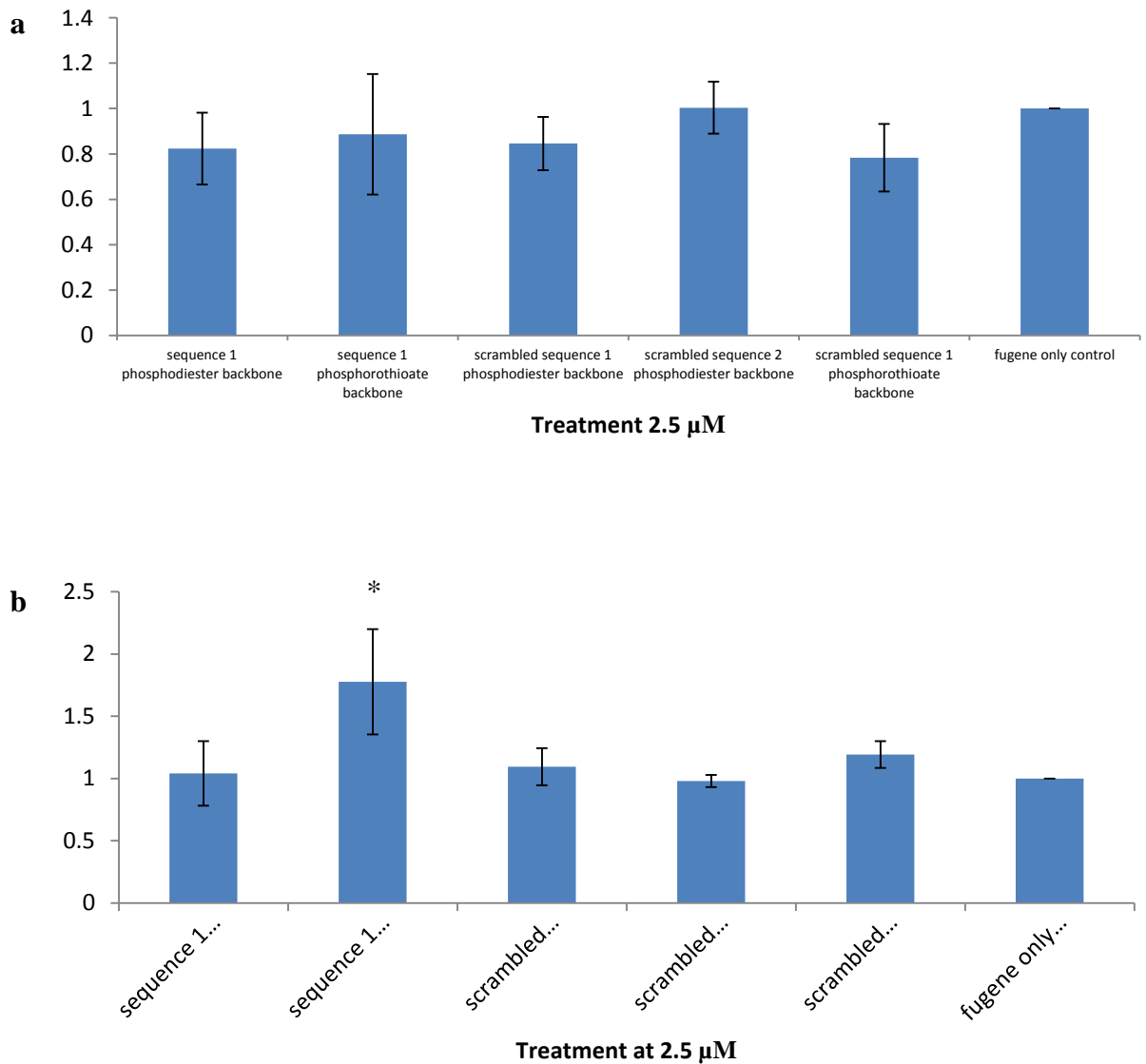


### Figure 4.9 Bmal1 mRNA significantly increases in response to 24 hours' treatment with a phosphorothioate asODNs

NIH 3T3 cells were seeded to be 60-70% confluent the following day. 2 hours prior to treatment the culture medium was refreshed. Thereafter they were treated as indicated above with asODNs, transfected with Fugene 6™. The cells were harvested a) 6 hours later b) 24 hours later and RNA was isolated for RT-PCR. All data were normalised to GAPDH and SDHA. Columns represent the fold change of Bmal1 mRNA expression with comparison to the control  $\pm$  SEM. One-way ANOVA with Bonferroni post-hoc test was used to test statistical differences.  $p < 0.05$

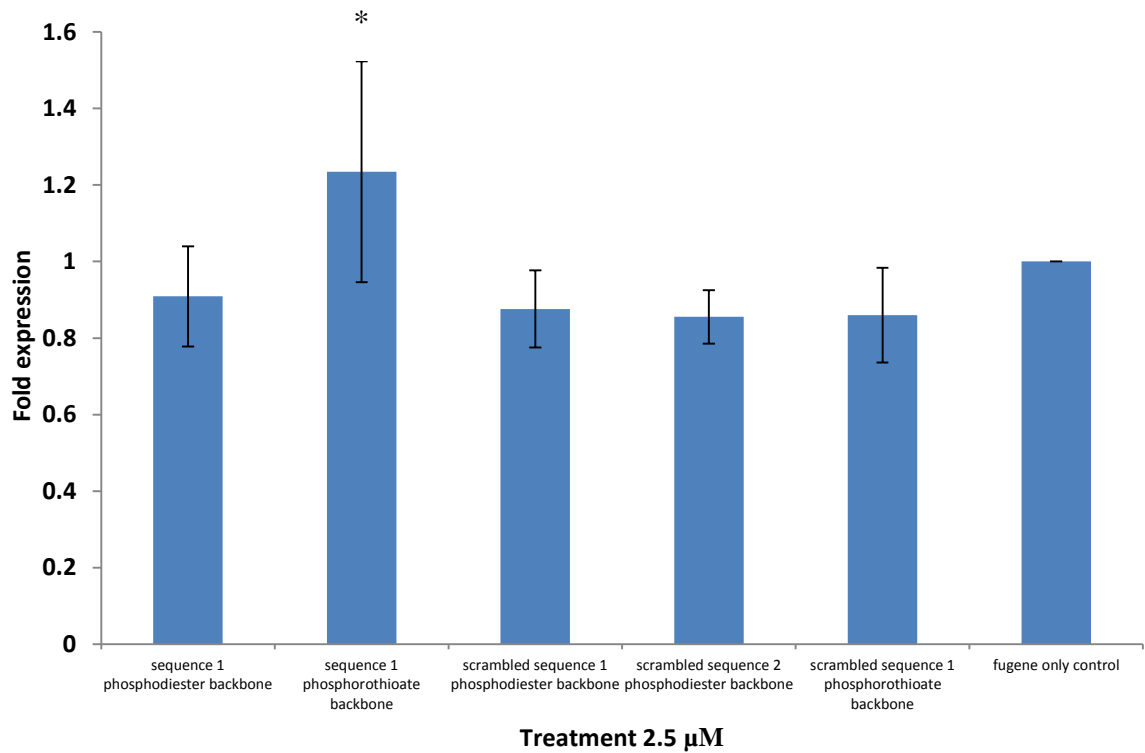


**Figure 4.10 Bmal1 mRNA significantly increases in response to 48 hours' treatment with a phosphorothioate asODNs**

NIH 3T3 cells were seeded to be 60-70% confluent the following day. 2 hours prior to treatment the culture medium was refreshed. Thereafter they were treated as indicated above with asODNs, transfected with Fugene 6™. The cells were harvested 48 hours later and RNA was isolated for RT-PCR. All data were normalised to GAPDH and SDHA. Columns represent the fold change of Bmal1 mRNA expression with comparison to the control  $\pm$  SEM. One-way ANOVA with Bonferroni post-hoc test was used to test statistical differences.  $p < 0.05$

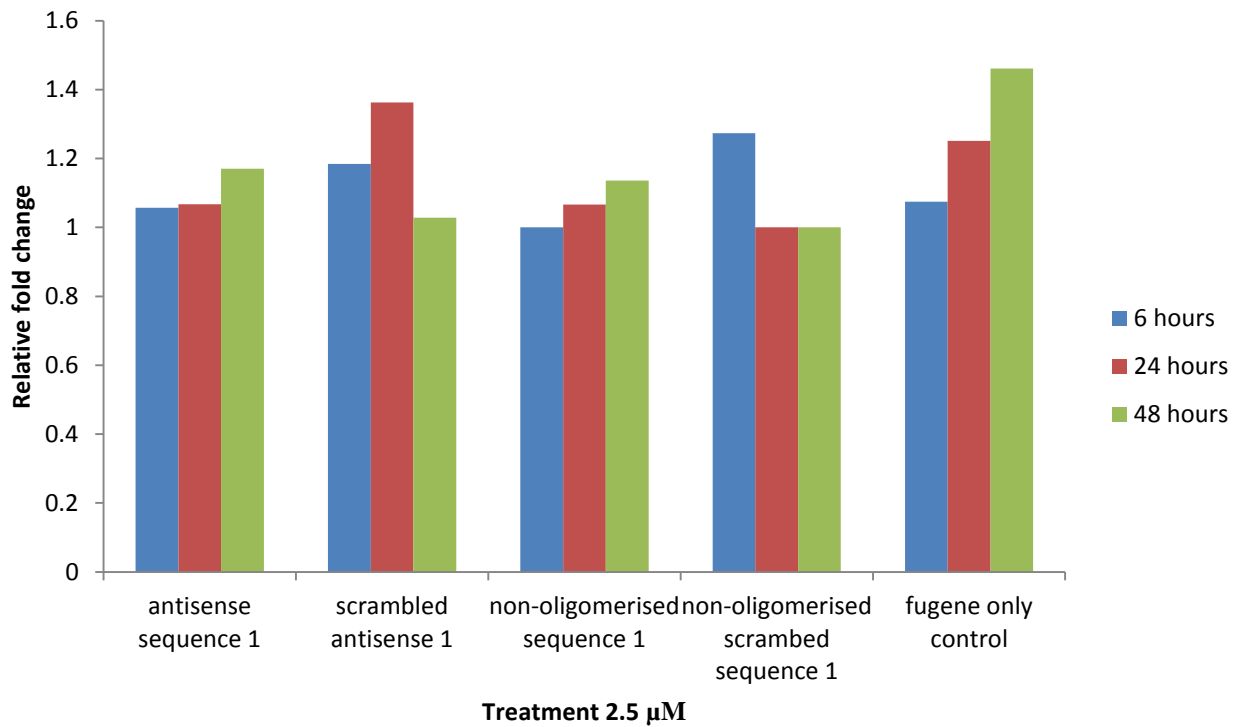


**Figure 4.11 Bmal1 mRNA is not affected by antisense or dNMPs**

NIH 3T3 cells were seeded to be 60-70% confluent the following day. 2 hours prior to treatment the culture medium was refreshed. Thereafter they were treated as indicated above with asODNs, transfected with Fugene 6™. The cells were harvested 6, 24 and 48 hours later and RNA was isolated for RT-PCR. All data were normalised to GAPDH and SDHA. Columns represent the fold change of Bmal1 mRNA expression.

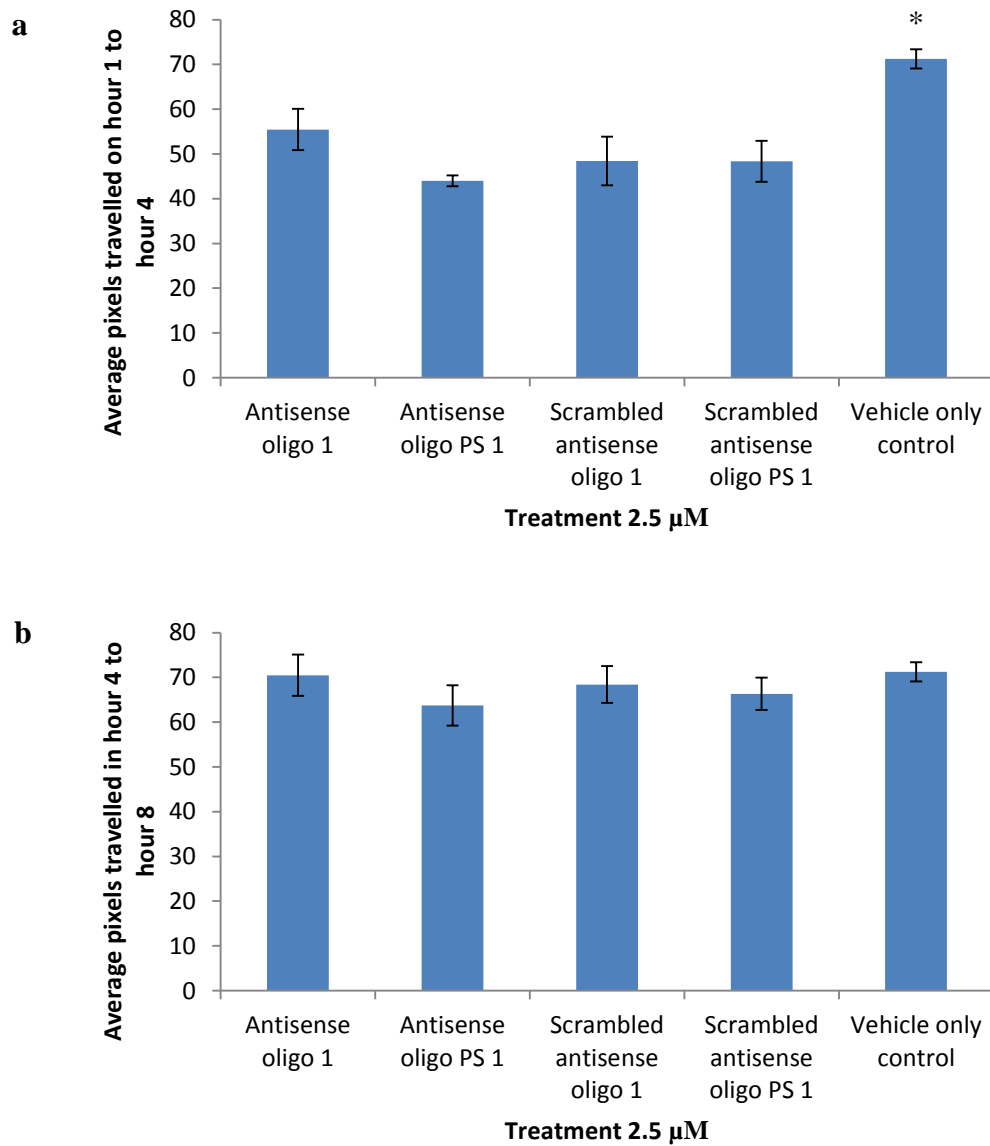


**Figure 4.12 asODNs do not increase migration rate of fibroblasts**

Scratch wound assays were prepared and average distance of cell migration was measured as described as per Methods 2.4. Columns represent mean pixels travelled in a) the first 4 hours b) the second 4 hours  $\pm$ SEM. One-way ANOVA with Bonferroni post-hoc test was used to test statistical differences.  $p < 0.05$

## 4.7. Discussion

The original basis for this project was to develop an antisense oligonucleotide strategy to transiently stop the circadian clock by knocking down Bmal1 as a topically applied pluronic based gel. Unfortunately the asODNs do not knock down Bmal1 on a sequence specific basis; the scrambled control sequence is as effective at knocking down Bmal1 as the targeted sequence. Additionally, the asODNs appear to have a toxic effect on the housekeeping proteins. The effect on Bmal1 protein at 48 hours post-treatment is the same for phosphodiester backbone sequence 1, scrambled phosphodiester backbone sequence 1 and non-oligomerised sequence 1 which suggests that the asODN is not entering the cells as an intact oligonucleotide, but is being rapidly catalysed and that it is the dNMPs which are exerting these effects on the cells as shown by earlier studies (Wickstrom, 1986; Maria Koziolkiewicz, Gendaszewska, Maszewska, Stein, & Stec, 2001)

Further, no knockdown of Bmal1 mRNA was seen with any of the asODNs or dNMPs at multiple time points when measured by RT-PCR. The only significant difference seen at the mRNA level was an increase in Bmal1 following 24 and 48 hour treatment with the phosphorothioate backbone analogue of antisense sequence 1. An increase in cell proliferation was seen by Koziolkiewicz et al (2001) when they treated HL-60 and HUVEC cells with dNMPSs; they hypothesized that this could be due to P2 receptors. It is possible that dNMPSs could have an effect on purinergic signalling. Regardless, these investigations have shown that antisense oligonucleotides in this format do not fulfil the requirements of the project so alternative methods of knocking down Bmal1 will be investigated in the following chapters. Functional assays showed that none of the asODNs had an effect on cell migration rate; in fact, they significantly reduced the rate of migration in the first 4 hours of the assay, perhaps as a result of the toxicity previously discussed.

# 5. Alternative methods of RNA interference

---

## 5.1. Ribonucleic acid interference (RNAi)

RNA interference is:

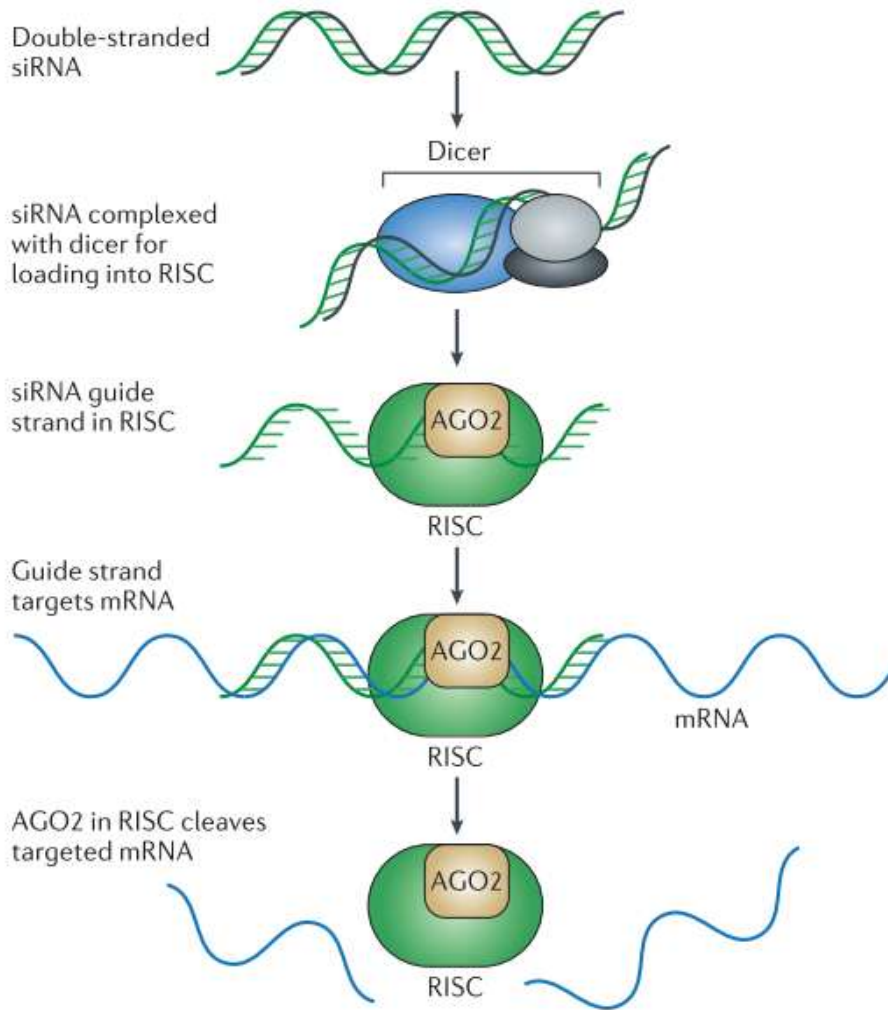
“RNA interference (RNAi). A form of post- transcriptional gene silencing in which the expression or transfection of double- stranded RNA induces degradation by nucleases of the homologous endogenous transcripts, resulting in the reduction or loss of gene activity.” (Kole et al., 2012)

RNA interference (RNAi) was first demonstrated in *Caenorhabditis elegans* (*c.elegans*) in 1997 with the introduction of double stranded ribonucleic acid (dsRNA) designed to interfere with the expression of *unc-22*, a gene that encodes a myofilament. The injected nematodes displayed the phenotype of a *unc-22*<sup>-/-</sup> following a dose representing only a few molecules of dsRNA per cell which led the investigators to conclude that there must be some amplification or catalytic effect to produce such a phenotype.(Fire et al., 1998) The mechanism involved the dsRNA being cleaved to several short interfering RNAs (siRNAs) approximately 21-22 nucleotides long which lead to an interaction with RNA-induced silencing complex (RISC). Within RISC the siRNA unfolds and the antisense strand binds to the mRNA which leads to the cleavage of the messenger RNA (mRNA) by argonaute 2. (Kole et al., 2012) The conversion of dsRNA to siRNAs is not possible in mammalian cells and it was not until 2001 that it was discovered that synthetic siRNA can target mRNA in human cells (Elbashir et al., 2001).

### 5.1.1. siRNA

The first *in vivo* study using siRNA was in mice in 2003 (Ashcroft et al., 2012) where siRNA targeted to knock down Fas was used to prevent cytotoxicity in hepatitis. One limitation found was that unmodified siRNA is degraded by endogenous nucleases very quickly. For that reason, in clinical trials there has been a focus on local delivery (Kole et al., 2012). Another potential pitfall with siRNA as a clinical tool is that there are possible off target effects; in particular the cleavage of the siRNA to smaller fragments can lead to microRNA-like silencing of off-target transcripts (Jackson et al., 2006; Jackson & Linsley, 2010). siRNA can also illicit an immune response via activation of Toll-like receptors resulting in the activation of pro-inflammatory pathways (de Fougerolles et al., 2007). Another possible outcome is the formation of triesters which inhibit global protein synthesis through binding to the terminus of tRNA and mRNA (Miller et al., 1977). For these reasons pharmaceutical companies reduced investment in siRNAs as systemically delivered therapies (Kole et al., 2012). It is still widely used *in vitro* in research to explore the effects of knocking down specific proteins. Several companies have developed bespoke modifications to enhance the longevity of the molecules (for example Silencer Select™, Life Technologies (Thermo Fisher Scientific Inc.)).

### a Small interfering RNA



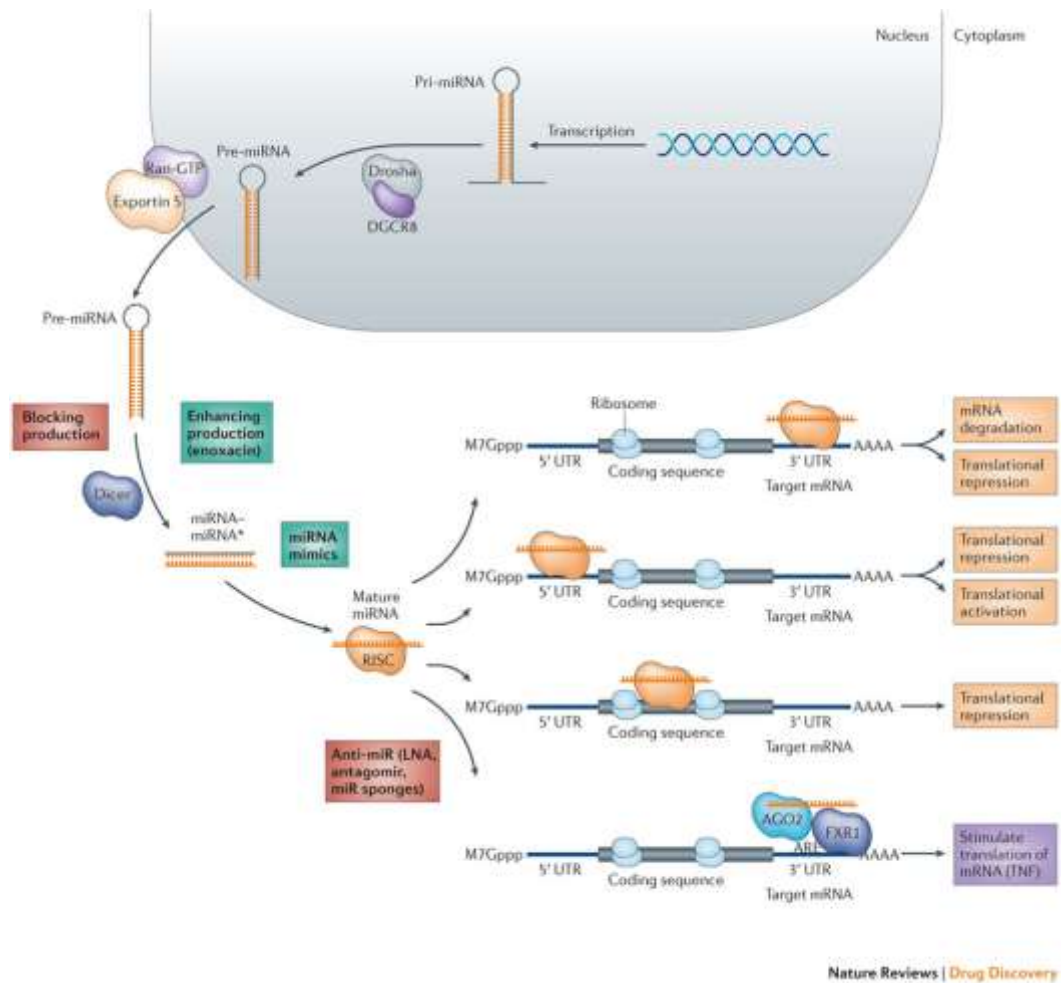
(Kole et al., 2012)

**Figure 5.1 The mechanism of action of siRNA**

### 5.1.2. microRNA

microRNA (miRNA) is a class of non-coding RNAs in the genomes of plants and mammals (Lagos-Quintana, Rauhut, Meyer, Borkhardt, & Tuschl, 2003). miRNAs were first discovered in *Caenorhabditis elegans* during the study of developmentally regulated *lin-4* and *let-7* (Reinhart et al., 2000). Mature miRNAs are approximately 21 nucleotides long. They are derived from 60-80 nucleotide double stranded hairpin RNA which are ultimately excised by Dicer RNase III in the cytoplasm (Lee, 2002). Originally it was thought that the 3' untranslated region of the miRNA binds to the

5'untranslated region of the mRNA via a 'seed' region of 6-7 nucleotides, leading to the repression of translation of the protein (Lagos-Quintana et al., 2003). Some miRNAs have been shown to activate translation (Vasudevan, Tong, & Steitz, 2007) and it is possible that other mechanisms for regulatory control by miRNAs are still to be discovered (Tay, Zhang, Thomson, Lim, & Rigoutsos, 2008; Ling, Fabbri, & Calin, 2013).



(Ling et al., 2013)

**Figure 5.2 Mechanisms of miRNA regulation of gene expression**

### 5.1.3. Short Hairpin RNA

Short hairpin RNA (shRNA) consists of 19-22 base pairs linked by a 4-11 nucleotide loop which bears a similarity to the natural hairpin structure seen in endogenous

microRNA. Once incorporated into the cell shRNA is cleaved into siRNA and then interferes with protein translation in the same way as siRNA. The predominant differences between siRNA and shRNA are that shRNA can be transfected in plasmid form or using viral vectors and that shRNA can be used to generate stable cells lines.(C. B. Moore, Guthrie, Huang, & Taxman, 2010) (more detail to follow in the section ‘Delivery methods’)

(Santa Cruz Biotechnology, n.d.)

#### **5.1.4. Overexpression of a dominant negative protein**

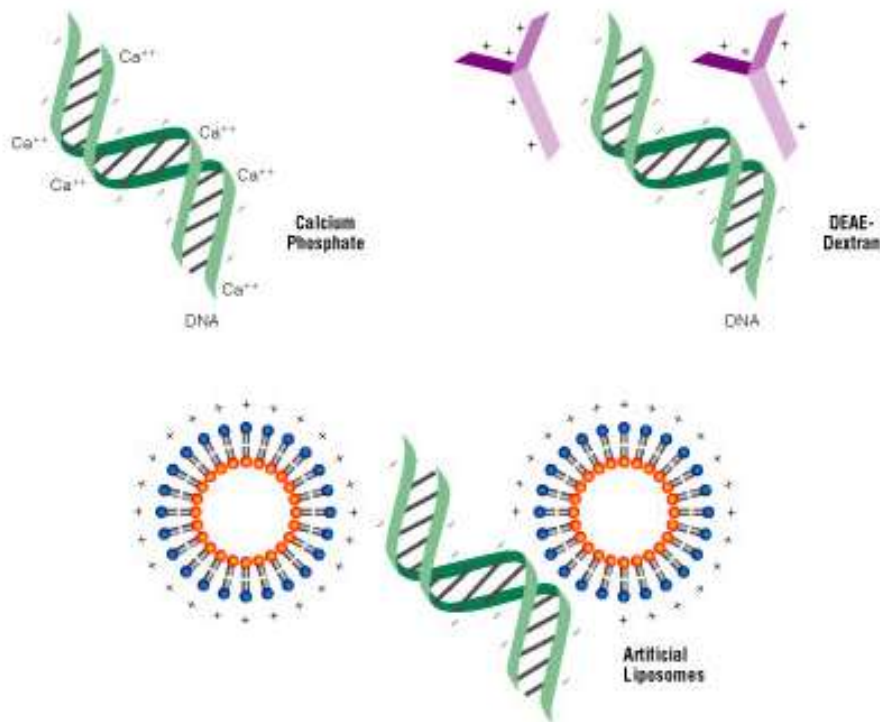
Another way to disrupt the function of a protein is to overexpress a truncated non-functional version. Bmal1 and CLOCK form a heterodimer that drives the transcription of downstream circadian proteins, therefore overexpression of a dominant negative mutant of Bmal1 that still maintains the moieties that enable it to bind to CLOCK but disable the transcriptional activity the circadian can be stopped (Kiyohara et al., 2006).

## **5.2. Delivery methods**

### **5.2.1. Transfection**

Transfection is the term used for the non-virally mediated introduction of nucleic acids into eukaryotic cells. Most laboratories use a transfection reagent of some type to facilitate this as naked nucleic acids are negatively charged so are repelled by the negatively charged cell membrane. One class of chemical transfection reagents are the cationic polymers such as Diethylaminoethyl-dextran (DEAE-dextran) (Pagano & Vaheri, 1965), or polybrene (Kawai & Nishizawa, 1984) which bind to the nucleic acids and gives the complex an overall positive charge. Another method to change the net charge is co-precipitation with calcium phosphate (Graham & van der Eb, 1973). Other positively charged polymers that have been used are polyethyleneimine (PEI) (Boussif

et al., 1995) and dendrimers; branched polyamidoamine polymers to effectively encapsulate the nucleic acids and enhance their uptake into the cytosol (Haensler & Szoka).



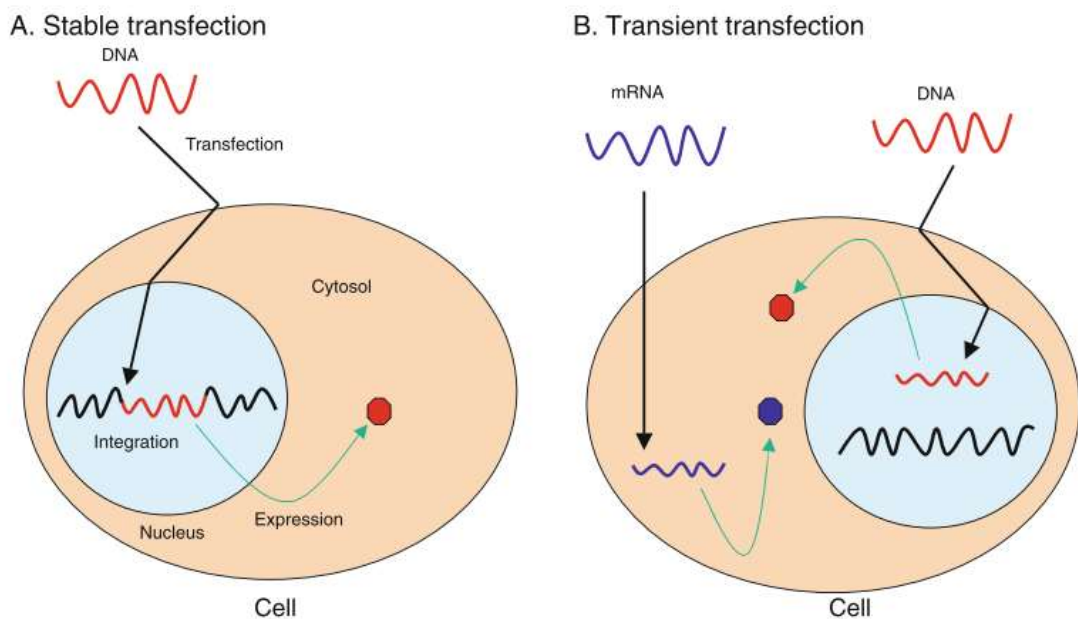
(Promega Corp, 2015)

### Figure 5.3 The mechanism of action of siRNA

Another class of delivery reagent is the cationic liposome family of reagents (sometimes this type of transfection is referred to as ‘lipofection’). The principle is the same; the aim is to change the charge on the nucleic acid-liposomal complex to facilitate permeation of the cell membrane and also to protect the encapsulated nucleic acids from enzymatic degradation. An additional benefit of this method is that it can be used *in vivo* (P. L. Felgner et al., 1987; J. Felgner, Bennett, & Felgner, 1993) and also to generate stably integrated nucleic acids into cells for long-term experiments. The majority of proprietary transfection reagents available commercially use versions of this chemistry (e.g. Lipofectamine, Life Technologies). A commonly used non-lipid based transfection reagent is Fugene 6 (Promega) which is popular with cell biologists as it can be used in serum-containing medium unlike lipofection reagents.

### 5.2.2. Transient versus Stable Transfection

In transiently transfected cells the nucleic acids introduced into them can either cause a protein to be over expressed (in the case of mRNA transfection) or knocked down transiently, i.e. for a few days, whilst the constructs are still present in the culture medium/cytosol. With stable transfection the targeted DNA is incorporated into the genome and the altered expression of the target protein persists. Typically the stably transfected cells are selected for inclusion of the desired construct via either antibiotic resistance or fluorescence-activated cell sorting (FACS). This is achieved by cloning antibiotic resistance to, for example, puromycin, into the RNAi construct or by adding a fluorescent tag. Post-transfection cells are incubated for a minimum of 48 hours to allow time for the expression of the resistance gene or fluorescent marker and are sorted by addition of puromycin (or other antibiotic selector such as G418 or hygromycin) to the culture medium, following which cells not expressing the desired construct will die off or can be sorted via FACS as mentioned above.



(T. K. Kim & Eberwine, 2010)

### 5.2.3. Physical methods of transfection

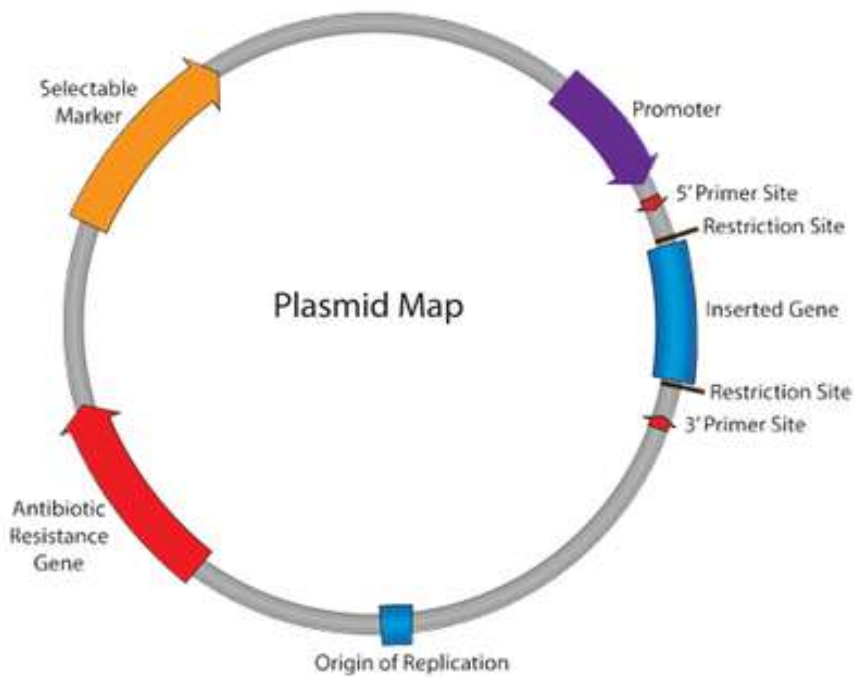
Nucleic acids have been delivered into hard-to-transfect cells via direct microinjection (Capecchi, 1980), biolistics (gene gun) or electroporation. Microinjection is very time-consuming and, for this reason, is not a popular method. Biolistics is the process of coating gold particles with the DNA and blasting it at the cells (Ye, Daniell, & Sanford, 1990). Electroporation involves suspension of the cells in a suitable buffer (for example growth medium) and passing an electrical current through specially made cuvettes. This perturbs the stability of the cells membranes transiently and enables the entry of the nucleic acids (Shigekawa & Dower, 1988). The main disadvantage of the latter two methods is that there is a high level of cell death.

#### **5.2.4. RNAi delivery vectors**

shRNA is delivered either via bacterial plasmids or a viral vector.

##### **Plasmids**

In order to be useful as a cloning tool, plasmids require a bacterial origin of replication, an antibiotic resistance gene, and one or more unique restriction enzyme sites. This permits the propagation of the plasmid within bacteria and allows selection against any bacteria not carrying the plasmid and the restriction enzyme site(s) allow for the cloning of a fragment of DNA into the plasmid. See Figure 5.4.



(Addgene, n.d.-b)

**Figure 5.4 A plasmid map displaying the qualities required for use in transfection**

### 5.2.5. Viral delivery

Viral delivery will be discussed in Chapter 6.

## 5.3. Methods and materials

### 5.3.1. siRNA

NIH 3T3 cells were seeded to be 70% confluent the following day. *Silencer Select*<sup>™</sup> siRNA sequences targeted to Bmal1, GAPDH (positive control) and non-targeting control (all Life Technologies Ltd.) were transfected at the recommended concentration (10 nM) using Fugene 6<sup>™</sup> as described in Methods 2.3.1. Protein expression was measured by Western blotting and mRNA by RT-PCR. In addition to these siRNA constructs a FAM-tagged siRNA was used to assess transfection efficiency. FAM is a fluorescein based fluorophore that is excited by 488 nm wavelength light. FAM-tagged siRNA was used to transfect NIH 3T3s using several different transfection reagents and

ratios of reagent to siRNA at multiple cells densities in order to ascertain the optimal transfection conditions.

### **5.3.2. miRNA**

NIH 3T3 cells were seeded to be 70% confluent the following day. Synthetic mirVana™ mimics and inhibitors (both mir-142-3P) and controls (all Life Technologies Ltd.) were transfected at the recommended concentration (10 nM) using Fugene 6™ as described in Methods 2.3.1. Protein expression was measured by Western blotting and mRNA by RT-PCR. mirVana™. miRNA mimics are designed to mimic the endogenous miRNA mir-142-3p that down-regulates Bmal1 protein translation (Tan et al., 2012). miRNA inhibitors are designed to bind to the miRNA and down-regulate their activity, so in this case should up-regulate the expression of Bmal1.

### **5.3.3. Dominant negative Bmal1**

A Bmal1 dominant negative (DN) plasmid and an empty vector (based on the p.CLNC backbone from Imgenex - a kind gift from T. Tamai) was transfected using Fugene 6™ as described in Methods 2.3.1.

On a separate occasion cells were electroporated with 50 µg Bmal1DN plasmid DNA using a BTX ECM 830 with the following settings taken from the BTX protocol database:

**Table 5.1 Electroporation settings**

Mode	T Set on 500V/CAPACITANCE/RESISTANCE (LV)
Capacitance	C 1500 $\mu$ F
Resistance	R R4 (72ohm)
Chamber Gap	BTX Disposable Cuvette P/N 620 (2mm gap)
Charging Voltage	S 350V
Desired Field Strength	E 1.75kV/cm
Desired Pulse Length	t 13 msec

The p.CLNC.Bmal1DN plasmid contains a FLAG tag which is a short polypeptide (Hopp et al., 1988) that enables identification of the protein by immunofluorescence using an anti-FLAG antibody and a fluorophore conjugated secondary antibody. By counterstaining with Hoescht and measuring the ratio of FLAG-positive cells to FLAG-negative cells the transfection efficiency can be assessed.

## 5.4. Transfection optimisation

As it became apparent that the RNAi was not having an effect, RT-PCR measurement of Bmal1 knockdown was repeated using the most successful transfection reagent for siRNA (Interferin). See Figure 5.9. Another approach used was co-transfection with enoxacin at 50  $\mu$ M (Sigma Ltd.). It is a broad-spectrum fluoroquinone based antibiotic reputed to have a beneficial effect on the transfection efficiency of siRNA and miRNA (Shan et al., 2008). Transfection efficiency was assessed by seeding the NIH 3T3s in Millipore 8 well chamberslides, transfecting them as per the manufacturers' instructions at a variety of concentrations and cell densities. 48 to 72 hours later cells were fixed in

4% PFA, permeabilised with PBS-Triton (0.1% v/v) and, in the case of the FLAG-tagged construct, incubated with mouse monoclonal anti-FLAG primary antibody for 2 hours at room temperature whilst on a shaker, washed three times with PBS-Triton and then incubated with goat anti-mouse Alexa 488 conjugated secondary antibody for an hour at room temperature. After more washes the cells were counterstained with Hoescht to stain the nuclei, the slides were mounted with glycerol-PBS mounting medium and coverslips were sealed with clear nail-varnish prior to imaging. Transfection efficiency was assessed visually as the proportion of green-stained cells to the number of blue-stained nuclei.

**Table 5.2 Transfection reagents tested**

<b>Transfection reagents</b>	<b>Manufacturer</b>
Lipofectamine L3000	Life Technologies
RNAiMAX	Life Technologies
Lipofectamine LTX	Life Technologies
Oligofectamine	Life Technologies
Interferin	Polyplus transfection
Jetprime	Polyplus transfection
Fugene 6	Promega
Fugene HD	Promega
TransIT	Mirus

## 5.5. Results

### 5.5.1. Short Interfering RNA

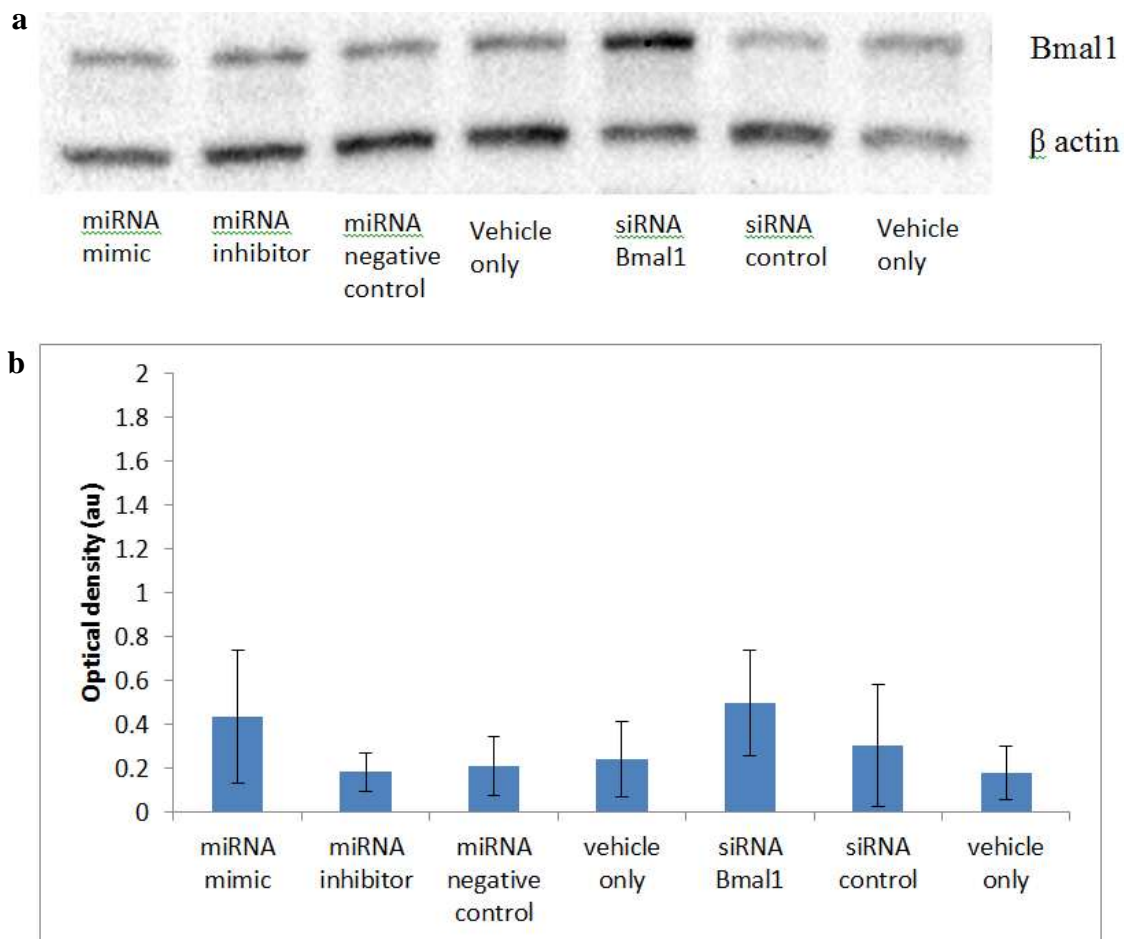


#### Figure 5.5 Neither miRNA nor siRNA knock down Bmal1 protein 48 hours post-treatment

NIH 3T3 cells were seeded to be 60-70% confluent the following day. 2 hours prior to treatment the culture medium was refreshed. Thereafter they were treated with 10 nM miRNA/siRNA, transfected with Fugene 6<sup>TM</sup>. The cells were harvested 48 hours later and protein was extracted for Western blot analysis. a) Representative image of the membrane post blotting. b) The columns represent mean  $\pm$  SEM Bmal1 protein relative to  $\beta$ -actin. n=3. One-way ANOVA with Bonferroni post-hoc test was used to test statistical differences. No significant differences were found.

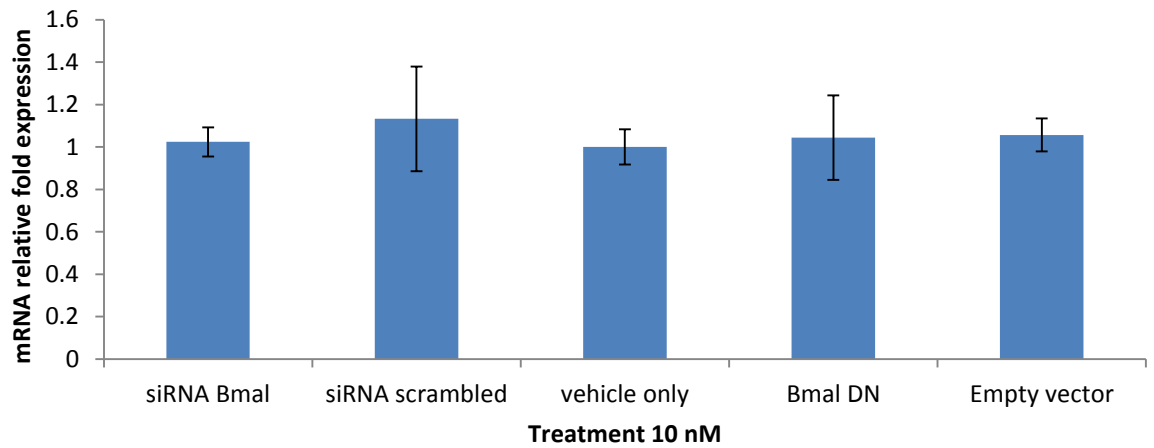


**Figure 5.6 neither siRNA nor overexpression of Bmal1 DN reduce the expression of Bmal1 48 hours post-treatment**

NIH 3T3s were seeded to be 60-70% confluent the following day. They were transfected with the siRNA sequences at 10 nM using Fugene 6™. They were harvested at the time points as indicated and RNA was isolated for RT-PCR as described in the Methods section. Columns represent Bmal1 mRNA fold expression  $\pm$  SEM relative to SDHA in NIH 3T3 cells, n = 3. Statistical analysis was done using one-way ANOVA on SPSS. There was no significant difference.

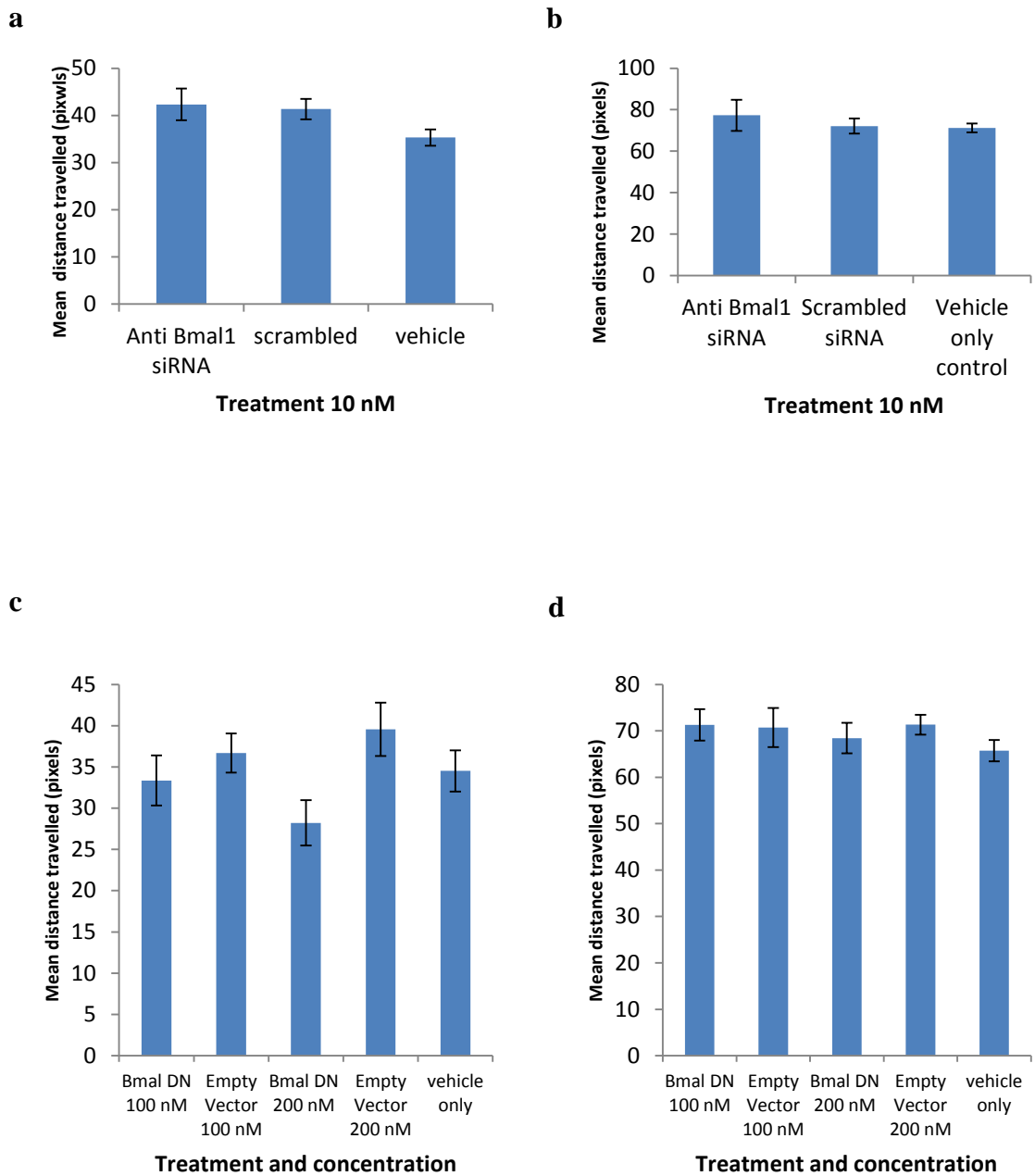


**Figure 5.7 Neither siRNA nor Bmal1 DN overexpression enhance the migration rate of NIH 3T3s**

NIH 3T3s were seeded to be ~70% confluent the day before transfection. 48 hours post-transfection the scratch wound assay was done as per Methods section 2.4. Columns represent mean distance travelled from the wound edge in pixels  $\pm$  SEM in the first 4 hours a) & c) then 4 to 8 hours in b) and d). n = 3 (8 biological replicates per experiment). Statistical analysis was done by one way ANOVA using SPSS. No statistical differences were found.

## 5.6. Micro RNA

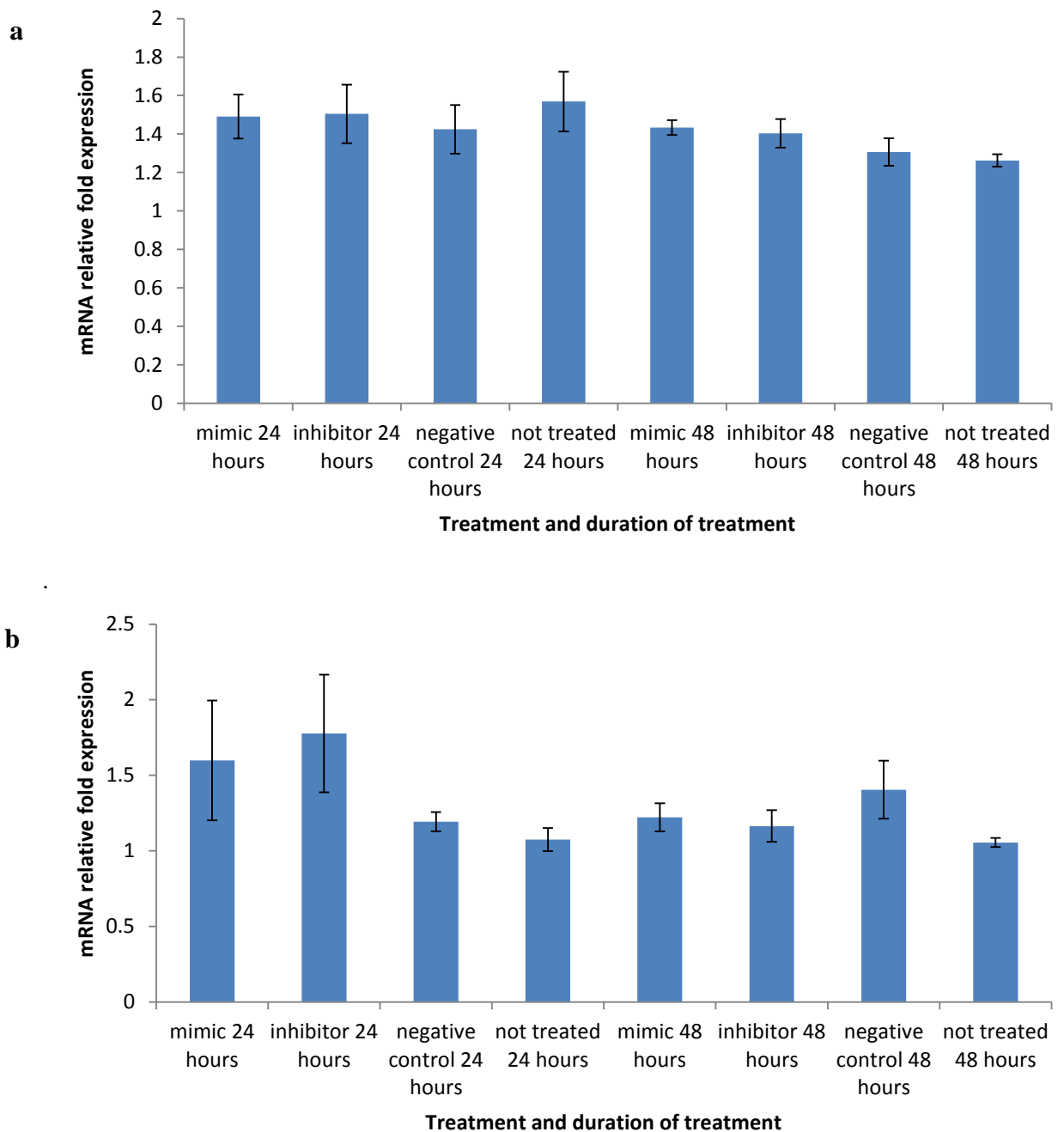


### Figure 5.8 miRNA mimics do not reduce mRNA expression of Bmal1

Fibroblasts were seeded to be 60-70% confluent the following day. They were transfected with the miRNA sequences at 10 nM using Fugene 6™. They were harvested at the time points as indicated and RNA was isolated for RT-PCR as described in the Methods section. Columns represent Bmal1 mRNA fold expression  $\pm$  SEM relative to SDHA in a) NIH 3T3 cells, b) primary murine fibroblasts  $n = 3$ . Statistical analysis was done using one-way ANOVA on SPSS. There was no significant difference between the treatments at both time points in either type of cell.

### 5.6.1. Transfection optimisation

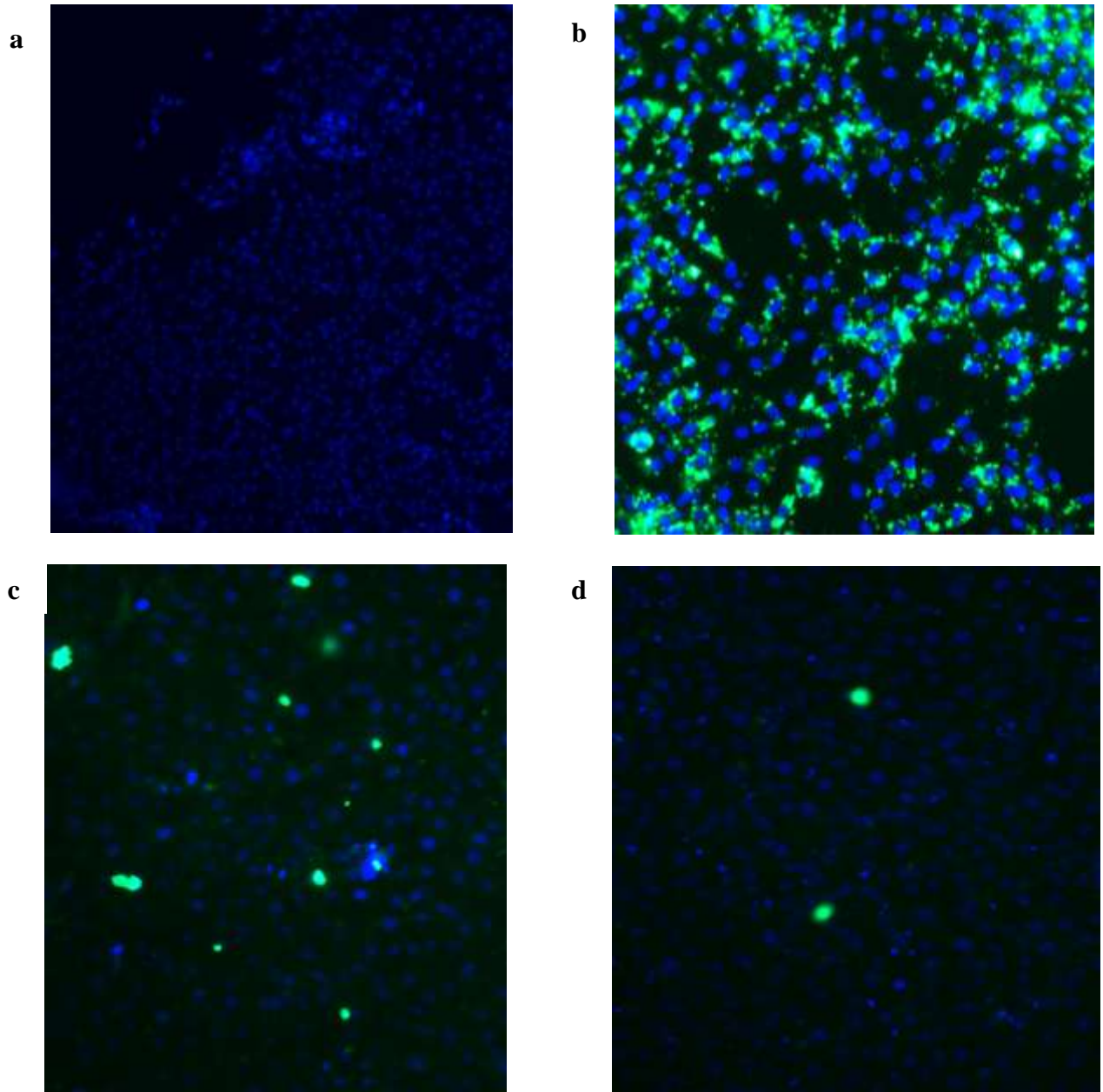


**Figure 5.9 Representative images of immunofluorescent assessment of transfection efficiency. Interferin is the most successful transfection reagent for FAM-tagged siRNA**

Blue = Hoechst nuclear stain. Green =

- a) Flag tagged Bmal1DN, immunofluorescence with Alexa 488 secondary antibody 48 hours post electroporation,
- b) FAM-tagged siRNA 72 hours post double transfection with Interferin
- c) Flag tagged Bmal1DN, immunofluorescence with Alexa 488 secondary antibody 48 hours post transfection with Eugene HD

d) Flag tagged Bmal1DN, immunofluorescence with Alexa 488 secondary antibody 48 hours post transfection with LTX

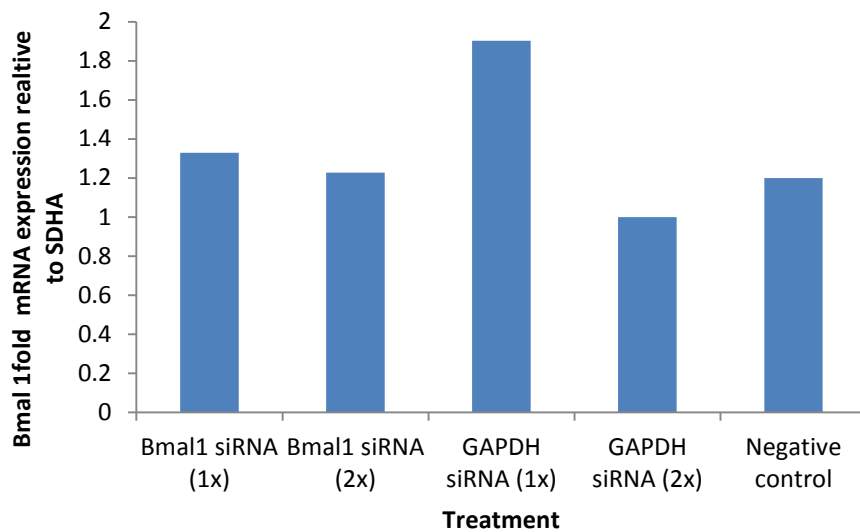


**Figure 5.10 The optimised Interferin transfection protocol conditions did not produce a knock-down of Bmal1 or GAPDH after 72 hours**

NIH 3T3s were seeded to be 60-70% confluent the following day. They were transfected with the siRNA sequences at 10 nM (1x) or 20 nM (2x) using Interferin™. The following day they were retransfected using half the dose of the previous day. They were harvested 72 hours after the first transfection and RNA was isolated for RT-PCR as described in the Methods section. Columns represent Bmal1 mRNA fold expression relative to SDHA.

## 5.7. Discussion

Despite multiple attempts to achieve a knock-down of Bmal1 with siRNA, miRNA and Bmal1 DN, none of these RNAi methods was successful.

Having obtained a fluorophore labelled siRNA and a FLAG-tagged Bmal1 DN construct to test the transfection efficiency of siRNA and plasmid DNA the reason for the failure of the RNAi to induce a knock-down appears to be that the transfection rate is too low to have any appreciable effect. Multiple concentrations of the RNA, ratios of RNA to several different transfection reagents and multiple cell seeding densities were used on the advice of the manufacturer of the siRNA and miRNA (Life Technologies). Additionally a representative from Sigma Aldrich kindly offered the help of their

technical support experts. Following lengthy conversations to troubleshoot the possible problems they concluded that the only problem could be that the cell line being used was difficult to transfect. Attempts to enhance transfection with enoxacin did not make any measurable difference. Even the GAPDH positive control failed to knock down GAPDH which indicates that the RNAi was not actually entering the cells rather than the problem being of sequence specificity to Bmal1. The greatest success in the myriad of reagents used was the use of the transfection reagent Interferin for transfecting FAM-tagged siRNA see Figure 5.9a. This was on the recommendation of a post-doctoral colleague who had used it successfully in the past. Unfortunately the conditions used for this successful transfection did not translate into positive results for the target siRNA. The target siRNA is a slightly different formulation (Silencer Select™ as opposed to Silencer™) so perhaps it is the proprietary stability modification of the Silencer Select™ which is preventing transfection.

Following this discovery other means of knocking-down the target were researched. It was hoped that it would be possible to obtain some epidermal tissue from Bmal1 knockout mice from another laboratory in order to produce primary cells to use but sadly there was a breeding problem with the Bmal1<sup>+/-</sup> mice. In the absence of a tool to use to test the theory of stopping the clock a lentiviral licence was obtained to permit the use of lentiviral vectors to introduce both an shRNA clone targeted to knocking down Bmal1 and also a Bmal1 luciferase reporter to assess the expression of Bmal1.

## 6. Lentiviral vectors & circadian clock synchronization *in vitro*

---

## **6.1. Introduction to lentiviral vectors**

As none of the alternative methods of RNAi were successful in knocking down Bmal1 in sufficient NIH 3T3 cells, the next approach was to use a lentiviral delivery system.

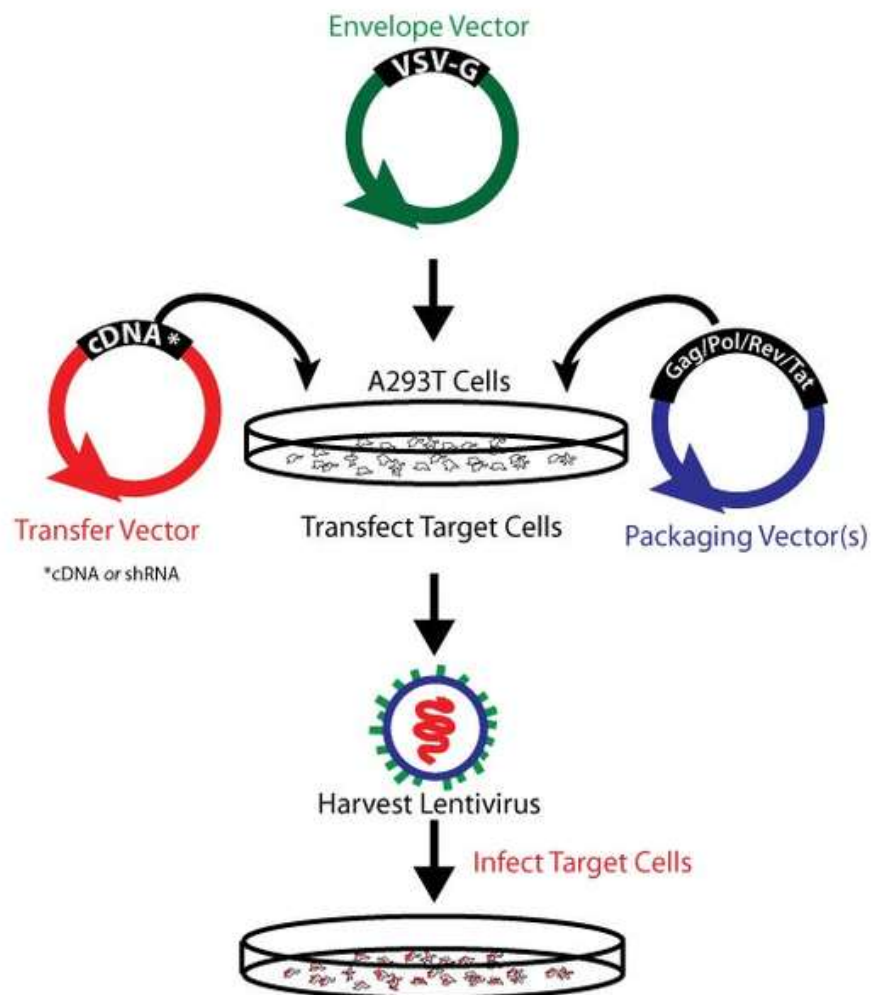
### **6.1.1. Virally mediated RNAi – transduction**

Transduction is the introduction of nucleic acids to eukaryotic cells via a viral vector. Both adenoviruses and lentiviruses can be used for this purpose. The prime advantage of using lentiviruses is that they are capable of transducing both dividing and non-dividing cells (Coffin, Hughes, & Varmus, 1997). The viral particles are made using a packaging cell line, typically a variant of HEK293 cells, such as 293FT (Life Technologies). These cells are transfected using an optimised ratio of transfer vector, containing the shRNA of interest, a packaging plasmid such as pCMV-dR8.2 dvpr with an envelope plasmid such as pCMV-VSV-G (Stewart, 2003). The reason for separating the genes that encode the packaging proteins and the envelope protein is for safety. The plasmid depository Addgene explains this fully as:

“The transfer vector encodes the gene of interest and contains the sequences that will incorporate into the host cell genome, but cannot produce functional viral particles without the genes encoded in the envelope and packaging vectors. Unless recombination occurs between the packaging, envelope, and transfer vectors, and the resulting construct is packaged into a viral particle, it is not possible for viruses normally produced from these systems to replicate and produce more virus after the initial infection.”

shRNA constructs are cloned into a suitable bacterial vector, this is amplified by growth in competent cells in Luria-Bertani (LB) broth overnight in a shaker at 37°C. The plasmid DNA is then isolated from the pelleted bacteria via Maxiprep (Qiagen). This can be transfected into the cells using a transfection reagent such as Fugene 6 and can be used to transiently transfect cells or produce stable cell lines via selection as mentioned previously.

The efficacy of the HIV based lentiviral vector is in part due to the *gag* matrix protein which directs it to the nucleus to enable incorporation of the viral DNA (Bukrinsky et al., 1993).

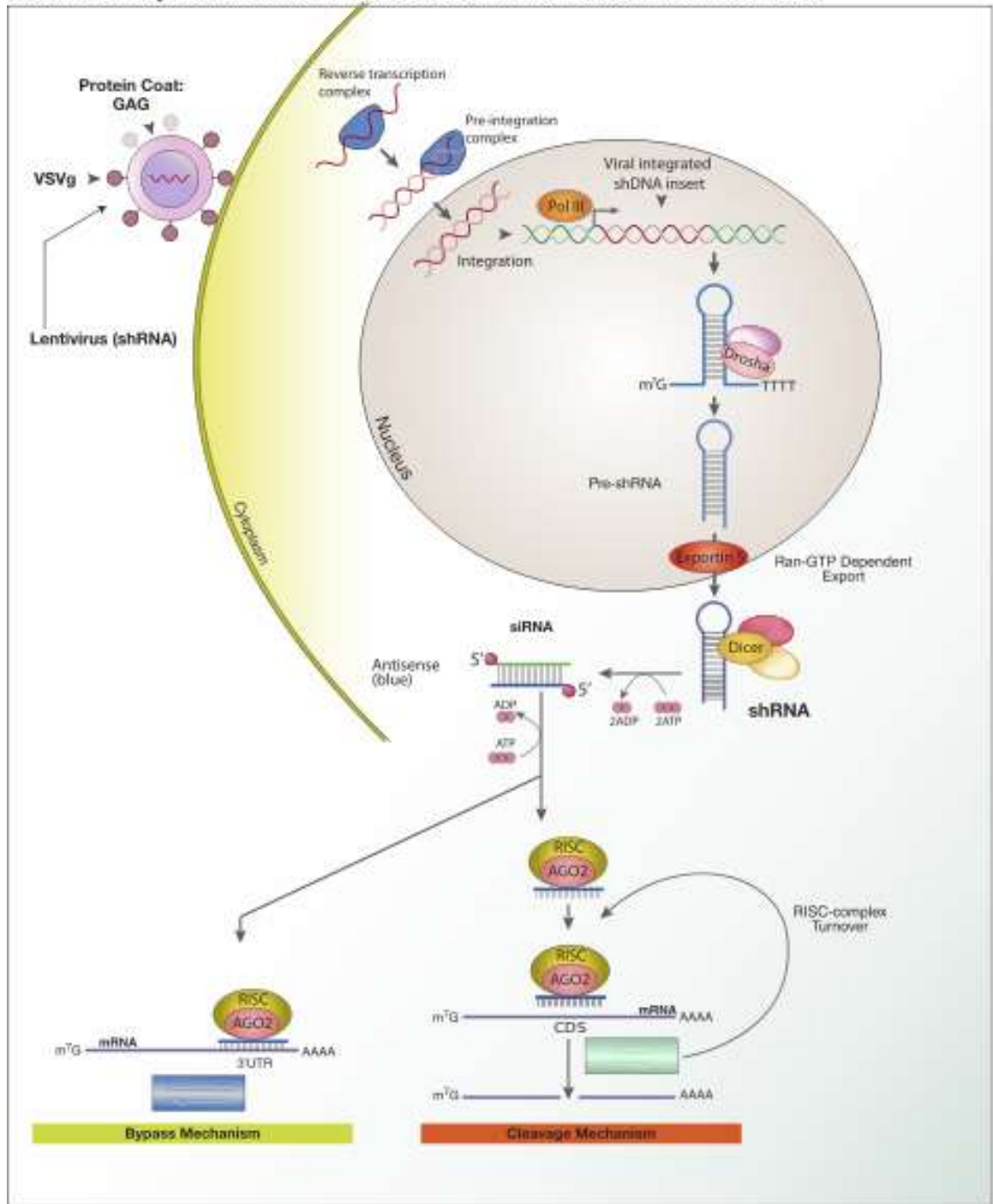


(Addgene, n.d.-a)

**Figure 6.1 Viral particles are made within 293FT cells following transfection with transfer, packaging and envelope plasmids**

Separating the components confers a higher level of biosafety for the user. The supernatant containing viral particles is used to transduce target cells to facilitate the introduction of the shRNA into the cells.

Lentiviral Delivery of shRNAs and the Mechanism of RNAi Interference in Mammalian Cells.



(Dan Cojocari, University Health Network, University of Toronto)

**Figure 6.2 Virally mediated transduction of shRNA constructs**

Viral pseudoparticles are used to facilitate the entry of the shRNA into the cell thereby enabling a higher rate of transduction.

## **6.2. Introduction to circadian clock synchronisation *in vitro***

In 1998, Balsalobre *et al* showed that mammalian cells in culture have a circadian clock that can be synchronised by simulating the cells with high serum medium (50% horse serum:50% DMEM). Subsequent to this several other compounds have been shown to cause a similar effect, for example, dexamethasone (Balsalobre *et al.*, 2000), forskolin (Kazuhiro Yagita & Okamura, 2000) and heat shock (43°C for 3 minutes) (Tamaru *et al.*, 2011). Each of these methods results in the oscillation of circadian genes for approximately three days before they start to dampen as they become desynchronised with each other (Welsh *et al.*, 2004; Nagoshi *et al.*, 2005).

## **6.3. Methods**

### **6.3.1. Lentiviral titre evaluation**

Lentiviral particles were generated as described in Section 2.3.2. An enzyme-linked immunosorbent assay (ELISA) was used to calculate the viral titre following disappointing initial results with using crude viral supernatant. (Alliance HIV-1 P24 Antigen ELISA Kit, Perkin Elmer). Centrifuged and filtered viral supernatants were diluted 1 in 5 with DMEM. A recombinant HIV-1 p24 stock solution was diluted with assay diluent to produce a standard curve. 225 µl of each standard and each filtered viral supernatant were added to 25 µl of Triton X-100 solution and incubated at 37 °C for 30 minutes to inactivate the samples. In duplicate, 110 µl of inactivated sample or standard were added to the anti-p24 antibody coated 96 well plate for 4 hours incubation at 37 °C. The wells were then emptied and washed three times with wash buffer. 100 µl FITC-conjugated anti-p24 monoclonal antibody (diluted 1:1000 in assay diluent) was added to each well and it was incubated at room temperature for an hour on a shaker. The wells were then washed three times as before and 100 µl HRP-conjugated anti-

FITC monoclonal antibody was added. The plate was incubated at room temperature for a further hour on the shaker. Following another three washes, 100 µl pre-warmed Substrate Solution was added to the wells until a colour change was seen. The enzyme reaction was stopped by adding 100 µl Stop Solution was added and the absorbance of each well was measured on a spectrophotometer at 450 nm. The value for the p24 concentration of each viral sample was obtained by plotting a standing curve in Microsoft Excel and applying a logarithmic scale to the x-axis and sigmoid curve. The formula for the curve was used to calculate the p24 concentration. The number of lentiviral particles (LPs) was calculated as follows:

$$1 \text{ ng p24} = 1.25 \times 10^7 \text{ LPs}$$

### **6.3.2. Transduction**

NIH 3T3s and Bmal1:LUC cells were seeded in 24 well plates at 50,000 cells per well. They were transduced 24 hours later in complete DMEM containing heat inactivated FBS (10%) and 5 µg/ml polybrene (Sigma-Aldrich Ltd) at a range of concentrations from 1 to 10,000 lentiviral particles per cell to ascertain the optimum transduction conditions. Cells were incubated at 4°C for 2 hours directly following transduction; they were then transferred to a cell culture incubator for an overnight incubation at 37°C, 5% CO<sub>2</sub>. The next morning the culture medium was replaced with complete DMEM without polybrene. Cells were split and replated as necessary. Three days after transduction the presence of mCherry fluorescence was assessed to quantify the transduction efficiency either on a chamberslide, counterstained with Hoescht as described in Methods 2.2.7 or by using an inverted microscope (Olympus) to visualise fluorescence in growing cells. Transduced cells were selected by the addition of puromycin (Life Technologies) at 2 µg/ml.



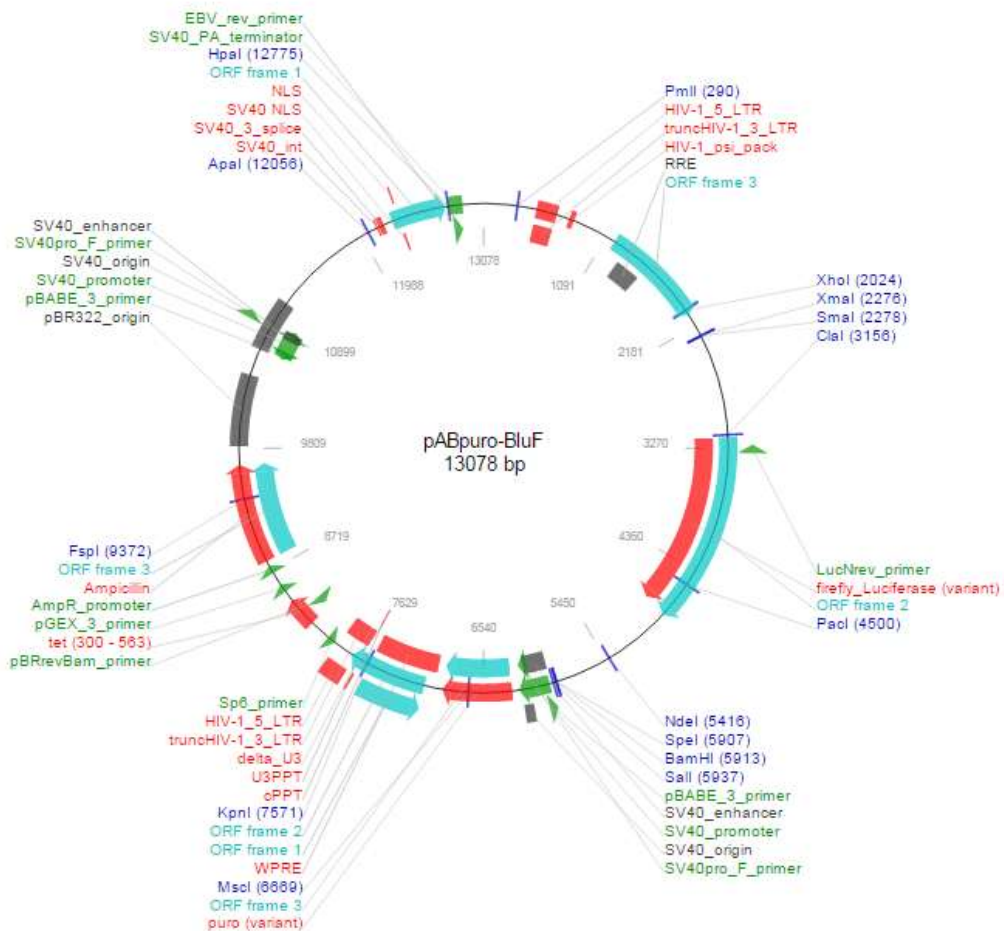


**Figure 6.4 Plasmid map of the Bmal1:LUC construct**

The Bmal1:LUC plasmid also encodes for puromycin resistance. There is no fluorophore in this plasmid.

### 6.3.3. Circadian clock synchronisation assay

Cells were synchronised either by treatment for 2 hours with 50% horse serum DMEM for 2 hours followed by 1% FBS DMEM or by a 30 minute treatment with 1  $\mu$ M dexamethasone (from a 1M stock dissolved in ethanol.) followed by normal growth medium (all Life Technologies).

### 6.3.4. RT-PCR

Cells were synchronised by the methods stated above. Controls were either a like-for like medium replacement or 0.001% ethanol (equating to the volume used to dilute the dexamethasone). They harvested at time 0 when the synchronisation started, thereafter every 4 or 6 hours and immediately lysed and stored at -80°C until the RNA was extracted. RT-PCR was executed as per Methods section 2.2.2.

### **6.3.5. Luciferase assay**

Cells were seeded at 5,000 cells per well in white flat bottomed 96 well plates 2 days prior to the experiment to ensure that they were all fully confluent at the start of the assay. Just prior to measuring the growth medium was replaced with phenol red-free HEPES buffered DMEM containing 10% (or 1% for serum shocked cells) FBS and penicillin-streptomycin at 100 U/ml (all Life Technologies Ltd.) containing 1 mM D-luciferin (Promega Corporation). The plates were sealed with Bio-Rad adhesive seals as used for RT-PCR. The photon counts were measured on a BMG Labtech Optima Fluostar preheated to 37°C every hour for 3 days. Controls included wells containing medium, but no cells, transduced cells with no luciferin and nontransduced cells with or without luciferin. The data was analysed in part by the bespoke BMG Labtech software (MARS) and in part by Microsoft Excel; in MARS the data were normalised to blank controls and the curve smoothing algorithm was applied (moving average). The data were then exported to Excel to calculate the average of a minimum of 5 biological replicates for each of 3 experiments and the standard deviation.

### **6.3.6. Incucyte scratch wound assay to assess functional effects of Bmal1 knockdown**

Cells were seeded 2 days prior to the assay at 5,000 cells per well in an Essen Image lock 96 well plate so that they would be confluent on the day of the experiment. The cells were scratched as per methods section 2.4. Images were acquired on an Incucyte Zoom of both brightfield and fluorescence in the red wavelength to differentiate between cells expressing the shRNA Bmal1 knockdown constructs and those that were not so as to be able to measure the relative migration rates of the different populations in the same well. Analysis was done using the Essen Zoom software using the tool that measures wound density.

## 6.4. Results

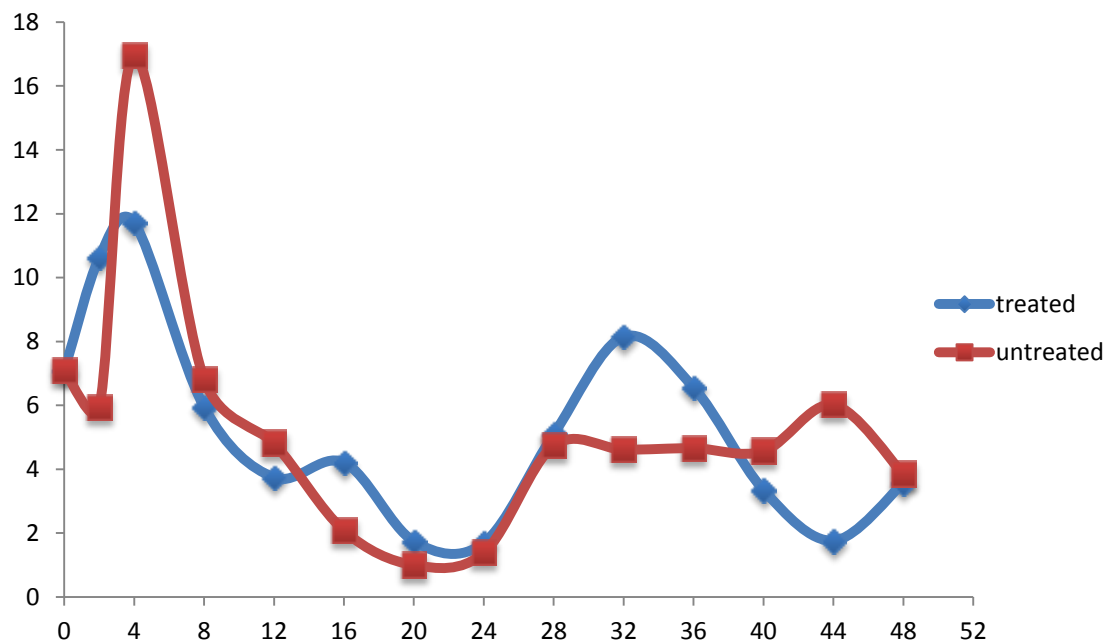


**Figure 6.5 The control has as much effect as the treatment in cell synchronisation of Bmal1 with serum shock**

This is a representative graph of many attempts to measure the effects of serum shock on NIH 3T3 cells. Cells were seeded 24 hours before the experiment in 6 well plates such that they were confluent the following day. They were harvested at 4 hour intervals following the serum shock. Data represents Bmal1 mRNA relative to SDHA and GAPDH.

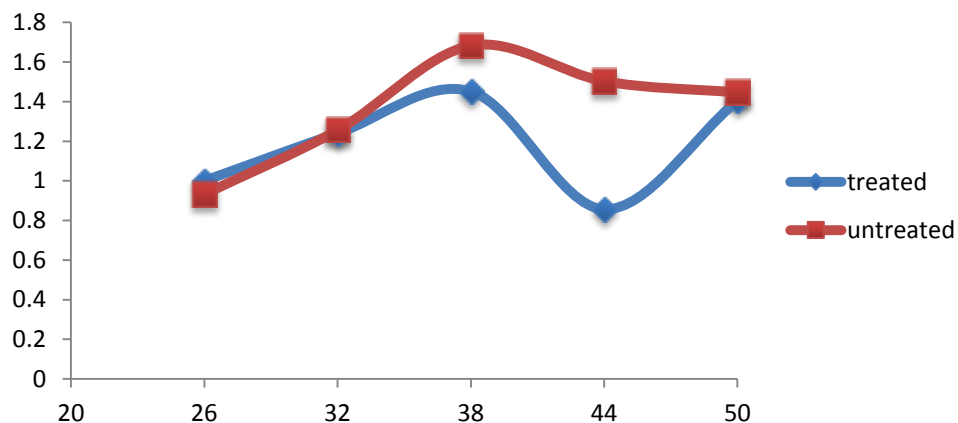


**Figure 6.6 Dexamethasone has no more effect than the control in the synchronisation of Bmal1 in NIH 3T3s**

This is a representative graph of many attempts to measure the effects of dexamethasone treatment on NIH 3T3 cells. Cells were seeded 24 hours before the experiment in 6 well plates such that they were confluent the following day. They were harvested at 4 hour intervals following the start of the dexamethasone treatment. Data represents Bmal1 mRNA relative to SDHA and GAPDH.

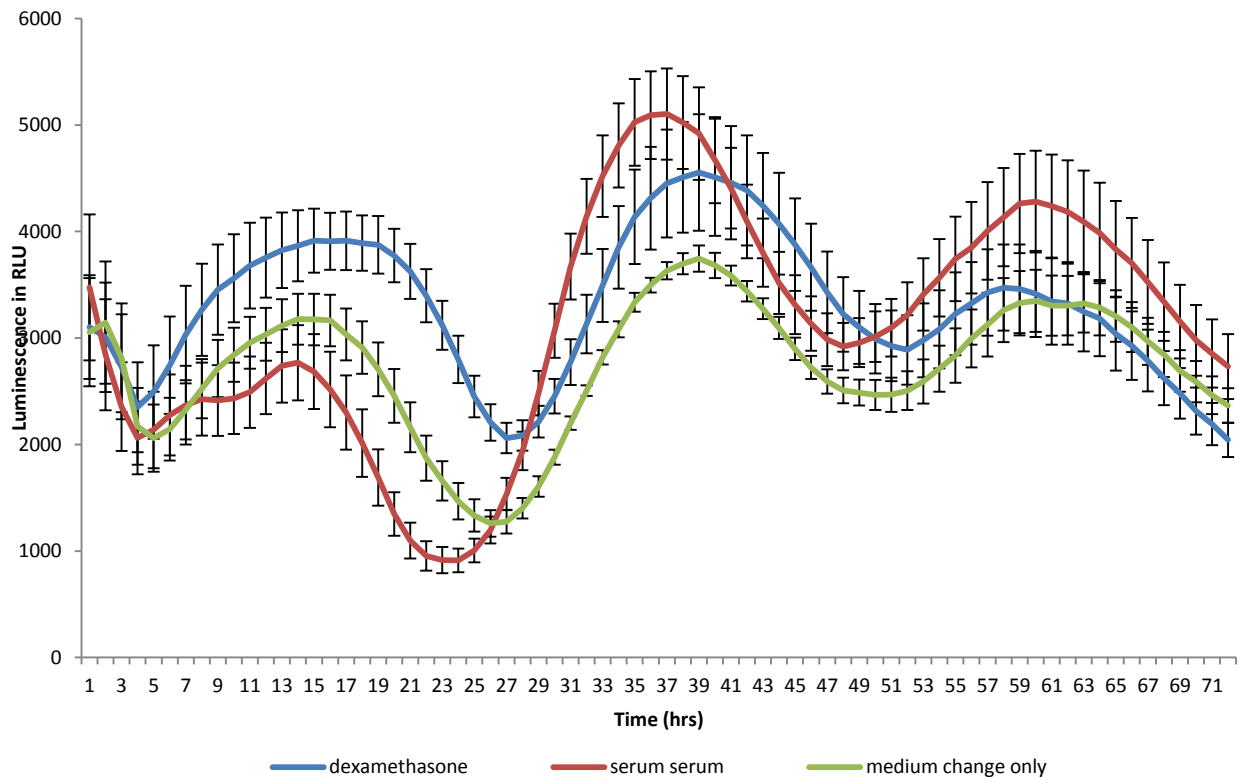


**Figure 6.7 Changing the culture medium for fresh culture medium induces circadian oscillations in Bmal1 as effectively as the cell synchronisation protocols widely used in the literature.**

At a constant temperature (37 °C) following treatment to synchronise the circadian clock, robust circadian oscillations are seen in NIH 3T3 cells stably expressing Bmal1:LUC with only a like-for-like serum change. Data is an average of  $\geq 15$  biological replicates  $\pm$  SEM. n = 3

There appears to be a phase shift of 2 hours between each treatment; the second trough appears at 24 hours in the serum shocked cells, 26 hours in the medium change cells and 28 hours in the dexamethasone treated cells. The following peak is at 48 hours, 50 hours and 52 hours respectively.

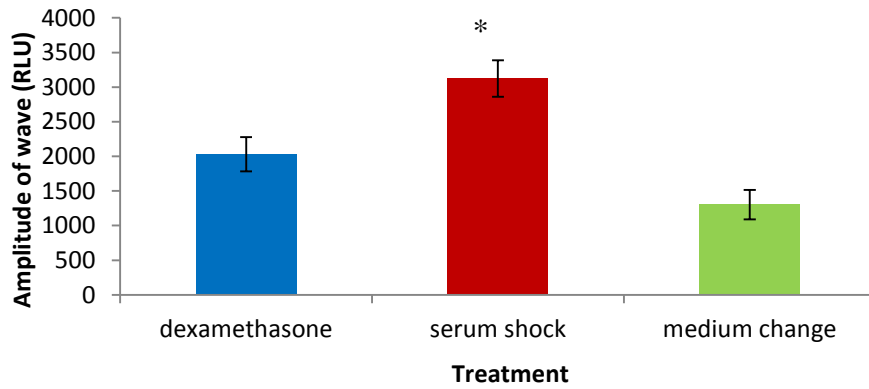


**Figure 6.8 The amplitude of the wave in circadian rhythm of Bmal1 with serum shock is larger than with dexamethasone or medium change.**

Data are the mean amplitude of the second wave measured by deducting the mean trough values from the mean peak value. Data is an average of  $\geq 15$  biological replicates  $\pm$  SEM.  $n = 3$ . Statistical differences were calculated by one way ANOVA  $*p < 0.05$  using SPSS.

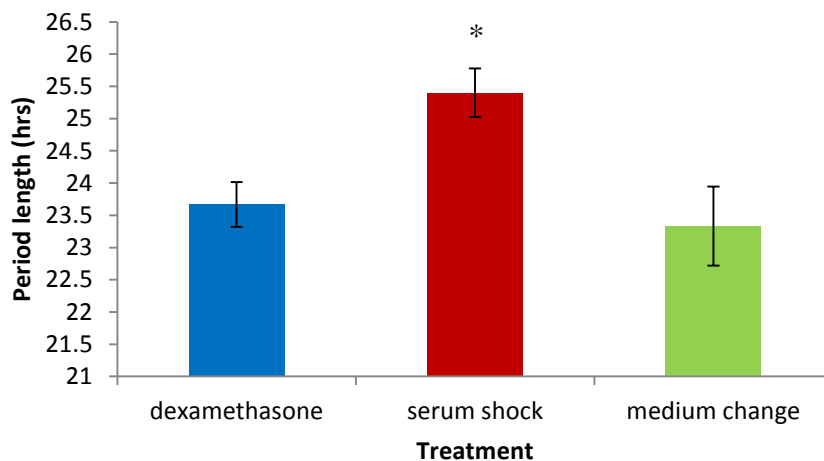


**Figure 6.9 Synchronisation by serum shock resulted in a longer period length than by the dexamethasone or medium change.**

Data are mean temporal frequency of peak amplitude minus trough  $\pm$  SEM. Data is an average of  $\geq 15$  biological replicates  $\pm$  SEM.  $n = 3$ . Statistical differences were calculated by one way ANOVA  $*p < 0.05$  using SPSS. Mean period length for cells undergoing synchronisation was as follows: 23.67 hours for dexamethasone, 25.4 hours for serum shock and 23.34 hours for medium change.

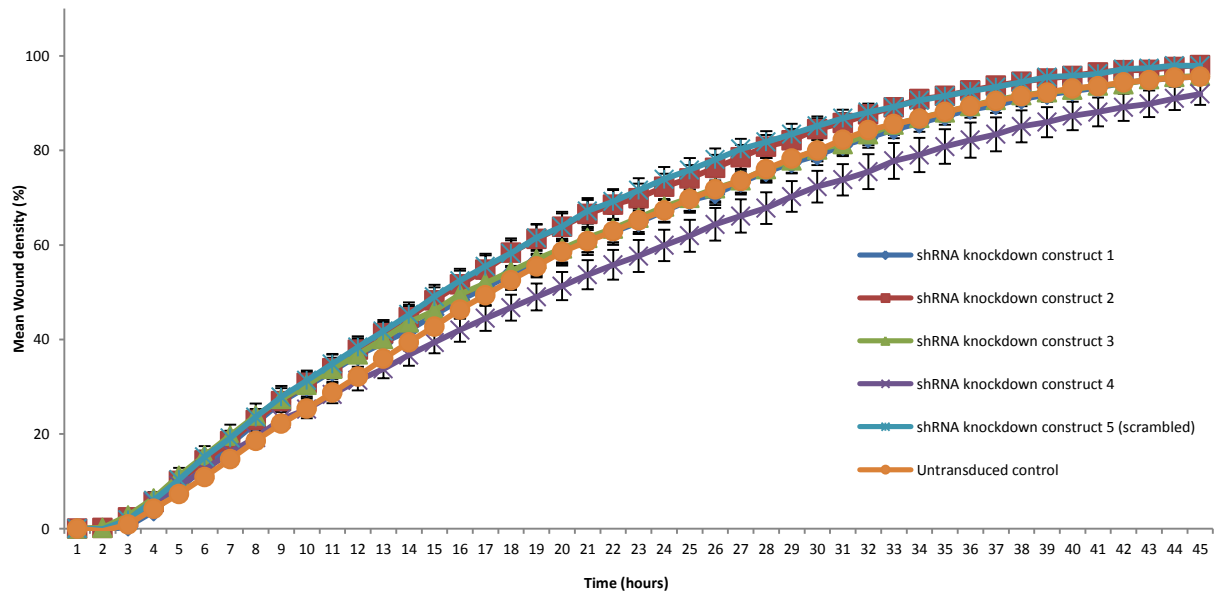


**Figure 6.10 ShRNA knockdown construct 4 significantly reduces the mean wound density of transduced NIH 3T3 fibroblasts**

NIH 3T3s expressing the shRNA knockdown constructs targeted to Bmal1 were seeded in Essen Image Lock™ 96 well plates 48 hours prior to the scratch wound assay. The assay was performed as per Methods section 2.4 with the exception that it was run on an Incucyte Zoom, using the brightfield and red fluorescence channels. NIH 3T3s transduced with the shRNA sequence 4 had a significantly reduced mean wound density with comparison to those transduced with the scrambled shRNA control. Statistical differences were tested using two way ANOVA with Dunnett’s post-hoc comparisons using GraphPad Prism. See table 6.1 for statistical differences across the time course. Data are mean wound density ± SEM. n = 16 wells (1 experiment only)

**Table 6.1 Statistical differences in mean wound density between NIH 3T3s transduced with shRNA construct 4 compared to NIH 3T3s transduced with the scrambled control**

Elapsed time post scratch wound	Statistical differences
up to 11 hours	ns
12 hours, 13 hours	$p \leq 0.05$
14 hours to 17 hours	$p \leq 0.01$
18 hours, 19 hours	$p \leq 0.001$
20 hours to 27 hours	$p \leq 0.0001$
28 hours to 31 hours	$p \leq 0.001$
32 hours to 36 hours	$p \leq 0.01$
37 hours to 41 hours	$p \leq 0.05$
42 hours to 45 hours	ns

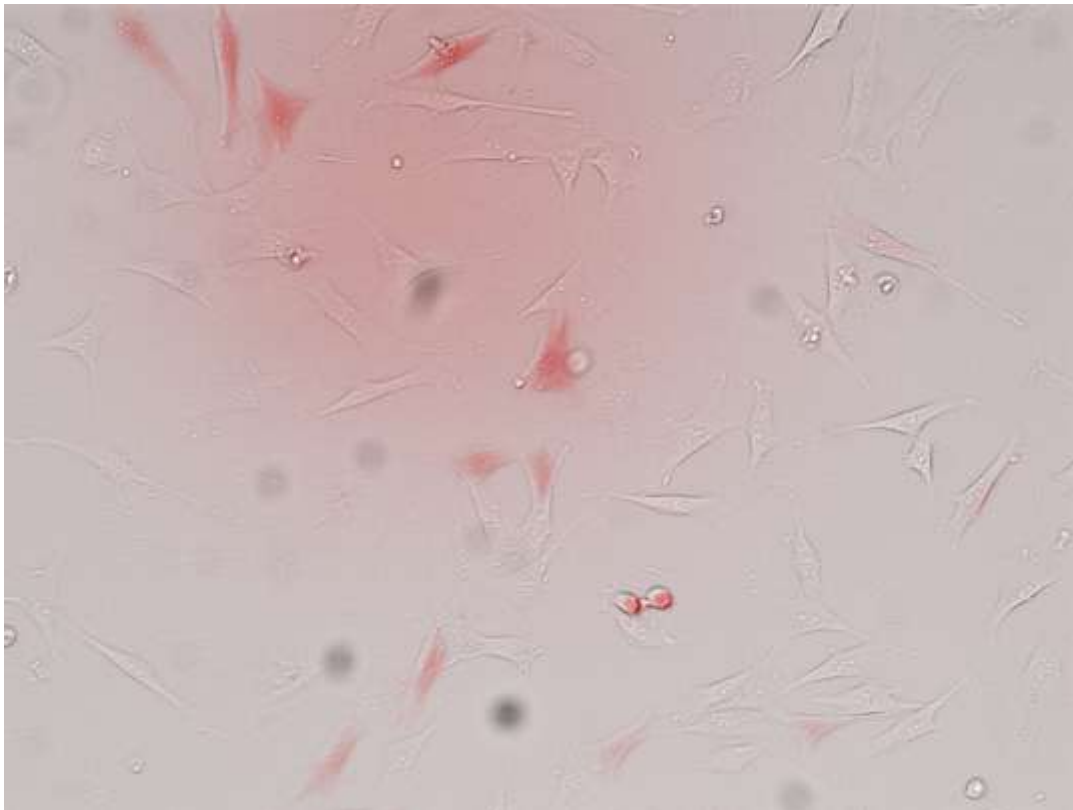


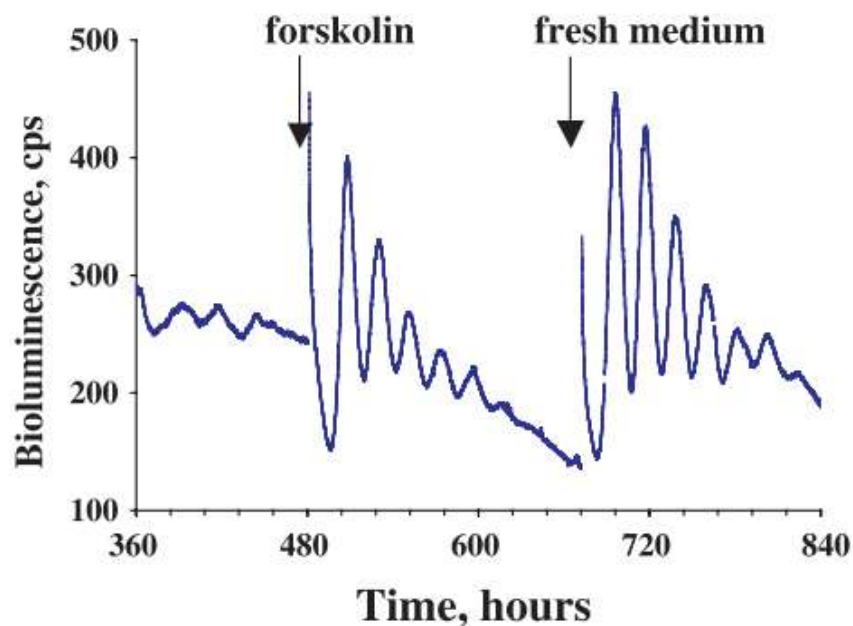
**Figure 6.11 Representative image of fluorescent cells expressing mCherry overlaid over a brightfield image of the same field of view (20 x)**

The Bmal1:LUC celled transduced with the mCherry expressing shRNA Bmal1 knockdown constructs were imaged in brightfield and with fluorescent excitation at 598 nm. Transduction efficiency was calculated by dividing the number of fluorescent cells by total cells and multiplied by 100 to gain a percentage. In Figure 6.11 the cells are Bmal1:LUC transduced with the shRNA construct number 4. 23.8% of the cells were fluorescent. Cells were counted using a plugin for ImageJ. The percentage of fluorescent Bmal1:LUC cells ranged from 16% to 24%.

## 6.5. Discussion

### 6.5.1. Circadian clock synchronisation *in vitro*

Merely feeding the cells with fresh culture medium is sufficient stimulus to elicit circadian clock synchronisation. This explains why the controls in the graphs of Bmal1 expression measured by RT-PCR had a similar profile to the serum shocked or dexamethasone treated cells. The absence of regular oscillations can be explained by the fact that the cells were seeded in 6 well plates with multiple time points per plate. Transient removal of the plates from the incubator to harvest a different time point could potentially be sufficient stimulus to ‘reset’ the circadian clock (personal communication, O’Neill laboratory, unpublished). The effect of medium change causing synchronisation has been observed previously. See **Figure 6.12**.



(Maywood et al., 2006, re drawn from Yamazaki, 2000)

**Figure 6.12 Per2 oscillations in NIH 3T3 cells expressing mPer2:LUC can be re-initiated by treatment with forskolin or by fresh medium.**

Acute treatment with fresh medium (either containing forskolin, an agent that raises cAMP, or without a pharmacological agent)

Despite this, the majority of the literature on circadian experimentation *in vitro* use some form of stimulus such as dexamethasone, forskolin, or serum shock to synchronise the cells. There is no statistical difference in the amplitude or period length in NIH 3T3 cells treated with dexamethasone versus a medium change not containing dexamethasone. The main difference in the synchronisation protocols seems to be the phase shift; dexamethasone shifts the cycle forward by 2 hours with comparison to the medium change and serum shock serum shift the cycle by 2 hours in the opposite direction. Dexamethasone has been shown to have this effect *in vivo* in the peripheral tissue of rats expressing a luciferase reporter (Stokkan, Yamazaki, Tei, Sakaki, & Menaker, 2001) and *in vitro* in NIH 3T3 cells expressing a Bmal1:luciferase reporter (Nagoshi, Saini, Bauer, Laroche, Naef, & Schibler, 2004).

The serum shock seems, in the short term at least, to amplify the circadian wave and shift the phase earlier. This could be explained by a recent study published earlier this year; Lipton et al (2015) discovered a new role for Bmal1 as a mediator of protein translation (in addition to the already known canonical role of transcription factor). In this study they demonstrated that Bmal1 is a substrate of the mammalian target of rapamycin (mTOR), a nutrient sensing protein. Briefly, Bmal1 is phosphorylated at serine 42 by the mTOR effector S6 kinase1 when there is an influx of growth factors and nutrients. This results in increased *de novo* protein synthesis. See **Figure 6.13**.

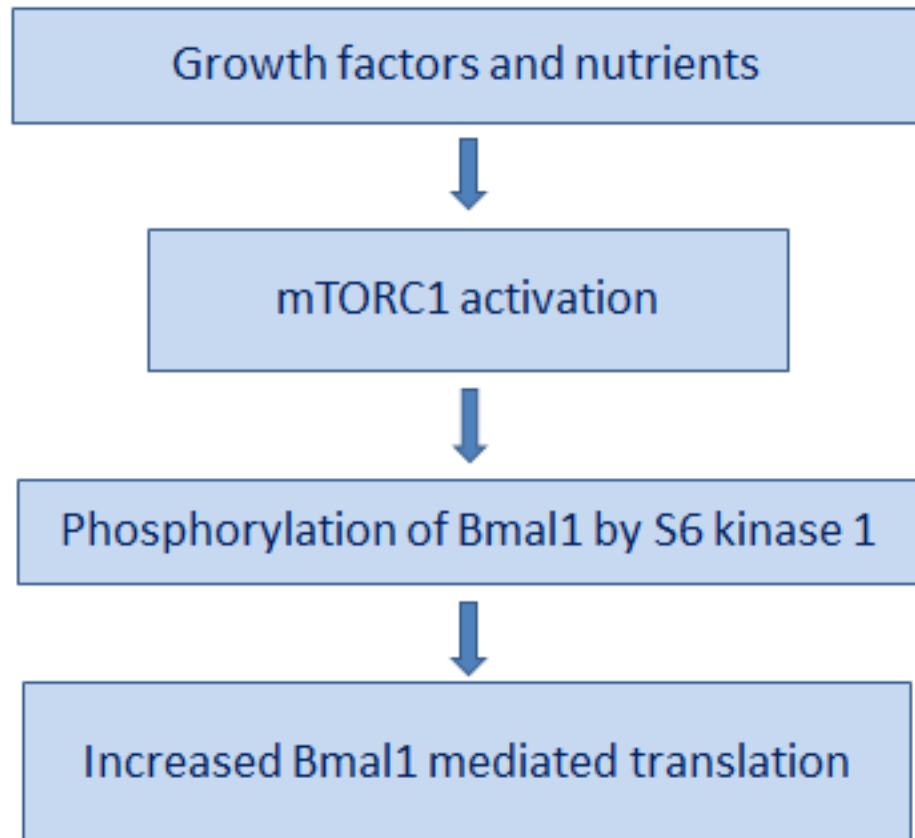


**Figure 6.13 Mechanism by which Bmal1 stimulates protein translation**

Protein translation is upregulated via the phosphorylation of Bmal1 in response to the presence of growth factors and nutrients being sensed by mTOR (mammalian target of rapamycin).

The anabolic effects of this pathway can be reversed by blocking the phosphorylation of Bmal1 by S6K1 or by blocking mTOR with rapamycin (Lipton et al., 2015).

Dexamethasone is a glucocorticoid receptor agonist. The effects of glucocorticoid signalling are in opposition to mTOR. (Shimizu et al., 2011)

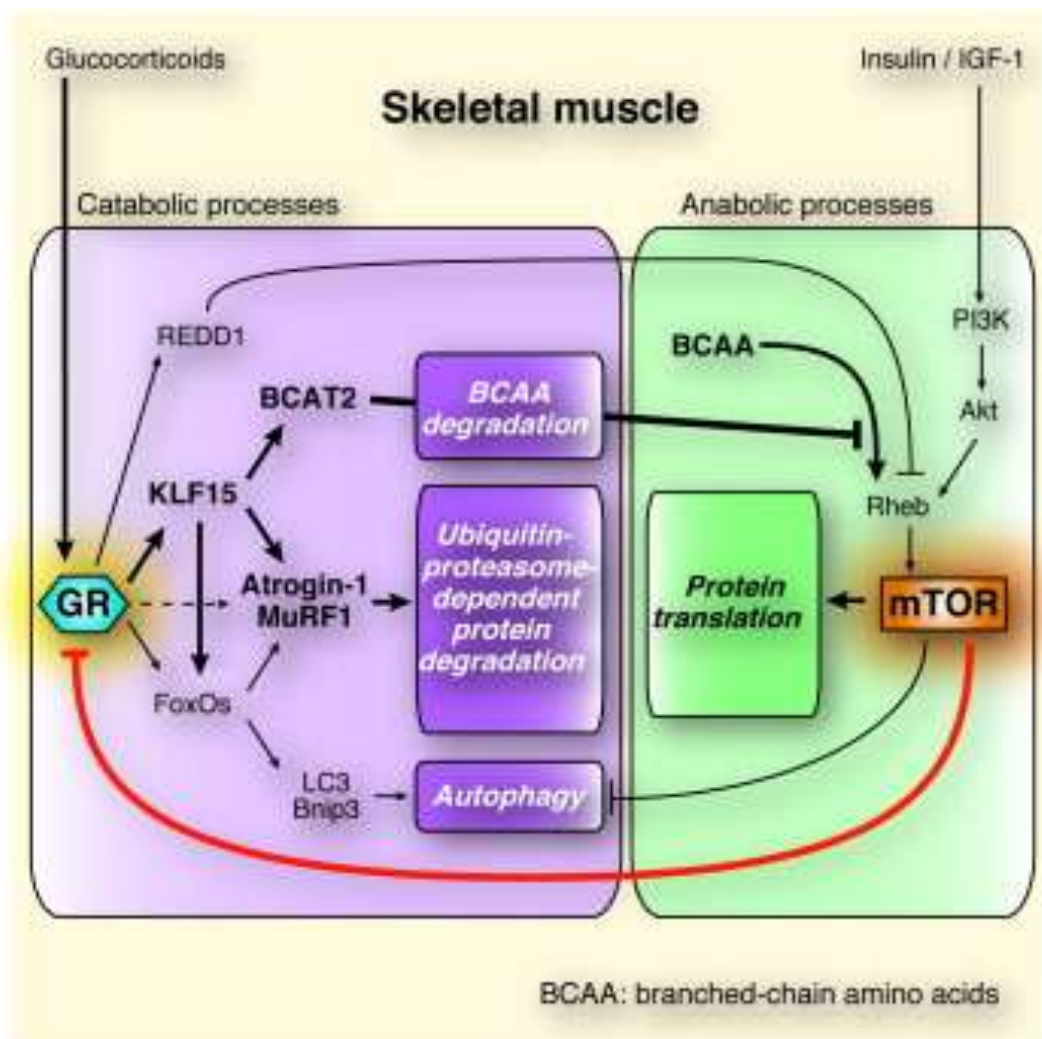


**Figure 6.14 The interaction between glucocorticoids and mTOR**  
(Shimizu et al., 2011)

Glucocorticoids and mTOR regulate each other via negative feedback. Additionally, the activation of mTOR upregulates protein translation.

It seems logical to deduce that if increasing the nutrients and growth factors *in vitro* with 50% serum treatment activates mTOR mediated signalling to Bmal1 then dexamethasone treatment would have the exact opposite effect. The mechanism by which the phase is shifted is not clear as the translational effects of Bmal1 have not yet been measured in the central circadian clock (Lipton et al., 2015). Given the increased amplitude seen in the Bmal1:LUC cells stimulated with 50% serum, it seems reasonable to hypothesize that the phosphorylation of Bmal1 leads to its own increased synthesis. This explains why the amplitude of the oscillations is greater in the serum shocked Bmal1:LUC cells. See **Figure 6.8**.

### 6.5.2. Scratch Wound Assay

shRNA sequence 4 significantly reduced the mean wound density in the scratch wound assay despite the fact that only approximately 24% of the cells were transduced. These cells also did not proliferate as quickly in culture which could indicate that Bmal1 is knocked down in these cells but without quantification of the knockdown by RT-PCR it is not possible to be certain. Despite having successfully created Bmal1:LUC expressing NIH 3T3s (3T3 /B:L) using a second generation lentiviral construct, followed by selection with puromycin to create stably expressing cells the equivalent treatment with shRNA knockdown constructs was not as straightforward. Transduction of NIH 3T3s with shRNA 4 did produce cells that expressed mCherry, however they failed to proliferate and died following puromycin selection. Despite considerable attempts to optimise the transduction and viral synthesis conditions the only cells that survived were 3T3/B:Ls that were already puromycin resistant, therefore not selectable by antibiotic treatment for shRNA expression. The probable explanation for this is that the promoter for puromycin resistance expression in the shRNA plasmids (IRES) is not as potent as the SV40 promoter in the Bmal1:LUC plasmid (personal communication, Genecopoeia technical support), therefore the puromycin concentration used for selection of these cells (2 µg) was too strong. If time permitted this would be repeated with a selection of lower concentrations to find the optimal conditions for this lentiviral system. Alternatively, the mCherry expressing 3T3/B:L cells could be isolated via fluorescent-assisted cell sorting (FACS), however this would require a large number of cells due to the attrition rate. Another technical issue that was not foreseen was that it was not possible to use the Incucyte Zoom data to measure migration rates of the separate populations of cells within the individual wells. The algorithm used to measure the migration of these cells was mean wound density which was designed by Essen Bioscience to control for initial cell density and cell proliferation, therefore normalising the mean wound density to the non-wounded areas in the wells.

Without determination of Bmal1 knockdown and the use of a functional assay on stably knocked down Bmal1 NIH 3T3s it is not possible to draw a definitive conclusion but the indications point towards Bmal1 knockdown, or ‘stopping the clock’ having a negative effect on wound healing. Further experiments are required to confirm this.

# 7. Discussion

---

## 7.1. General discussion

The importance of chronobiology in medicine has been given substantial attention in recent years. This includes various aspects of health and disease such as the association of working night shifts with increased cancer risk (Stevens, Brainard, Blask, Lockley, & Motta, 2014), the importance of timing of cancer chemotherapy administration for optimal effect (Lévi, Okyar, Dulong, Innominato, & Clairambault, 2010) and the importance of maintaining the circadian rhythms in cancer treatment (Innominato et al., 2014). Several studies have addressed the issue of sleep deprivation in intensive care units (Huang et al., 2015) and the skin damaging effects, dependent on circadian time of day, of exposure to ultra-violet radiation (Desotelle, Wilking, & Ahmad; Geyfman & Andersen, 2009; Gaddameedhi, Selby, Kaufmann, Smart, & Sancar, 2011b; Geyfman et al., 2012). My study has focused on the effects of manipulating the circadian clock on wound healing, with a view to meeting the as yet unmet need for effective treatments for chronic wounds. Several approaches to this problem have been investigated, ranging from physical treatments, such as the use of compression bandages, to biochemical methods such as the use of a variety of growth factors. A meta-analysis in 2012 identified venous leg ulcers as being the predominant type of chronic wound; they are most frequently healed by the use of compression bandages. The basis for this is that the cause of the ulcers is venous incompetence which results in venous hypertension. This can be ameliorated (and prevented) with compression bandages/stockings. The meta-analysis sought to compare the benefits of stronger compression versus medium compression and the finding was somewhat inconclusive, mainly due to the lack of information about other concurrent treatments being used in the various trials assessed. The authors, Nelson et al, (2012) stated that there was a need to determine the biological mechanism involved in ulcer healing. Another meta-analysis, originally published in 2012, but updated earlier this year, sought to assess the evidence for the use of

hyperbaric oxygen therapy (HBOT) for chronic ulcers of the lower leg. The benefits shown were marginal; they reported a small, short term benefit using HBOT for treating diabetic foot ulcers and a possible reduction of wound size in chronic ulcers caused by venous incompetence. There was no evidence, positive or negative, for its use in treating ulcers caused by arterial insufficiency. The authors highlighted problems found conducting the meta-analysis being caused by differences in the studies making them difficult to compare; there were many small studies, often with different end points and often measuring ulcers of multiple aetiology (Peter Kranke et al., 2015). Another line of investigation has been the activation of epidermal stem cells (Plikus et al., 2012). The circadian clock has been shown to be important in several areas of health and disease at the whole organism level. On a cellular level it controls the cell cycle (Smaaland, 1996) and the skin cells of mice and humans are known to be under circadian control (Tanioka et al., 2009; Sandu et al., 2012). For these reasons it seems reasonable to test whether manipulation of the circadian clock can have beneficial effects on wound healing.

The aims of the present study were:

- 4) Optimisation of asODNs by continuing *in vivo* experiments and by *in silico* expansion of the sequences to ensure a more biologically stable asODN.
- 5) Development of a tool to knockdown Bmal1 in order to disrupt the circadian clock for use in proof of concept *in vitro* experiments.
- 6) Measuring the functional effects of Bmal1knockdown on wound healing *in vitro*.

In summary, the findings of the study were as follows:

- 1) The unmodified asODNs did not have a beneficial effect on wound healing *in vivo*. The initial positive macroscopic results were due to an artefact introduced by the established standard laboratory procedure at that time. It became evident that the effects seen were position-dependent, not asODN treatment dependent,

so an experiment was designed to challenge the theory (using the same drug in three positions and alternating the direction of the skin fold for the purpose of wounding). This experiment conclusively proved that the suspicions were valid. Following the discovery of the artefact, the standard operating procedure was altered and the treatments were randomised and blinded to the investigator until analysis had taken place to reduce the possibility of operator bias. Following the negative results from the original asODN 16 mer sequences, it was hypothesised that the asODNs were being degraded by endonucleases too quickly to take effect so, thereafter, the sequences were expanded to 30 mer asODNs using several criteria (see section 2.6) to filter the possible candidates to 18 sequences to be tested *in vitro*. Again, initially the results looked promising until a proper control scrambled sequence was used, at which point it became apparent that the knock down was not sequence specific. Additionally, the 30 mer asODNs knocked down the three commonly used housekeeping proteins (GAPDH,  $\alpha$ -tubulin and  $\beta$ -actin). It seems likely that this is due to the toxic effects of the dNMP by-products of the catalysis of the phosphodiester backboned asODNs (de Fouw, Ma, Michalevycz, Gray, & Hoffbrand, 1984). Phosphorothiate backboned asODNs were tested as they have been shown to be more stable *in vitro* (A. R. Thierry & Dritschilo, 1992). They did not knock down Bmal1 either. Further, none of the asODNs were shown to be effective in a functional assay (scratch wound assay).

- 2) In light of the discoveries regarding the asODNs, other methods of RNAi were investigated, such as microRNA, siRNA and the overexpression of Bmal1 dominant negative. Despite considerable efforts, these methods did not knock down Bmal1 or disrupt the circadian clock. At the same time, a tool for assessing the circadian oscillations was developed. There were several problems

with measuring this by RT-PCR, as detailed in Chapter 6, so a Bmal1:LUC expressing lentiviral plasmid was obtained. This permitted the measurement of luminescence driven by the Bmal1 promoter at a constant temperature and produced robust oscillations. This tool also facilitated the discovery of the phase shifts caused by serum shock (SS), and dexamethasone treatment (dex) proved that fresh medium is sufficient to synchronise mammalian cells for at least three days. This is of note as the majority of reports in the literature are needlessly using SS or dex in their circadian experiments (Dibner et al., 2010; Lipton et al., 2015). The discovery of the phase shift changes caused by SS/dex is in concordance with a study published earlier this year linking Bmal1 to mTOR signalling (Lipton et al., 2015).

- 3) Partial transduction of Bmal1:LUC expressing NIH 3T3s with shRNA Bmal1 knockdown lentiviral constructs was achieved, but further optimisation is required to produce NIH 3T3s with Bmal1 knockdown that can be selected with puromycin to confer a stably knocked down cell line. This will permit quantification of the knockdown by RT-PCR and further scratch wound assays with a homologous population of Bmal1 knock down NIH 3T3s. The indications from the preliminary experiments are that the Bmal1 knockdown reduces cell migration into the wound *in vitro*, but further work is needed to confirm this.

In light of this, it seems reasonable to speculate as to the probability of a tool to knock down Bmal1 being used as a topical treatment for chronic wound healing.

The majority of the literature suggests that knocking down Bmal1 would have a pejorative effect on wound healing. In 2013, Kowalska et al observed wound healing defects in multiple circadian clock deficient mouse models, marked by a lack of re-epithelisation and irregular granulation tissue.

“Most wounds in *bmal1*<sup>-/-</sup> mice consisted mainly of an inflammatory fibrin clot with hardly any fibroblast or keratinocyte proliferation” (Kowalska et al., 2013)

It is important to consider that this work was done using total genetic knockout animals as opposed to tissue specific *Bmal1* deficiency or in a skin cell line. This is of great significance as the phenotype of *Bmal1*<sup>-/-</sup> mouse is severe; females are infertile (Boden, Varcoe, Voultios, & Kennaway, 2010), they display signs of premature ageing and have a shorter life-span than their wild type littermates (Kondratov, Kondratova, Gorbacheva, Vykhovanets, & Antoch, 2006). Another group were able to rescue the premature ageing phenotype by re-expression of *Bmal1* in these animals (McDearmon et al., 2006). *Bmal1* null mice also have a propensity for type II diabetes; both *CLOCK* and *Bmal1* mutant mice have impaired glucose tolerance and other indicators of metabolic syndrome (Turek et al., 2005; Bass & Takahashi, 2010). That being said, lentiviral mediated over-expression of *Bmal1* in NIH 3T3s results in increased cell proliferation (Lin, Chen, Li, Zhao, & Tan, 2013), and the silencing of *Bmal1* results in the suppression of malignant plural mesothelioma cell proliferation and increased their rate of apoptosis (Elshazley et al., 2012).

Conversely, circadian studies related to skin suggest that knocking down *Bmal1* could have a positive effect on wound healing. Several studies have looked at the circadian control of metabolism and ultraviolet B (UVB) radiation induced damage to skin (Kang, Lindsey-Boltz, Reardon, & Sancar, 2010; Gaddameedhi et al., 2011a; Geyfman et al., 2012). These studies suggest that *Bmal1* has a protective role in the skin. Wildtype (WT) mice have *Bmal1* controlled cell proliferation and metabolic phenotype:

“In sum, time-of-day-dependent variation in cell proliferation in the epidermis is controlled by *BMAL1* intrinsic to keratinocytes, and this variation correlates with a time-of-day dependent differential sensitivity to UVB-induced DNA damage.”(Geyfman et al., 2012)”

In the skin of WT mice, the period at which the majority of cells are undergoing S phase (night) correlates with the lowest levels of oxidative phosphorylation generated reactive oxygen species (ROS) and UVB exposure (Geyfman et al., 2012). Another study measuring the metabolism of epidermal stem cells *in vivo* showed that in WT mice they exhibit a glycolytic phenotype at night, presumably to reduce the levels of ROS during S phase (Stringari et al., 2015). In *Bmal1*<sup>-/-</sup> mice, these oscillations are obliterated so ROS levels are constitutively elevated and the time control of S phase is also lost. The authors surmised that this could lead to more mutations which would explain their premature ageing phenotype. In mice with a keratinocyte specific *Bmal1* knockdown a constant and elevated rate of cell proliferation was seen in the interfollicular epidermis (Geyfman et al., 2012). Epidermal stem cells derived from the hair follicle bulb have been shown to contribute to wound repair (Ito et al., 2005). These cells are known to be at different states of activity. When *Bmal1* is deleted in the basal keratinocyte compartment *in vivo*, an accumulation of dormant stem cells is seen, along with an increase in epidermal ageing and reduced tumorigenesis (Janich et al., 2011). A subsequent study by the same group demonstrated that the timing of the function of epidermal stem cells is under circadian control (Janich et al., 2013). It is possible that manipulation of the circadian clock in this population of cells could ameliorate wound healing. Given the multiplicity of effects seen in the manipulation of the circadian clock in different tissues it is hard to predict what effect the knockdown of *Bmal1* would have.

## 7.2.Future directions

Further experiments to create a homogenous population of Bmal1 knock down cells are ongoing in order to elucidate the effects on wound healing *in vitro*. Dependent on the results it might be possible to develop a topical treatment to knockdown (or upregulate) Bmal1 for use in chronic wounds. Due to the difficulties with transient transfection, these experiments have been conducted using NIH 3T3 fibroblasts expressing a stable Bmal1 knockdown. For translation to a safe therapy in humans it would be prudent to develop a method to transiently modulate Bmal1 within the wound to reduce the risk of off-target effects.

# References

---

- Aartsma-Rus, A., van Vliet, L., Hirschi, M., Janson, A. A. M., Heemskerk, H., de Winter, C. L., ... van Ommen, G.-J. B. (2009). Guidelines for antisense oligonucleotide design and insight into splice-modulating mechanisms. *Molecular Therapy : The Journal of the American Society of Gene Therapy*, 17(3).
- Abe, H., Honma, S., Namihira, M., Tanahashi, Y., Ikeda, M., & Honma, K. (1998). Circadian rhythm and light responsiveness of BMAL1 expression, a partner of mammalian clock gene Clock, in the suprachiasmatic nucleus of rats. *Neuroscience Letters*, 258(2). Retrieved from <http://www.ncbi.nlm.nih.gov/pubmed/9875535>
- Addgene. (n.d.-a). Addgene: Lentiviral Protocols & Resources. Retrieved June 19, 2015, from <https://www.addgene.org/lentiviral/protocols-resources/>
- Addgene. (n.d.-b). Addgene: What is a Plasmid? Retrieved June 19, 2015, from <https://www.addgene.org/mol-bio-reference/plasmid-background/>
- Agrawal, S., Mayrand, S. H., Zamecnik, P. C., & Pederson, T. (1990). Site-specific excision from RNA by RNase H and mixed-phosphate-backbone oligodeoxynucleotides. *Proceedings of the National Academy of Sciences of the United States of America*, 87(4). Retrieved from <http://www.pubmedcentral.nih.gov/articlerender.fcgi?artid=53483&tool=pmcentrez&rendertype=abstract>
- Akiyama, M., Kouzu, Y., Takahashi, S., Wakamatsu, H., Moriya, T., Maetani, M., ... Shibata, S. (1999). Inhibition of light- or glutamate-induced mPer1 expression represses the phase shifts into the mouse circadian locomotor and suprachiasmatic firing rhythms. *The Journal of Neuroscience : The Official Journal of the Society for Neuroscience*, 19(3). Retrieved from <http://www.ncbi.nlm.nih.gov/pubmed/9920673>
- Armstrong, D. G., Wrobel, J., & Robbins, J. M. (2007). Guest Editorial: are diabetes-related wounds and amputations worse than cancer? *International Wound Journal*, 4(4).
- Ashcroft, G. S., Jeong, M.-J., Ashworth, J. J., Hardman, M., Jin, W., Moutsopoulos, N., ... Wahl, S. M. (2012). Tumor necrosis factor-alpha (TNF- $\alpha$ ) is a therapeutic target for impaired cutaneous wound healing. *Wound Repair and Regeneration : Official Publication of the Wound Healing Society [and] the European Tissue Repair Society*, 20(1).
- Asher, G., & Schibler, U. (2006). A CLOCK-less clock. *Trends in Cell Biology*, 16(11).
- Bahou, W. F., & Gnatenko, D. V. (2004). Platelet transcriptome: the application of microarray analysis to platelets. *Seminars in Thrombosis and Hemostasis*, 30(4).
- Balsalobre, A., Brown, S. a, Marcacci, L., Tronche, F., Kellendonk, C., Reichardt, H. M., ... Schibler, U. (2000). Resetting of circadian time in peripheral tissues by glucocorticoid signaling. *Science (New York, N.Y.)*, 289(5488). Retrieved from <http://www.ncbi.nlm.nih.gov/pubmed/11009419>
- Balsalobre, ADamiola, F., & Schibler, U. (1998). A serum shock induces circadian gene expression in mammalian tissue culture cells. *Cell*, 93(6). Retrieved from <http://www.ncbi.nlm.nih.gov/pubmed/9635423>
- Barrientos, S., Brem, H., Stojadinovic, O., & Tomic-Canic, M. (2014). Clinical

Application of Growth Factors and Cytokines in Wound Healing. *Wound Repair and Regeneration*.

- Bass, J., & Takahashi, J. S. (2010). Circadian integration of metabolism and energetics. *Science (New York, N.Y.)*, 330(6009).
- Baum, D. A., & Silverman, S. K. (2008). Deoxyribozymes: useful DNA catalysts in vitro and in vivo. *Cellular and Molecular Life Sciences : CMLS*, 65(14).
- Becker, D., Lin, J., & Green, C. (1999). *Antisense technology in the central nervous system*. (H. R. Ron A. Leslie, J. Hunter, Ed.). Oxford: Oxford University Press.
- Bergan, R. C., Kyle, E., Connell, Y., & Neckers, L. (1995). Inhibition of protein-tyrosine kinase activity in intact cells by the aptameric action of oligodeoxynucleotides. *Antisense Research and Development*, 5(1). Retrieved from <http://www.ncbi.nlm.nih.gov/pubmed/7542047>
- Bianchi, M. E. (2007). DAMPs, PAMPs and alarmins: all we need to know about danger. *Journal of Leukocyte Biology*, 81(1).
- Bjarnason, G. a, Jordan, R. C., Wood, P. a, Li, Q., Lincoln, D. W., Sothorn, R. B., ... Ben-David, Y. (2001). Circadian expression of clock genes in human oral mucosa and skin: association with specific cell-cycle phases. *The American Journal of Pathology*, 158(5).
- Bock, L. C., Griffin, L. C., Latham, J. A., Vermaas, E. H., & Toole, J. J. (1992). Selection of single-stranded DNA molecules that bind and inhibit human thrombin. *Nature*, 355(6360).
- Boden, M. J., Varcoe, T. J., Voultzios, A., & Kennaway, D. J. (2010). Reproductive biology of female Bmal1 null mice. *Reproduction (Cambridge, England)*, 139(6).
- Boussif, O., Lezoualc'h, F., Zanta, M. a, Mergny, M. D., Scherman, D., Demeneix, B., & Behr, J. P. (1995). A versatile vector for gene and oligonucleotide transfer into cells in culture and in vivo: polyethylenimine. *Proceedings of the National Academy of Sciences of the United States of America*, 92(16). Retrieved from <http://www.pubmedcentral.nih.gov/articlerender.fcgi?artid=41326&tool=pmcentrez&rendertype=abstract>
- Brown, S. A., Fleury-Olela, F., Nagoshi, E., Hauser, C., Juge, C., Meier, C. A., ... Schibler, U. (2005). The period length of fibroblast circadian gene expression varies widely among human individuals. *PLoS Biology*, 3(10).
- Brown, S. A., Kunz, D., Dumas, A., Westermark, P. O., Vanselow, K., Tilmann-Wahnschaffe, A., ... Kramer, A. (2008). Molecular insights into human daily behavior. *Proceedings of the National Academy of Sciences of the United States of America*, 105(5).
- Brown, W. (1991). A review and mathematical analysis of circadian rhythms in cell proliferation in mouse, rat and human epidermis. *Journal of Investigative Dermatology*. Retrieved from <http://www.nature.com/jid/journal/v97/n2/abs/5612416a.html>
- Buijs, R. M., Wortel, J., Van Heerikhuizen, J. J., Feenstra, M. G., Ter Horst, G. J., Romijn, H. J., & Kalsbeek, a. (1999). Anatomical and functional demonstration of a multisynaptic suprachiasmatic nucleus adrenal (cortex) pathway. *The European Journal of Neuroscience*, 11(5). Retrieved from <http://www.ncbi.nlm.nih.gov/pubmed/10215906>

- Bukrinsky, M. I., Haggerty, S., Dempsey, M. P., Sharova, N., Adzhubel, A., Spitz, L., ... Stevenson, M. (1993). A nuclear localization signal within HIV-1 matrix protein that governs infection of non-dividing cells. *Nature*, *365*(6447).
- Bunger, M. K., Wilsbacher, L. D., Moran, S. M., Clendenin, C., Radcliffe, L. A., Hogenesch, J. B., ... Bradfield, C. A. (2000). Mop3 is an essential component of the master circadian pacemaker in mammals. *Cell*, *103*(7). Retrieved from <http://www.pubmedcentral.nih.gov/articlerender.fcgi?artid=3779439&tool=pmcentrez&rendertype=abstract>
- Cailotto, C., Lei, J., van der Vliet, J., van Heijningen, C., van Eden, C. G., Kalsbeek, A., ... Buijs, R. M. (2009). Effects of nocturnal light on (clock) gene expression in peripheral organs: a role for the autonomic innervation of the liver. *PloS One*, *4*(5).
- Caldelas, I., Poirel, V.-J., Sicard, B., Pvet, P., & Challet, E. (2003). Circadian profile and photic regulation of clock genes in the suprachiasmatic nucleus of a diurnal mammal *arvicantha ansorgei*. *Neuroscience*, *116*(2).
- Capecchi, M. R. (1980). High efficiency transformation by direct microinjection of DNA into cultured mammalian cells. *Cell*, *22*(2 Pt 2). Retrieved from <http://www.ncbi.nlm.nih.gov/pubmed/6256082>
- Coffin, J. M., Hughes, S. H., & Varmus, H. E. (1997). Retroviruses. Cold Spring Harbor Laboratory Press. Retrieved from <http://www.ncbi.nlm.nih.gov/books/NBK19370/>
- Coogan, A. N., & Piggins, H. D. (2003). Circadian and Photic Regulation of Phosphorylation of ERK1 / 2 and Elk-1 in the Suprachiasmatic Nuclei of the Syrian Hamster, *23*(7).
- D'Amico, G., Frascaroli, G., Bianchi, G., Transidico, P., Doni, a, Vecchi, a, ... Mantovani, a. (2000). Uncoupling of inflammatory chemokine receptors by IL-10: generation of functional decoys. *Nature Immunology*, *1*(5).
- Da Costa, R. M., Jesus, F. M. R., Aniceto, C., & Mendes, M. (1999). Randomized, double-blind, placebo-controlled, dose- ranging study of granulocyte-macrophage colony stimulating factor in patients with chronic venous leg ulcers. *Wound Repair and Regeneration*, *7*(1).
- Damiola, F. (2000). Restricted feeding uncouples circadian oscillators in peripheral tissues from the central pacemaker in the suprachiasmatic nucleus. *Genes & Development*, *14*(23).
- Davis, M. W. (n.d.). ApE- A plasmid Editor. Retrieved February 1, 2013, from <http://biologylabs.utah.edu/jorgensen/wayned/ape/>
- de Fougères, A., Vornlocher, H.-P., Maraganore, J., & Lieberman, J. (2007). Interfering with disease: a progress report on siRNA-based therapeutics. *Nature Reviews. Drug Discovery*, *6*(6).
- de Fouw, N. J., Ma, D. D., Michalevicz, R., Gray, D. a, & Hoffbrand, a V. (1984). Differential cytotoxicity of deoxyguanosine and 8-aminoguanosine for human leukemic cell lines and normal bone marrow progenitor cells. *Hematological Oncology*, *2*(2).
- Debruyne, J. P., Noton, E., Lambert, C. M., Maywood, E. S., Weaver, D. R., & Reppert, S. M. (2006). A clock shock: mouse CLOCK is not required for circadian oscillator function. *Neuron*, *50*(3).

- DeBruyne, J. P., Weaver, D. R., & Reppert, S. M. (2007). CLOCK and NPAS2 have overlapping roles in the suprachiasmatic circadian clock. *Nature Neuroscience*, 10(5).
- Desotelle, J. A., Wilking, M. J., & Ahmad, N. The circadian control of skin and cutaneous photodamage. *Photochemistry and Photobiology*, 88(5).
- Dibner, C., Schibler, U., & Albrecht, U. (2010). *The mammalian circadian timing system: organization and coordination of central and peripheral clocks. Annual review of physiology* (Vol. 72).
- Diegelmann, R. F., & Evans, M. C. (2004). Wound healing: An overview of acute, fibrotic and delayed healing. *Frontiers in Bioscience : A Journal and Virtual Library*, (4).
- Dovi, J. V., Szpadarska, A. M., & DiPietro, L. A. (2004). Neutrophil function in the healing wound: adding insult to injury? *Thrombosis and Haemostasis*, 92(2).
- Dunlap, J. C. (1999). Molecular Bases for Circadian Clocks Review, 96.
- Elbashir, S. M., Harborth, J., Lendeckel, W., Yalcin, A., Weber, K., & Tuschl, T. (2001). Duplexes of 21-nucleotide RNAs mediate RNA interference in cultured mammalian cells. *Nature*, 411(6836).
- Elshazley, M., Sato, M., Hase, T., Yamashita, R., Yoshida, K., Toyokuni, S., ... Hasegawa, Y. (2012). The circadian clock gene BMAL1 is a novel therapeutic target for malignant pleural mesothelioma. *International Journal of Cancer. Journal International Du Cancer*, 131(12).
- Eming, S. a, Krieg, T., & Davidson, J. M. (2007). Inflammation in wound repair: molecular and cellular mechanisms. *The Journal of Investigative Dermatology*, 127(3).
- Felgner, J., Bennett, F., & Felgner, P. L. (1993). Cationic Lipid-Mediated Delivery of Polynucleotides. *Methods*, 5(1).
- Felgner, P. L., Gadek, T. R., Holm, M., Roman, R., Chan, H. W., Wenz, M., ... Danielsen, M. (1987). Lipofection: a highly efficient, lipid-mediated DNA-transfection procedure. *Proceedings of the National Academy of Sciences of the United States of America*, 84(21). Retrieved from <http://www.pubmedcentral.nih.gov/articlerender.fcgi?artid=299306&tool=pmcentrez&rendertype=abstract>
- Fire, A., Xu, S., Montgomery, M. K., Kostas, S. A., Driver, S. E., & Mello, C. C. (1998). Potent and specific genetic interference by double-stranded RNA in *Caenorhabditis elegans*. *Nature*, 391(6669).
- Froy, O. (2011). Circadian rhythms, ageing, and life span in mammals. *Physiology (Bethesda, Md.)*, 26(4).
- Froy, O., Chang, D. C., & Reppert, S. M. (2002). Redox potential: differential roles in dCRY and mCRY1 functions. *Current Biology : CB*, 12(2). Retrieved from <http://www.ncbi.nlm.nih.gov/pubmed/11818067>
- Fuchs, E. (2008). Skin stem cells: rising to the surface. *The Journal of Cell Biology*, 180(2).
- Gaddameedhi, S., Selby, C. P., Kaufmann, W. K., Smart, R. C., & Sancar, A. (2011a). Control of skin cancer by the circadian rhythm. *Proceedings of the National*

- Academy of Sciences of the United States of America*, 108(46).
- Gaddameedhi, S., Selby, C. P., Kaufmann, W. K., Smart, R. C., & Sancar, A. (2011b). Control of skin cancer by the circadian rhythm. *Proceedings of the National Academy of Sciences of the United States of America*, 108(46).
- Genecopoeia. (n.d.). shRNA Knockdown, shRNA Clones, Lentiviral shRNA | Genecopoeia. Retrieved June 19, 2015, from <http://www.genecopoeia.com/product/shrna-clones/>
- Geyfman, M., & Andersen, B. (2009). How the skin can tell time. *The Journal of Investigative Dermatology*, 129(5).
- Geyfman, M., Kumar, V., Liu, Q., Ruiz, R., Gordon, W., Espitia, F., ... Andersen, B. (2012). Brain and muscle Arnt-like protein-1 (BMAL1) controls circadian cell proliferation and susceptibility to UVB-induced DNA damage in the epidermis. *Proceedings of the National Academy of Sciences of the United States of America*, 109(29).
- Giles, R. V., Spiller, D. G., Green, J. A., Clark, R. E., & Tidd, D. M. (1995). Optimization of antisense oligodeoxynucleotide structure for targeting bcr-abl mRNA. *Blood*, 86(2). Retrieved from <http://www.ncbi.nlm.nih.gov/pubmed/7606003>
- Graham, F. L., & van der Eb, A. J. (1973). A new technique for the assay of infectivity of human adenovirus 5 DNA. *Virology*, 52(2). Retrieved from <http://www.ncbi.nlm.nih.gov/pubmed/4705382>
- Grewal, S. S., York, R. D., & Stork, P. J. (1999). Extracellular-signal-regulated kinase signalling in neurons. *Current Opinion in Neurobiology*, 9(5).
- Haensler, J., & Szoka, F. C. Polyamidoamine cascade polymers mediate efficient transfection of cells in culture. *Bioconjugate Chemistry*, 4(5). Retrieved from <http://www.ncbi.nlm.nih.gov/pubmed/8274523>
- Hanft, J. R., Pollak, R. A., Barbul, A., Gils, C. va., Kwon, P. S., Gray, S. M., ... Breen, T. J. (2008). Phase I trial on the safety of topical rhVEGF on chronic neuropathic diabetic foot ulcers. *Journal of Wound Care*, 17(1).
- Hannibal, J., Ding, J. M., Chen, D., Fahrenkrug, J., Larsen, P. J., Gillette, M. U., & Mikkelsen, J. D. (1997). Pituitary adenylate cyclase-activating peptide (PACAP) in the retinohypothalamic tract: a potential daytime regulator of the biological clock. *The Journal of Neuroscience : The Official Journal of the Society for Neuroscience*, 17(7). Retrieved from <http://www.ncbi.nlm.nih.gov/pubmed/9065523>
- Haslett, C. (1992). Resolution of acute inflammation and the role of apoptosis in the tissue fate of granulocytes. *Clinical Science (London, England : 1979)*, 83(6). Retrieved from <http://www.ncbi.nlm.nih.gov/pubmed/1336433>
- Hastings, M., O'Neill, J. S., & Maywood, E. S. (2007). Circadian clocks: Regulators of endocrine and metabolic rhythms. *Journal of Endocrinology*, 195(2).
- Hattar, S., Liao, H. W., Takao, M., Berson, D. M., & Yau, K. W. (2002). Melanopsin-containing retinal ganglion cells: architecture, projections, and intrinsic photosensitivity. *Science (New York, N.Y.)*, 295(5557).
- Hinz, B. (2007). Formation and function of the myofibroblast during tissue repair. *The Journal of Investigative Dermatology*, 127(3).

- Hirota, T., Okano, T., Kokame, K., Shirotani-Ikejima, H., Miyata, T., & Fukada, Y. (2002). Glucose down-regulates Per1 and Per2 mRNA levels and induces circadian gene expression in cultured Rat-1 fibroblasts. *The Journal of Biological Chemistry*, 277(46).
- Hopp, T. P., Prickett, K. S., Price, V. L., Libby, R. T., March, C. J., Pat Cerretti, D., ... Conlon, P. J. (1988). A Short Polypeptide Marker Sequence Useful for Recombinant Protein Identification and Purification. *Bio/Technology*, 6(10).
- Huang, H.-W., Zheng, B.-L., Jiang, L., Lin, Z.-T., Zhang, G.-B., Shen, L., & Xi, X.-M. (2015). Effect of oral melatonin and wearing earplugs and eye masks on nocturnal sleep in healthy subjects in a simulated intensive care unit environment: which might be a more promising strategy for ICU sleep deprivation? *Critical Care (London, England)*, 19(1).
- Iliina, O., & Friedl, P. (2009). Mechanisms of collective cell migration at a glance. *Journal of Cell Science*, 122(Pt 18).
- Innominato, P. F., Roche, V. P., Palesh, O. G., Ulusakarya, A., Spiegel, D., & Lévi, F. A. (2014). The circadian timing system in clinical oncology. *Annals of Medicine*, 46(4).
- Ishida, A., Mutoh, T., Ueyama, T., Bando, H., Masubuchi, S., Nakahara, D., ... Okamura, H. (2005). Light activates the adrenal gland: timing of gene expression and glucocorticoid release. *Cell Metabolism*, 2(5).
- Ito, M., Liu, Y., Yang, Z., Nguyen, J., Liang, F., Morris, R. J., & Cotsarelis, G. (2005). Stem cells in the hair follicle bulge contribute to wound repair but not to homeostasis of the epidermis. *Nature Medicine*, 11(12).
- Jackson, A. L., Burchard, J., Schelter, J., Chau, B. N., Cleary, M., Lim, L., & Linsley, P. S. (2006). Widespread siRNA "off-target" transcript silencing mediated by seed region sequence complementarity. *RNA (New York, N.Y.)*, 12(7).
- Jackson, A. L., & Linsley, P. S. (2010). Recognizing and avoiding siRNA off-target effects for target identification and therapeutic application. *Nature Reviews. Drug Discovery*, 9(1).
- Janich, P., Pascual, G., Merlos-Suárez, A., Batlle, E., Ripperger, J., Albrecht, U., ... Benitah, S. A. (2011). The circadian molecular clock creates epidermal stem cell heterogeneity. *Nature*, 480(7376).
- Janich, P., Toufighi, K., Solanas, G., Luis, N. M., Minkwitz, S., Serrano, L., ... Benitah, S. A. (2013). Human epidermal stem cell function is regulated by circadian oscillations. *Cell Stem Cell*, 13(6).
- Kaneko, M., Hiroshige, T., Shinsako, J., & Dallman, M. F. (2012). Diurnal changes in amplification of hormone rhythms in the adrenocortical system Diurnal rhythms changes in amplification of hormone in the adrenocortical system.
- Kang, T.-H., Lindsey-Boltz, L. A., Reardon, J. T., & Sancar, A. (2010). Circadian control of XPA and excision repair of cisplatin-DNA damage by cryptochrome and HERC2 ubiquitin ligase. *Proceedings of the National Academy of Sciences of the United States of America*, 107(11).
- Kawai, S., & Nishizawa, M. (1984). New procedure for DNA transfection with polycation and dimethyl sulfoxide. *Molecular and Cellular Biology*, 4(6). Retrieved from

<http://www.pubmedcentral.nih.gov/articlerender.fcgi?artid=368888&tool=pmcentrez&rendertype=abstract>

- Kim, M.-H., Liu, W., Borjesson, D. L., Curry, F.-R. E., Miller, L. S., Cheung, A. L., ... Simon, S. I. (2008). Dynamics of neutrophil infiltration during cutaneous wound healing and infection using fluorescence imaging. *The Journal of Investigative Dermatology*, 128(7).
- Kim, T. K., & Eberwine, J. H. (2010). Mammalian cell transfection: the present and the future. *Analytical and Bioanalytical Chemistry*, 397(8).
- Kippenberger, S., Bernd, A., Loitsch, S., Guschel, M., Müller, J., Bereiter-Hahn, J., & Kaufmann, R. (2000). Signaling of mechanical stretch in human keratinocytes via MAP kinases. *The Journal of Investigative Dermatology*, 114(3).
- Kiss, J., Leranath, C., & Halasz, B. (1984). Serotonergic endings on VIP-neurons in the suprachiasmatic nucleus and on ACTH-neurons in the arcuate nucleus of the rat hypothalamus . A combination of high resolution autoradiography and electron microscopic immunocytochemistry, 44.
- Kiyohara, Y. B., Tagao, S., Tamanini, F., Morita, A., Sugisawa, Y., Yasuda, M., ... Yagita, K. (2006). The BMAL1 C terminus regulates the circadian transcription feedback loop. *Proceedings of the National Academy of Sciences of the United States of America*, 103(26).
- Kobayashi, H., Aiba, S., Yoshino, Y., & Tagami, H. (2003). Acute cutaneous barrier disruption activates epidermal p44/42 and p38 mitogen-activated protein kinases in human and hairless guinea pig skin. *Experimental Dermatology*, 12(6).
- Kole, R., Krainer, A. R., & Altman, S. (2012). RNA therapeutics: beyond RNA interference and antisense oligonucleotides. *Nature Reviews. Drug Discovery*, 11(2). Retrieved from <http://dx.doi.org/10.1038/nrd3625>
- Kondratov, R. V, Kondratova, A. A., Gorbacheva, V. Y., Vykhoanets, O. V, & Antoch, M. P. (2006). Early ageing and age-related pathologies in mice deficient in BMAL1, the core component of the circadian clock. *Genes & Development*, 20(14).
- Kornhauser, J. M., Mayo, K. E., & Takahashi, J. S. (1996). Light, immediate-early genes, and circadian rhythms. *Behavior Genetics*, 26(3). Retrieved from <http://www.ncbi.nlm.nih.gov/pubmed/8754249>
- Kowalska, E., Ripperger, J. A., Hoegger, D. C., Bruegger, P., Buch, T., Birchler, T., ... Brown, S. A. (2013). NONO couples the circadian clock to the cell cycle. *Proceedings of the National Academy of Sciences of the United States of America*, 110(5).
- Koziolekiewicz, M. (2001). The mononucleotide-dependent, nonantisense mechanism of action of phosphodiester and phosphorothioate oligonucleotides depends upon the activity of an ecto-5'-nucleotidase. *Blood*, 98(4).
- Koziolekiewicz, M., Gendaszewska, E., Maszewska, M., Stein, C. a., & Stec, W. J. (2001). The mononucleotide-dependent, nonantisense mechanism of action of phosphodiester and phosphorothioate oligonucleotides depends upon the activity of an ecto-5'-nucleotidase. *Blood*, 98(4).
- Kranke, P., Bennett, M. H., Martyn-St James, M., Schnabel, A., Debus, S. E., & Weibel, S. (2015). Hyperbaric oxygen therapy for chronic wounds. *The Cochrane Database of Systematic Reviews*, 6.

- Kranke, P., Mh, B., M, M. J., Schnabel, A., & Se, D. (2012). Hyperbaric oxygen therapy for chronic wounds ( Review ), (4).
- Lagos-Quintana, M., Rauhut, R., Meyer, J., Borkhardt, A., & Tuschl, T. (2003). New microRNAs from mouse and human. *RNA (New York, N.Y.)*, 9(2). Retrieved from <http://www.pubmedcentral.nih.gov/articlerender.fcgi?artid=1370382&tool=pmcentrez&rendertype=abstract>
- Law, L., Zhang, W., & Stott, N. (2006). In vitro optimization of antisense oligodeoxynucleotide design: an example using the connexin gene family. *Journal of Biomeolecular Techniques*, 17(4). Retrieved from <http://www.ncbi.nlm.nih.gov/pmc/articles/PMC2291797/>
- Lee, Y. (2002). MicroRNA maturation: stepwise processing and subcellular localization. *The EMBO Journal*, 21(17).
- Lévi, F., Okyar, A., Dulong, S., Innominato, P. F., & Clairambault, J. (2010). Circadian timing in cancer treatments. *Annual Review of Pharmacology and Toxicology*, 50.
- Liang, C.-C., Park, A. Y., & Guan, J.-L. (2007). In vitro scratch assay: a convenient and inexpensive method for analysis of cell migration in vitro. *Nature Protocols*, 2(2).
- Lin, F., Chen, Y., Li, X., Zhao, Q., & Tan, Z. (2013). Over-expression of circadian clock gene Bmal1 affects proliferation and the canonical Wnt pathway in NIH-3T3 cells. *Cell Biochemistry and Function*, 31(2).
- Ling, H., Fabbri, M., & Calin, G. A. (2013). MicroRNAs and other non-coding RNAs as targets for anticancer drug development. *Nature Reviews. Drug Discovery*, 12(11).
- Lipton, J. O., Yuan, E. D., Boyle, L. M., Ebrahimi-Fakhari, D., Kwiatkowski, E., Nathan, A., ... Sahin, M. (2015). The Circadian Protein BMAL1 Regulates Translation in Response to S6K1-Mediated Phosphorylation. *Cell*, 161(5).
- Mathias, J. R., Perrin, B. J., Liu, T., Kanki, J., Look, A. T., & Huttenlocher, A. (2006). Resolution of inflammation by retrograde chemotaxis of neutrophils in transgenic zebrafish flammation is a critical process during normal im-, 80(December).
- McDearmon, E. L., Patel, K. N., Ko, C. H., Walisser, J. a, Schook, A. C., Chong, J. L., ... Takahashi, J. S. (2006). Dissecting the functions of the mammalian clock protein BMAL1 by tissue-specific rescue in mice. *Science (New York, N.Y.)*, 314(5803).
- Mendoza-Naranjo, A., Cormie, P., Serrano, A. E., Hu, R., O'Neill, S., Wang, C. M., ... Becker, D. L. (2012). Targeting cx43 and N-cadherin, which are abnormally upregulated in venous leg ulcers, influences migration, adhesion and activation of rho GTPases. *PloS One*, 7(5).
- Menger, G. J., Allen, G. C., Neuendorff, N., Nahm, S.-S., Thomas, T. L., Cassone, V. M., & Earnest, D. J. (2007). Circadian profiling of the transcriptome in NIH/3T3 fibroblasts: comparison with rhythmic gene expression in SCN2.2 cells and the rat SCN. *Physiological Genomics*, 29(3).
- Miller, P. S., Braiterman, L. T., & Ts'o, P. O. P. (1977). Effects of a trinucleotide ethyl phosphotriester, G m p(Et)G m p(Et)U, on mammalian cells in culture. *Biochemistry*, 16(9).
- Mitchison, T. J., & Cramer, L. P. (1996). Actin-based cell motility and cell locomotion. *Cell*, 84(3). Retrieved from <http://www.ncbi.nlm.nih.gov/pubmed/8608590>

- Moore, C. B., Guthrie, E. H., Huang, M. T.-H., & Taxman, D. J. (2010). Short hairpin RNA (shRNA): design, delivery, and assessment of gene knockdown. *Methods in Molecular Biology (Clifton, N.J.)*, 629.
- Moore, R. Y. (1997). Circadian rhythms: basic neurobiology and clinical applications. *Annual Review of Medicine*, 48.
- Moore, R. Y., & Card, J. P. (1994). Intergeniculate leaflet: an anatomically and functionally distinct subdivision of the lateral geniculate complex. *The Journal of Comparative Neurology*, 344(3).
- Moore, R. Y., & Lenn, N. J. (1972). A retinohypothalamic projection in the rat. *The Journal of Comparative Neurology*, 146(1).
- Mrosovsky, N., Edelstein, K., Hastings, M. H., & Maywood, E. S. (2001). Cycle of period Gene Expression in a Diurnal Mammal (*Spermophilus tridecemlineatus*): Implications for Nonphotic Phase Shifting. *Journal of Biological Rhythms*, 16(5).
- Nagoshi, E., Brown, S. A., Dibner, C., Kornmann, B., & Schibler, U. (2005). Circadian gene expression in cultured cells. *Methods in Enzymology*, 393.
- Nagoshi, E., Saini, C., Bauer, C., Laroche, T., Naef, F., & Schibler, U. (2004). Circadian gene expression in individual fibroblasts: cell-autonomous and self-sustained oscillators pass time to daughter cells. *Cell*, 119(5).
- Nagoshi, E., Saini, C., Bauer, C., Laroche, T., Naef, F., Schibler, U., ... Geneva, U. of. (2004). Circadian Gene Expression in Individual Fibroblasts : Oscillators Pass Time to Daughter Cells. *Cell*, 119.
- Nelson, E. A., Bell-syer, S. E. M., Cullum, N. A., & Webster, J. (2012). Compression for preventing recurrence of venous ulcers ( Review ) Compression for preventing recurrence of venous ulcers. *Cochrane Database of Systematic Reviews*, (8).
- Nguyen, B. P., Gil, S. G., & Carter, W. G. (2000). Deposition of laminin 5 by keratinocytes regulates integrin adhesion and signaling. *The Journal of Biological Chemistry*, 275(41).
- Noli, C., & Miolo, A. (2001). The mast cell in wound healing. *Veterinary Dermatology*, 12(6). Retrieved from <http://www.ncbi.nlm.nih.gov/pubmed/11844219>
- Nuccitelli, R., Nuccitelli, P., Ramlatchan, S., Sanger, R., & Smith, P. J. S. Imaging the electric field associated with mouse and human skin wounds. *Wound Repair and Regeneration : Official Publication of the Wound Healing Society [and] the European Tissue Repair Society*, 16(3).
- Nurden, A. T., Nurden, P., Sanchez, M., Andia, I., & Anitua, E. (2008). Platelets and wound healing. *Frontiers in Bioscience : A Journal and Virtual Library*, 13. Retrieved from <http://www.ncbi.nlm.nih.gov/pubmed/18508453>
- Obrietan, K., Impey, S., & Storm, D. R. (1998). Light and circadian rhythmicity regulate MAP kinase activation in the suprachiasmatic nuclei. *Nature Neuroscience*, 1(8).
- Oishi, K., Miyazaki, K., & Ishida, N. (2002). Functional CLOCK is not involved in the entrainment of peripheral clocks to the restricted feeding: entrainable expression of mPer2 and BMAL1 mRNAs in the heart of Clock mutant mice on Jcl:ICR background. *Biochemical and Biophysical Research Communications*, 298(2). Retrieved from <http://www.ncbi.nlm.nih.gov/pubmed/12387815>

- Osland, T. M., Fernø, J., Håvik, B., Heuch, I., Ruoff, P., Lærum, O. D., & Steen, V. M. (2011). Lithium differentially affects clock gene expression in serum-shocked NIH-3T3 cells. *Journal of Psychopharmacology (Oxford, England)*, 25(7).
- Pagano, J. S., & Vaheri, A. (1965). Enhancement of infectivity of poliovirus RNA with diethylaminoethyl-dextran (DEAE-D). *Archiv Für Die Gesamte Virusforschung*, 17(3). Retrieved from <http://www.ncbi.nlm.nih.gov/pubmed/4286824>
- Paterson, B. M., Robertst, B. E., & Kuff, E. L. (1977). Structural gene identification and mapping by DNA \* mRNA hybrid-arrested cell-free translation *Biochemistry* :, 74(10).
- Pearson, W. R. (n.d.). FASTA Sequence Comparison. Retrieved November 10, 2012, from [http://fasta.bioch.virginia.edu/fasta\\_www2/fasta\\_www.cgi?rm=select&pgm=fa](http://fasta.bioch.virginia.edu/fasta_www2/fasta_www.cgi?rm=select&pgm=fa)
- Pearson, W. R., & Lipman, D. J. (1988). Improved tools for biological sequence comparison. *Proceedings of the National Academy of Sciences of the United States of America*, 85(8). Retrieved from <http://www.pubmedcentral.nih.gov/articlerender.fcgi?artid=280013&tool=pmcentrez&rendertype=abstract>
- Perretti, M., & Gavins, F. N. E. (2012). Annexin 1 : An Endogenous Anti-Inflammatory Protein.
- Pevet, P., & Challet, E. (2011). Melatonin: both master clock output and internal time-giver in the circadian clocks network. *Journal of Physiology, Paris*, 105(4-6).
- Pilcher, B. K., Wang, M., Qin, X. J., Parks, W. C., Senior, R. M., & Welgus, H. G. (1999). Role of matrix metalloproteinases and their inhibition in cutaneous wound healing and allergic contact hypersensitivity. *Annals of the New York Academy of Sciences*, 878. Retrieved from <http://www.ncbi.nlm.nih.gov/pubmed/10415717>
- Plikus, M. V., Gay, D. L., Treffeisen, E., Wang, A., Supapannachart, R. J., & Cotsarelis, G. (2012). Epithelial stem cells and implications for wound repair. *Seminars in Cell & Developmental Biology*, 23(9).
- Preitner, N., Damiola, F., Zakany, J., Duboule, D., Albrecht, U., & Schibler, U. (2002). The Orphan Nuclear Receptor REV-ERB  $\alpha$  Controls Circadian Transcription within the Positive Limb of the Mammalian Circadian Oscillator University of Geneva University of Geneva, 110.
- Promega Corp. (2015). Transfection. Retrieved June 17, 2015, from <http://www.promega.co.uk/resources/product-guides-and-selectors/protocols-and-applications-guide/transfection/>
- Qiu, C., Coutinho, P., Frank, S., Franke, S., Law, L., Martin, P., ... London, W. C. E. (2003). Targeting Connexin43 Expression Accelerates the Rate of Wound Repair. *Current*, 13.
- Reinhart, B. J., Slack, F. J., Basson, M., Pasquinelli, A. E., Bettinger, J. C., Rougvie, A. E., ... Ruvkun, G. (2000). The 21-nucleotide let-7 RNA regulates developmental timing in *Caenorhabditis elegans*. *Nature*, 403(6772).
- Rennert, R. C., Rodrigues, M., Wong, V. W., Duscher, D., Hu, M., Maan, Z., ... Longaker, M. T. (2013). Biological therapies for the treatment of cutaneous wounds: phase III and launched therapies. *Expert Opinion on Biological Therapy*, 13(11).

- Reppert, S. M., & Weaver, D. R. (2002). Coordination of circadian timing in mammals. *Nature*, *418*(6901).
- Ripperger, J. a., & Schibler, U. (2001). Circadian regulation of gene expression in animals. *Current Opinion in Cell Biology*, *13*(3). Retrieved from <http://www.ncbi.nlm.nih.gov/pubmed/11343908>
- Robinson, R. (2004). RNAi therapeutics: how likely, how soon? *PLoS Biology*, *2*(1).
- Ruble, B. K., Richards, J. L., Cheung-Lau, J. C., & Dmochowski, I. J. (2012). Mismatch Discrimination and Efficient Photomodulation with Split 10-23 DNAzymes. *Inorganica Chimica Acta*, *380*(null).
- Sandu, C., Dumas, M., Malan, A., Sambakhe, D., Marteau, C., Nizard, C., ... Felder-Schmittbuhl, M.-P. (2012). Human skin keratinocytes, melanocytes, and fibroblasts contain distinct circadian clock machineries. *Cellular and Molecular Life Sciences : CMLS*.
- Santa Cruz Biotechnology. (n.d.). Gene Silencers. Retrieved June 17, 2015, from [https://www.scbt.com/gene\\_silencers.html](https://www.scbt.com/gene_silencers.html)
- Santoro, S. W., & Joyce, G. F. (1997). A general purpose RNA-cleaving DNA enzyme. *Proceedings of the National Academy of Sciences of the United States of America*, *94*(9). Retrieved from <http://www.ncbi.nlm.nih.gov/pubmed/16790281>
- Santoro, S. W., & Joyce, G. F. (1998). Mechanism and utility of an RNA-cleaving DNA enzyme. *Biochemistry*, *37*(38).
- Sato, T. K., Panda, S., Miraglia, L. J., Reyes, T. M., Rudic, R. D., McNamara, P., ... Hogenesch, J. B. (2004). A functional genomics strategy reveals Rora as a component of the mammalian circadian clock. *Neuron*, *43*(4).
- Schäfer, M., & Werner, S. (2008). Oxidative stress in normal and impaired wound repair. *Pharmacological Research : The Official Journal of the Italian Pharmacological Society*, *58*(2).
- Schwab, J. M., Chiang, N., Arita, M., & Serhan, C. N. (2007). Resolvin E1 and protectin D1 activate inflammation-resolution programmes. *Nature*, *447*(7146).
- Schwanhäusser, B., Busse, D., Li, N., Dittmar, G., Schuchhardt, J., Wolf, J., ... Selbach, M. (2011). Global quantification of mammalian gene expression control. *Nature*, *473*(7347).
- Shan, G., Li, Y., Zhang, J., Li, W., Szulwach, K. E., Duan, R., ... Jin, P. (2008). A small molecule enhances RNA interference and promotes microRNA processing. *Nature Biotechnology*, *26*(8).
- Shaykhiev, R., Behr, J., & Bals, R. (2008). Microbial patterns signaling via Toll-like receptors 2 and 5 contribute to epithelial repair, growth and survival. *PloS One*, *3*(1).
- Shi, S., Hida, A., McGuinness, O. P., Wasserman, D. H., Yamazaki, S., & Johnson, C. H. (2010). Circadian clock gene *Bmal1* is not essential; functional replacement with its paralog, *Bmal2*. *Current Biology : CB*, *20*(4).
- Shigekawa, K., & Dower, W. J. (1988). Electroporation of eukaryotes and prokaryotes: a general approach to the introduction of macromolecules into cells. *BioTechniques*, *6*(8). Retrieved from <http://www.ncbi.nlm.nih.gov/pubmed/3273636>

- Shimizu, N., Yoshikawa, N., Ito, N., Maruyama, T., Suzuki, Y., Takeda, S., ... Tanaka, H. (2011). Crosstalk between glucocorticoid receptor and nutritional sensor mTOR in skeletal muscle. *Cell Metabolism*, 13(2).
- Sigma. (n.d.). Sigma Genosys DNA calculator. Retrieved February 1, 2013, from <http://www.sigma-genosys.com/calc/DNACalc.asp>
- Silver, R., LeSauter, J., Tresco, P., & Lehman, M. (1996). A diffusible coupling signal from the transplanted suprachiasmatic nucleus controlling circadian locomotor rhythms. *Nature*. Retrieved from [http://www.columbiauniversity.org/cu/psychology/silver/publications/090Silver et al 1996.PDF](http://www.columbiauniversity.org/cu/psychology/silver/publications/090Silver%20et%20al%201996.PDF)
- Smaaland, R. (1996). Circadian rhythm of cell division. *Progress in Cell Cycle Research*, 2. Retrieved from <http://www.ncbi.nlm.nih.gov/pubmed/9552400>
- Smiell, J. M., Wieman, T. J., Steed, D. L., Perry, B. H., Sampson, A. R., & Schwab, B. H. (1999). Efficacy and safety of becaplermin (recombinant human platelet-derived growth factor-BB) in patients with nonhealing, lower extremity diabetic ulcers: a combined analysis of four randomized studies. *Wound Repair and Regeneration*, 7(5).
- Stephan, F. K. (2002). The “Other” Circadian System: Food as a Zeitgeber. *Journal of Biological Rhythms*, 17(4).
- Stephenson, M. L., & Zamecnik, P. C. (1978). Inhibition of Rous sarcoma viral RNA translation by a specific oligodeoxyribonucleotide. *Proceedings of the National Academy of Sciences of the United States of America*, 75(1). Retrieved from <http://www.pubmedcentral.nih.gov/articlerender.fcgi?artid=411231&tool=pmcentrez&rendertype=abstract>
- Stevens, R. G., Brainard, G. C., Blask, D. E., Lockley, S. W., & Motta, M. E. (2014). Breast cancer and circadian disruption from electric lighting in the modern world. *CA: Cancer J Clin.*, 64(3).
- Stewart, S. A. (2003). Lentivirus-delivered stable gene silencing by RNAi in primary cells. *RNA*, 9(4).
- Stokkan, K. A., Yamazaki, S., Tei, H., Sakaki, Y., & Menaker, M. (2001). Entrainment of the circadian clock in the liver by feeding. *Science (New York, N.Y.)*, 291(5503).
- Stringari, C., Wang, H., Geyfman, M., Crosignani, V., Kumar, V., Takahashi, J. S., ... Gratton, E. (2015). In vivo single-cell detection of metabolic oscillations in stem cells. *Cell Reports*, 10(1).
- Summerton, J., & Weller, D. (1997). Morpholino antisense oligomers: design, preparation, and properties. *Antisense & Nucleic Acid Drug Development*, 7(3). Retrieved from <http://www.ncbi.nlm.nih.gov/pubmed/9212909>
- Takahashi, J. S., Hong, H.-K., Ko, C. H., & McDearmon, E. L. (2008). The genetics of mammalian circadian order and disorder: implications for physiology and disease. *Nature Reviews. Genetics*, 9(10).
- Tamaru, T., Hattori, M., Honda, K., Benjamin, I., Ozawa, T., & Takamatsu, K. (2011). Synchronization of circadian Per2 rhythms and HSF1-BMAL1:CLOCK interaction in mouse fibroblasts after short-term heat shock pulse. *PloS One*, 6(9).
- Tan, X., Zhang, P., Zhou, L., Yin, B., Pan, H., & Peng, X. (2012). Clock-controlled mir-142-3p can target its activator, Bmal1. *BMC Molecular Biology*, 13(1).

- Tanioka, M., Yamada, H., Doi, M., Bando, H., Yamaguchi, Y., Nishigori, C., & Okamura, H. (2009). Molecular clocks in mouse skin. *The Journal of Investigative Dermatology*, 129(5).
- Tay, Y., Zhang, J., Thomson, A. M., Lim, B., & Rigoutsos, I. (2008). MicroRNAs to Nanog, Oct4 and Sox2 coding regions modulate embryonic stem cell differentiation. *Nature*, 455(7216).
- Thierry, a R., & Dritschilo, a. (1992). Intracellular availability of unmodified, phosphorothioated and liposomally encapsulated oligodeoxynucleotides for antisense activity. *Nucleic Acids Research*, 20(21).
- Thierry, A. R., & Dritschilo, A. (1992). Intracellular availability of unmodified, phosphorothioated and liposomally encapsulated oligodeoxynucleotides for antisense activity. *Nucleic Acids Research*, 20(21).
- Todaro, G. J., & Green, H. (1963). Quantitative studies of the growth of mouse embryo cells in culture and their development into established lines. *The Journal of Cell Biology*, 17(2).
- Tonnesen, M. G., Feng, X., & Clark, R. A. (2000). Angiogenesis in wound healing. *The Journal of Investigative Dermatology. Symposium Proceedings / the Society for Investigative Dermatology, Inc. [and] European Society for Dermatological Research*, 5(1).
- Tsuchiya, Y., Minami, I., Kadotani, H., & Nishida, E. (2005). Resetting of peripheral circadian clock by prostaglandin E2. *EMBO Reports*, 6(3).
- Turek, F. W., Joshu, C., Kohsaka, A., Lin, E., Ivanova, G., McDearmon, E., ... Bass, J. (2005). Obesity and metabolic syndrome in circadian Clock mutant mice. *Science (New York, N.Y.)*, 308(5724).
- Ulrich, M. M. W., Verkerk, M., Reijnen, L., Vlig, M., van den Bogaardt, A. J., & Middelkoop, E. (2007). Expression profile of proteins involved in scar formation in the healing process of full-thickness excisional wounds in the porcine model. *Wound Repair and Regeneration : Official Publication of the Wound Healing Society [and] the European Tissue Repair Society*, 15(4).
- Vaerman, J. L., Moureau, P., Deldime, F., Lewalle, P., Lammineur, C., Morschhauser, F., & Martiat, P. (1997). Antisense Oligodeoxyribonucleotides Suppress Hematologic Cell Growth Through Stepwise Release of Deoxyribonucleotides. *Blood*, 90(1). Retrieved from <http://bloodjournal.hematologylibrary.org/cgi/content/abstract/90/1/331>
- van den Pol, a N., & Tsujimoto, K. L. (1985). Neurotransmitters of the hypothalamic suprachiasmatic nucleus: immunocytochemical analysis of 25 neuronal antigens. *Neuroscience*, 15(4). Retrieved from <http://www.ncbi.nlm.nih.gov/pubmed/2413388>
- Vasudevan, S., Tong, Y., & Steitz, J. A. (2007). Switching from repression to activation: microRNAs can up-regulate translation. *Science (New York, N.Y.)*, 318(5858).
- Vitaterna, M. H., King, D. P., Chang, a M., Kornhauser, J. M., Lowrey, P. L., McDonald, J. D., ... Takahashi, J. S. (1994). Mutagenesis and mapping of a mouse gene, Clock, essential for circadian behavior. *Science (New York, N.Y.)*, 264(5159). Retrieved from <http://www.ncbi.nlm.nih.gov/pubmed/8171325>

- Vosko, A. M., Hagenauer, M. H., Hummer, D. L., & Lee, T. M. (2009). Period gene expression in the diurnal degu (*Octodon degus*) differs from the nocturnal laboratory rat (*Rattus norvegicus*). *American Journal of Physiology. Regulatory, Integrative and Comparative Physiology*, 296(2).
- Welsh, D. K., Yoo, S.-H., Liu, A. C., Takahashi, J. S., & Kay, S. A. (2004). Bioluminescence imaging of individual fibroblasts reveals persistent, independently phased circadian rhythms of clock gene expression. *Current Biology : CB*, 14(24).
- Werner, S., & Grose, R. (2003). Regulation of wound healing by growth factors and cytokines. *Physiological Reviews*, 83(3).
- Wickstrom, E. (1986). Oligodeoxynucleotide stability in subcellular extracts and culture media. *Journal of Biochemical and Biophysical Methods*, 13(2).
- Wu, A. G., Joshi, S. S., Chan, W. C., Iversen, P. L., Jackson, J. D., Kessinger, A., ... Verbik, D. J. (1995). Effects of BCR-ABL antisense oligonucleotides (AS-ODN) on human chronic myeloid leukemic cells: AS-ODN as effective purging agents. *Leukemia & Lymphoma*, 20(1-2).
- Wynn, T. A. (2008). Cellular and molecular mechanisms of fibrosis. *The Journal of Pathology*, 214(2).
- Yagita, K., & Okamura, H. (2000). Forskolin induces circadian gene expression of rPer1, rPer2 and dbp in mammalian rat-1 fibroblasts. *FEBS Letters*, 465(1).
- Yagita, K., & Okamura, H. (2000). Forskolin induces circadian gene expression of rPer1, rPer2 and dbp in mammalian rat-1 fibroblasts. *FEBS Letters*, 465(1). Retrieved from <http://www.ncbi.nlm.nih.gov/pubmed/10620710>
- Yagita, K., Tamanini, F., van Der Horst, G. T., & Okamura, H. (2001). Molecular mechanisms of the biological clock in cultured fibroblasts. *Science (New York, N.Y.)*, 292(5515).
- Yamazaki, S. (2000). Resetting Central and Peripheral Circadian Oscillators in Transgenic Rats. *Science*, 288(5466).
- Ye, G.-N., Daniell, H., & Sanford, J. C. (1990). Optimization of delivery of foreign DNA into higher-plant chloroplasts. *Plant Molecular Biology*, 15(6).
- Zamecnik, P. C., & Stephenson, M. L. (1978). Inhibition of Rous sarcoma virus replication and cell transformation by a specific oligodeoxynucleotide. *Biochemistry : Zamecnik and Stephenson*, 75(1).
- Zanello, S. B., Jackson, D. M., & Holick, M. F. (2000). Expression of the circadian clock genes clock and period1 in human skin. *The Journal of Investigative Dermatology*, 115(4).

# Appendix A

---

Reference: RA002562/1

Sign-off Status: Authorised

<b>Date Created:</b>	11/12/2014	<b>Confidential?</b>	No
<b>Assessment Title:</b>	The use of lentiviral vectors for the introduction and knockdown of genes that control the circadian clock in cell culture models		
<b>Assessment Outline:</b>	This is a new activity		
<b>Area Responsible (for management of risks)</b>		<b>Location of Risks</b>	
<b>Division, School, Faculty, Institute:</b>	Faculty of Life Sciences	<b>Building:</b>	Rockefeller Building
<b>Department:</b>	Div of Biosciences	<b>Area:</b>	Ground and Above
<b>Group/Unit:</b>	Cell & Developmental Biology	<b>Sub Area:</b>	Laboratory
<b>Further Location Information:</b>	Cell culture room 532 and equipment room 521		
<b>Assessment Start Date:</b>	23/01/2015	<b>Review or End Date:</b>	23/01/2016
<b>Relevant Attachments:</b>			
Description of attachments:			
Location of non-electronic documents:			
<b>Assessor(s):</b>	Heath, Katherine		
<b>Approver(s):</b>	JILLIAN DEANS LANGFORD, TONY		
<b>Signed Off:</b>	LANGFORD, TONY (16/01/2015 17:52) JILLIAN DEANS (23/01/2015 14:53)		
<b>Distribution List:</b>	TONY LANGFORD (T.langford@ucl.ac.uk) - 11/12/2014		

**PEOPLE AT RISK (from the Activities covered by this Risk Assessment)**

<b>CATEGORY</b>
Employees
Post-Graduates
Undergraduates
Contractors
Members of the Public
Visitors
Disabled Persons
Inexperienced Workers/Trainees
Women of Child-bearing Age
Young Persons
Other Vulnerable Persons
Other

**Summary of Activities, Hazards, Controls**

1. <b>GMM Class 1 Risk Assessment</b>	With Controls -----
---------------------------------------	---------------------

Who Made By	Date/Time Received	Comments
DEANS, JILLIAN	16/01/2015	Rejected: Please could you be more explicit (at 1.2) as to why the GMMs are low hazard - in particular addressing the biosafety features of the vector and the nature of the gene(s) to be knocked down is why there will no/negligible biological effect should such genes be switched off in the event of operator exposure. At 2.6.3 you indicate that GMMs will not be taken outside of the laboratory but you have indicated elsewhere that they will be moved from the lab a -80°C freezer in another room - please could you indicate the containment to be used when you are carrying out this process.